12-1986

Deep-ocean Bottom Pressure and Temperature Sensors Report: Methods and Data

D. Randolph Watts

H. Kontoyiannis

TRACEY

DEEP-OCEAN BOTTOM PRESSURE AND TEMPERATURE SENSORS REPORT: METHODS AND DATA

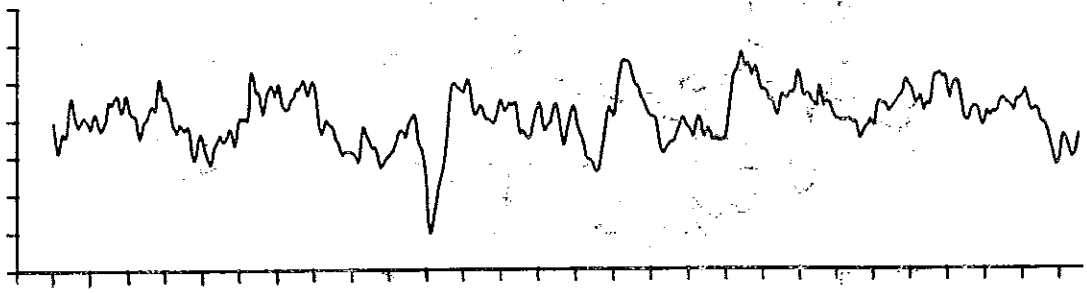

by

D. R. WATTS

and

H. KONTOYIANNIS

University of Rhode Island

Graduate School of Oceanography

Narragansett, Rhode Island 02882

GSO Technical Report Number 86-8

December, 1986

GRADUATE SCHOOL OF OCEANOGRAPHY
UNIVERSITY OF RHODE ISLAND
NARRAGANSETT, RHODE ISLAND

DEEP-OCEAN BOTTOM PRESSURE AND TEMPERATURE SENSORS

REPORT: METHODS AND DATA

by

D. R. Watts and H. Kontoyiannis

December, 1986

GSO Technical Report No. 86-8

This research program has been sponsored by the
National Science Foundation under grant number OCE82-01222
And by the Office of Naval Research under contract N00014-81-C-0062.

ABSTRACT

This report documents ocean bottom pressure data collected from September 1983 to May 1985 in eleven deployments of pressure sensors under the Gulf Stream northeast of Cape Hatteras in depths of 3300 to 3900 m, as part of the Gulf Stream Dynamics Experiment.

In past experiments, pressure sensors suitable for ocean depths have typically exhibited systematic drifts in calibration that seriously contaminate any observed periodicities longer than a few days. We used Digiquartz sensors (manufactured by Paroscientific, Inc.), because these sensors offered potentially much lower drift than other commercially available sensors. In these sensors, either a bellows or a Bourdon tube applies stress to an oscillating quartz-crystal beam, causing its oscillation frequency to vary.

Several factors influence the amount of drift: bellows vs. Bourdon-tube construction, the applied pressure, the duration of deployment, and, for some sensors, high-pressure preconditioning in the lab. For the sensors deployed in the Gulf Stream, the total drift during deployments lasting from 3 to 12 months ranged from undetectable ($\leq$0.01 dbar) to 0.20 to 0.50 dbar. About half of the total drift typically occurred within the first 6 days of deployment.

We estimate the residual error in the final pressure records, after the "dedrifting" calculations, to be typically 0.02 dbar r.m.s. (or 0.06 dbar r.m.s.) if the first 6 days of the record are excluded (or included, respectively). This low drift-error opens many possibilities for studies that require knowledge of the low-frequency dynamic pressure signal in the deep ocean.

Part I on Methods contains a short review of bottom pressure measurement in the deep ocean, a description of the sensors that we used, a discussion of their performance and drift relative to type of construction and prior pressurization history ("preconditioning"), and estimates of the accuracy of the dedrifted pressure records.

In Part II of this report, the full data processing is described, including calibration parameters, corrections for the influence of temperature variations on the pressure sensor, and parameterization to remove sensor drift errors by least-squares regression onto an exponentially decaying time-dependence. Time series are plotted which illustrate several steps in the processing: the edited half-hourly pressure records, the detided pressures with drift-model curves superimposed, and the low-pass filtered, "dedrifted" pressure records (i.e., after subtracting the estimated drift curve).

TABLE OF CONTENTS

TABLE OF CONTENTS, CONTINUED

LIST OF TABLES

PART I

Part II

LIST OF FIGURES

PART I

PART II

LIST OF FIGURES, CONTINUED

PART I. METHODS

1. BOTTOM PRESSURE MEASUREMENT IN THE DEEP OCEAN

Physical oceanographers have long desired to have instrumentation capable of accurately monitoring the small variations in bottom pressures in the deep ocean (Baker, 1981) in order to observe the oceanic pressure field in analogy with the use of barometers by meteorologists. The measurement problem has been challenging because the dynamic pressure fluctuations are only ~0.10 to 0.01 dbar in an ambient pressure of 4000 dbar, requiring resolution and stability of ~1 ppm.

In the last fifteen years, deep-ocean bottom pressure measurements have been conducted in several studies on ocean tides (Filloux, 1971; Zetler et al., 1975), the ocean eddy pressure field (Brown et al., 1975), weather-induced bottom pressure fluctuations (Beardsley et al., 1977), and the performance of the pressure instruments themselves (Snodgrass et al., 1975). The most common pressure instruments used in the above studies have been strain gauges (Wunsch and Wimbush, 1977), Vibrotron sensors (Wimbush, 1977), metal Bourdon tubes (Filloux, 1971; Mofjeld and Wimbush, 1977), and quartz-crystal transducers (Snodgrass et al., 1975).

Although the requirement of adequate sensitivity and short-term stability is of great importance, the chief difficulty in dealing with pressure instruments is the instrumental noise of low frequency, i.e., drift, whose magnitude typically increases with applied pressure. Consequently, it has been most difficult to measure bottom pressures of the deep ocean. The drift contaminates the observed spectrum most at low frequencies. (A simple example is that a linear drift would add a red noise spectrum of slope f^{-2}.) Consequently, earlier studies with

deep pressure gauges have tended to focus on the higher frequency (less contaminated) aspects of the data.

In Part I, we present the experimental setting and measurements (Section 2), and we describe the pressure and temperature sensors (Section 3). We next discuss the observed pressure drifts in relation to sensor construction and to prior history of pressurization (Section 4). Next, we describe our techniques to model and remove the drift (Section 5), and finally we attempt to estimate the uncertainties in the drift removal, i.e., the accuracy of the final records (Section 6). All the time series plots of the data are shown in Part II.

2. EXPERIMENTAL SETTING AND MEASUREMENTS

2.1 Experiment Description and Overview

As part of the Gulf Stream Dynamics Experiment, data were collected using deep-ocean bottom pressure and temperature sensors in the Gulf Stream northeast of Cape Hatteras from September 1983 to May 1985. The measurements were made under the combined support of an NSF project entitled "The Dynamics of Gulf Stream Meanders" and an ONR project entitled "Observations on the Current Structure and Energetics of Gulf Stream Fluctuations Downstream of Cape Hatteras". Other data collected as part of this program are documented in separate reports (Tracey et al., 1985; Tracey and Watts, 1986b; Friedlander et al., 1986).

The deployment sites and the overall study area are shown in Figure 2.1. Inverted echo sounders were deployed at all the sites, whereas pressure sensors, along with temperature sensors, were deployed only at the sites indicated by the solid circles. The data records in this report are labelled by (a) the letters "PIES", indicating that a pressure sensor,

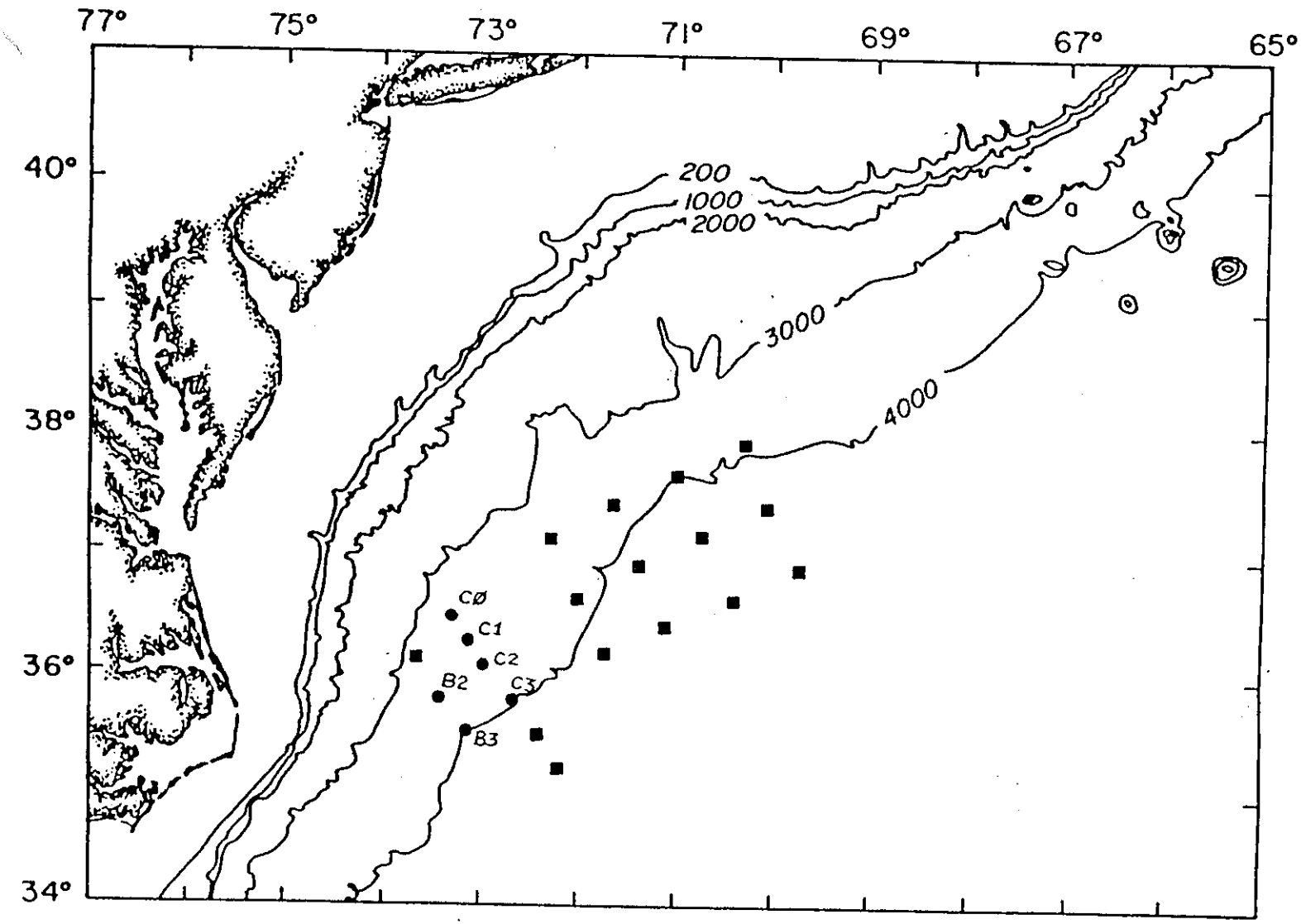

Figure 2.1 Study area and deployment sites. Inverted echo sounders were deployed at all 21 sites. Pressure sensors and temperature sensors were deployed at sites indicated by solid circles.

a temperature sensor, and an inverted echo sounder were deployed at the site, (b) the last two digits of the year (84 or 85) in which the instrument was recovered, (c) the site designation indicated in Figure 2.1, and (d) the letters "CM" between the line letter and the site number if a current meter mooring was also at the site. For example, PIES84BCM2 means the data record collected in 1984 at site B2 where a current meter mooring had also been deployed.

The time series plots of the raw, half-hourly bottom pressure and temperature measurements are given. Processing of the bottom pressure records included removal of the tides and, in particular, the long-term drift; these records are also shown. This report details the methods used to estimate and remove the drift, and to estimate the residual uncertainty. Subsequently, both the bottom pressure and temperature measurements were low-pass filtered, subsampled at six-hour intervals, and plotted. First order statistics (minimum, maximum, mean, and standard deviation) are listed for all data shown.

2.2 Data Recovery

In the 20-month period from September 1983 to May 1985, seven different pressure instruments (Table 2.1) were used for a total of eleven deployments at six sites (Table 2.2). These instruments were launched, recovered, and redeployed on five cruises aboard the R/V ENDEAVOR (EN106, 22-30 September 1983; EN107, 1-3 November 1983; EN118, 1-18 June 1984; EN124, 11-20 January 1985; EN130, 7-21 May 1985) and one cruise aboard the R/V OCEANUS (OC144, 9-19 January 1984).

In the eleven deployments of the deep-ocean pressure and temperature sensors, all instruments were recovered, giving an instrument recovery rate of 100%. Due to a malfunction of the electronic board controlling one pressure sensor, no pressure measurements were obtained for that

TABLE 2.1 Pressure sensors used

Sensor	Serial Number	Model	Working Range (dbar)	Type
1	8181	75K-002	0-3450	bellows
2	8180	75000	0-3450	bellows
3	17848	76KB-032	0-4100	Bourdon-tube
4	17849	76KB-032	0-4100	Bourdon-tube
5	17911	76KB-032	0-4100	Bourdon-tube
6	18426	76KB-032	0-4100	Bourdon-tube
7	19327	46K-032	0-4100	Bourdon-tube

TABLE 2.2 Deployment period (represented by the length of each rectangle) and pressure sensor used for each record.

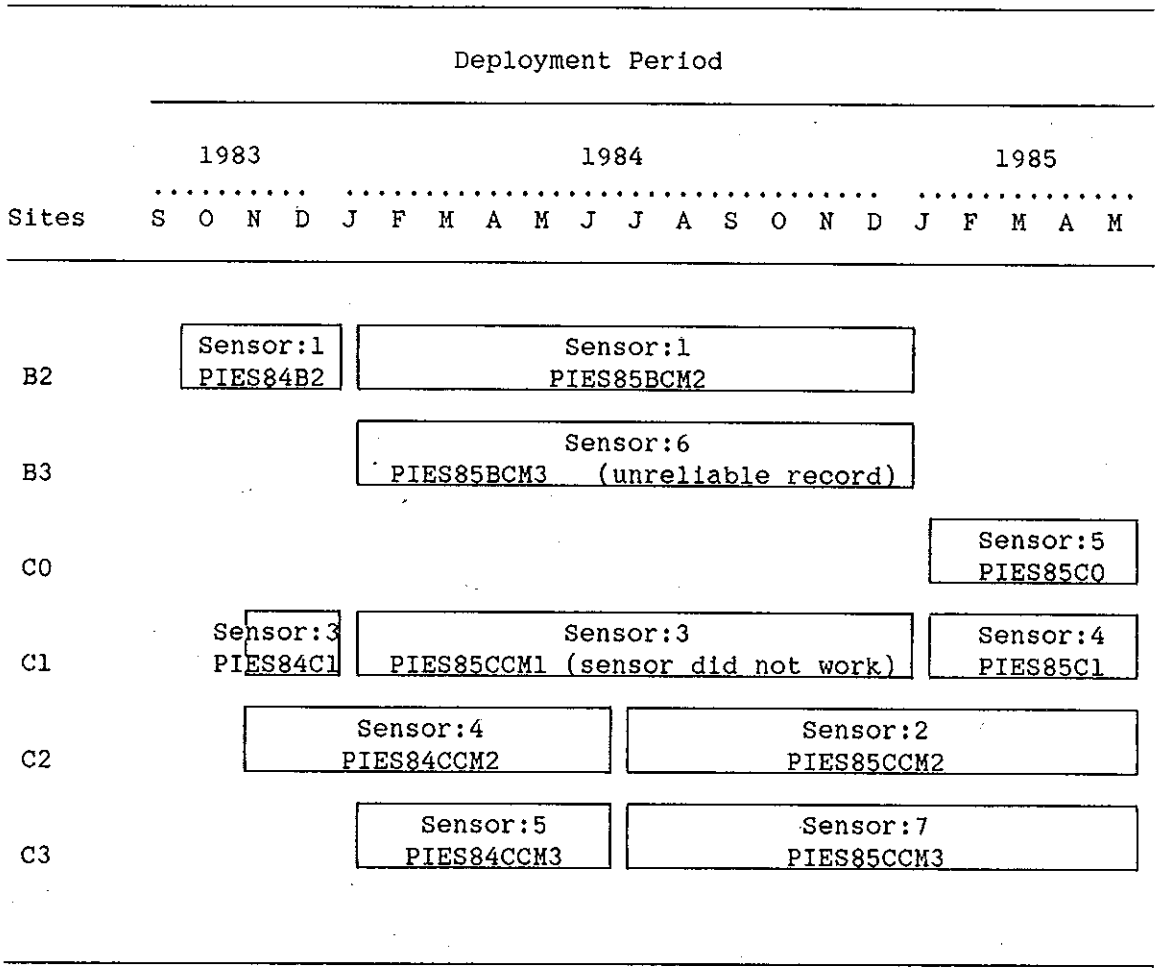

instrument during one deployment period (record PIES85CCM1). During the same deployment period, another pressure sensor malfunctioned; large steps (both positive and negative) were observed in the measured pressures (record PIES85BCM3). All nine remaining instruments performed successfully, giving an 82% data return for the pressure measurements. Complete records were obtained for all eleven deployments of the temperature sensors; thus the return rate was 100% for those data.

3. DESCRIPTION OF SENSORS

3.1 Pressure sensor and mounting

All the sensors we used have been manufactured by Paroscientific, Inc. A detailed description of the digital pressure transducers we used is given by Paros (1976) and by Wearn and Larson (1982). Briefly, the key sensing element in the pressure transducer is an oscillating, beam-shaped quartz crystal, which is piezoelectrically induced to vibrate in its lowest resonant flexural mode by an oscillator circuit. The oscillation frequency of the crystal varies with the stress load applied to it through a lever arm attached to either a bellows or Bourdon tube (Figure 3.1). The bellows or Bourdon tube is pressurized at the full ambient pressure of the ocean via a long, thin capillary tube filled with mineral oil. The measurement of fluid pressure is made by counting the output frequency of the oscillator circuit.

The pressure sensors were powered and controlled by Sea Data Corp. model XP35 electronics cards installed in inverted echo sounders (IESs). The IES circuitry and mooring configuration are described by Chaplin and Watts (1984). These instruments were tethered less than 1 m above the ocean floor, in order to have minimal vertical motion of the instrument in

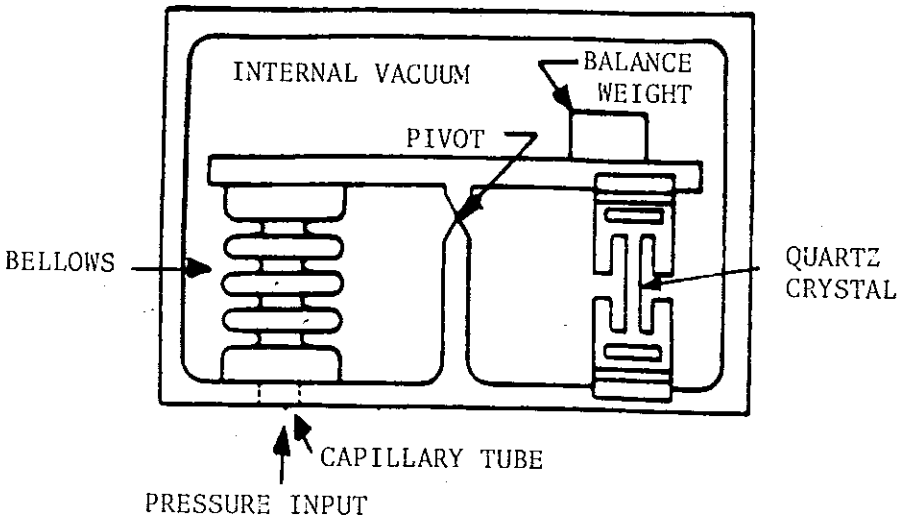

Figure 3.1 Schematic of the bellows-type Digiquartz pressure sensor (Paroscientific, Inc.). In the Bourdon-tube type of sensor, the bellows is replaced by a Bourdon tube. The sensor is connected to the environment through a small capillary tube filled with mineral oil.

response to bottom currents; we estimate less than 0.5 cm vertical excursion in the peak observed deep current speeds (~30 cm/s) in this area.

Another potential concern for bottom pressure measurements is the stability of the mounting on the sea floor. Most evidence indicates no tendency in these deployments for the anchors to sink into the mud or for the bottom to slump downslope: all but one of the observed pressure drifts discussed in the following section are toward lower (rather than higher) pressures. Moreover, the acoustic travel times (τ) measured simultaneously on these IESs show no indication of depth change, although only large or sudden depth changes would be likely to show up in the τ records.

3.2 Temperature sensor

Because temperature also affects the oscillation frequency of the quartz crystal in the pressure sensor, it is essential to independently measure the temperature of the crystal. A thermistor (Yellow Springs International Corp., model 44032) was placed as close as possible to each sensor.

The thermistor was powered and controlled by Sea Data Corp. model DC37 electronics cards installed in the IESs. This circuitry produces an output frequency that varies with the temperature-dependent resistance of the thermistor.

3.3 Time base and recording

The frequency-counting periods for the above measurements were controlled by a quartz-crystal clock in the IES; the circuitry is described by Chaplin and Watts (1984). The stability of the crystal (JAN Crystals, model HC33/U AT cut 4.194304 MHz) and timing circuitry used in these deployments was reported by the company to be 25 ppm/^{o}C and

20 ppm in the first year. However, these stability specifications are not as good as they need to be; the JAN crystals were mistakenly used as a less expensive replacement for an earlier, better crystal. The JAN crystals had all been baked at elevated temperatures and aged before deployment; however, clock-frequency drift could still be responsible for most of the observed drifts in the measured pressures. (After these deployments, we discovered our error and upgraded the time bases.)

All the data were recorded digitally on the IES data cassettes using a Sea Data model 610 recorder.

4. OBSERVED DRIFTS OF PRESSURE SENSORS

4.1 General description of performance

In many records a long-term drift is apparent when we remove the mean and the tides. Some characteristics of this drift are summarized in Table 4.1, and plots of the detided pressures are shown in Part II (Figures 11.1 to 11.10).

Several features are common to these records: 1) During the first few hours ($\lesssim$12 h) there is a rapid slewing toward higher pressure readings as the sensors come to thermal equilibrium at the ocean bottom. 2) During the next 3 to 12 months of deployment, several (five of the ten) pressure records drift by several tenths of a decibar, with the rate of drift decreasing greatly with increasing time. 3) Superimposed on the drift is the "ocean pressure signal", with obvious 5- to 30-day periodicities and 0.1- to 0.2-dbar pressure changes; these are the dynamic pressure signals of central scientific interest that we wish to study uncontaminated by drift. 4) There is high-frequency variability of roughly $\pm$0.02 dbar,

TABLE 4.1 Drift characteristics for each deployment.

	Sensor			Preconditioning		Deployment			Drift	
Record	Number	Type	Serial Number	Duration (months)	Pressure (dbar)	Dates	Duration (months)	Pressure (dbar)	Initial 6 days (dbar)	Entire record (dbar)
PIES84B2	1	bellows	8181	24	3200	Oct 83 - Jan 84	3	3625	-0.15	-0.21
PIES85BCM2	1	bellows	8181	3	3625	Jan 84 - Jan 85	12	3645	-0.17	-0.37
PIES85CCM2	2	bellows	8180	4	3900	Jun 84 - May 85	11	3730	+0.15	+0.48
PIES84C1	3	Bourdon-tube	17848	3	1400	Nov 83 - Jan 84	2	3514		none
PIES85CCM1	3	Bourdon-tube	17848	2	3514	Jan 84 - Jan 85	12	*	*	*
PIES84CCM2	4	Bourdon-tube	17849	-	-	Nov 83 - Jun 84	8	3730	0.12	-0.45
PIES85C1	4	Bourdon-tube	17849	-	-	Jan 85 - May 85	5	3530		none
PIES84CCM3	5	Bourdon-tube	17911	-	-	Jan 84 - Jun 84	6	3990		none
PIES85C0	5	Bourdon-tube	17911	-	-	Jan 85 - May 85	5	3340		none
PIES85BCM3	6	Bourdon-tube	18426	-	-	Jan 84 - Jan 85	12	†	†	†
PIES85CCM3	7	Bourdon-tube	19327	-	-	Jun 84 - May 85	11	3990	-0.08	-0.21

* Electronics failed.
† Record jumpy and unusable.

which exceeds measurement noise or our estimates of instrument depth variation.

Table 4.1 also summarizes the drift characteristics found for all the deployments; for simplicity, only the total change during the first 6 days and the total change from start to end of the record are listed. Several other factors are also listed that could be expected to influence the amount of drift. These include the ambient pressure (fairly similar at 3340 to 3990 dbar for all these deployments), the sensor construction (bellows vs. Bourdon tube), and whether the sensor was "preconditioned" to high pressure for some period before deployment. The following subsections discuss the amount of drift in relation to these factors, although we must caution that we have very few replicate cases for comparison.

4.2 Bellows vs. Bourdon-tube construction

We first categorize the drift performance by bellows vs. Bourdon-tube construction (Table 4.1). There were two bellows sensors with three deployment records, all of which showed significant drift (~0.20 to 0.50 dbar). Five Bourdon-tube sensors used in eight deployments produced seven records; in the second deployment of sensor 3 (record PIES85CCM1), the electronics did not work. In four of the seven recovered records, there was no detectable drift, but in the other three records, the sensors unfortunately performed unpredictably: One sensor (4; record PIES84CCM2) had one of the worst drifts of all (0.45 dbar) in its first deployment but none in its next (record PIES85C1). (This sensor was used in two different IESs. Clock-frequency drift could be responsible for this difference.) Another sensor (7; record PIES85CCM3) had ~0.20 dbar drift. A third sensor (6; record PIES85BCM3) recorded numerous discontinuous jumps (~0.20 dbar) of varying size and sign (again, possibly

attributable to the time base crystal), as shown in Figure 11.3. Only one Bourdon-tube sensor (5) did not drift in both of its deployments.

4.3 Effect of prior pressurization ("preconditioning")

Secondly, we categorize performance according to whether the sensors were "preconditioned" at high pressure. Both bellows sensors were preconditioned. One bellows sensor (1), which was pressurized at 3200 dbar for 24 months prior to its deployment (at 3625 dbar), drifted only about half as much as the other bellows sensor (2). That sensor was pressurized at 3900 dbar for 4 months prior to deployment (at 3730 dbar) and drifted with opposite sign. (This is surprising, because Wearn and Larson (1982) suggest that all internally pressurized bellows sensors ought to drift in the same direction.) The opposite direction of drift may possibly be explained by the fact that the preconditioning was at a slightly higher pressure than that of the deployment.

The only Bourdon-tube sensor (3) that was preconditioned showed no drift, but other Bourdon-tube sensors had no drift without preconditioning.

5. METHOD OF DRIFT ESTIMATION AND REMOVAL

5.1 Introduction to drift modeling

Historically, investigators have modeled the drift of various pressure sensors by either a power-law [$\sim(t - t_0)^{\beta}$, $0<\beta<1$], logarithmic ["log-law", $\sim\ln(t - t_0)$] or exponential {$\sim\exp[-\alpha(t - t_0)]$} dependence on time, t, after initial pressurization at $t = t_0$. Although the exact cause of the drift is unknown, it is believed to result from mechanical creep of materials subjected to high stress. The above three

dependencies have been used to describe creep in laboratory and geophysical studies, as has been reviewed by Wunsch and Wimbush (1977) and Wearn and Larson (1982).

It had been hoped and asserted (Wearn and Larson, 1980) that by careful measurement of drift characteristics of a sensor in the laboratory, the drift curve for it in an open ocean deployment might be accurately predicted. Skepticism has probably always been appropriate about applying such predictions, because the drift processes may not be reversible or reproducible. Moreover, for the deep-ocean pressure sensors it has not yet been practical to monitor the drift in the lab at the required ~1-ppm accuracy for long time periods. In one of the best attempts (Wearn and Larson, 1980), the required level of absolute pressure and temperature stability was not achieved even by their high-quality calibration instruments.

In these deployments, the approach to drift removal has been to make least-squares fits of the above mathematical models to the records themselves. We used the non-linear least-squares regression routine, P3R, in the BMDP-79 package of computer programs (Dixon and Brown, 1979). Since the records are long compared to the time scales of the deep-ocean pressure variability, the "ocean pressure signal" will tend to average out in estimating the drift. We tried fitting our data to all three of the above drift dependencies and to an exponential-linear dependency; the results are compared in this section. The accuracy of the best-fit drift-curve models is discussed in Section 6.

5.2 Log-law vs. power-law least-squares fit

We first made a comparison between the power-law and the log-law types of drift, described by the following formulas, respectively:

$$P_{drift} = P_1 (t - t_0)^{P_2} + P_3$$

and

$$P_{drift} = P_1 \ln(t - t_0) + P_2$$

where t is the time in hours, t_0 is the time when the drift starts (13 hours before the first data point used, as explained in Section 8.3 in Part II), and P_1, P_2, and P_3 are free parameters whose values are individually determined for each record by the nonlinear regression subroutine.

The residual deviations of the measurements from the fitted curves are essentially the same for both laws and are shown in Table 5.1. The two types of curves, when plotted, are virtually indistinguishable within the measurement interval. The log law is preferred because of its computational simplicity and its rapid convergence to unique parameters. (By contrast, the regression for the power law converges slowly and the final parameters are affected by the starting values in the iteration process.) Values of P_1 and P_2 for the logarithmic drift curve model are listed in Table 5.2, with the r.m.s. deviations repeated for each record.

The logarithmic curves superimposed on our drift data are shown in the left-hand column of Figure 5.1. The fitted log-curves lie within the scatter of the data and approximate the existing drift remarkably well. However, in the first part (~30 days) of the records PIES84CCM2 and PIES85BCM2, the predicted drift rates are probably unreal (overestimated for PIES84CCM2 and underestimated for PIES85BCM2).

TABLE 5.1 The r.m.s. deviations of drift curves from the detided pressures. The r.m.s. $\Delta P_i = [\Sigma(\Delta P_i)^2 N^{-1}]^{1/2}$, where ΔP_i is the difference between P_{drift} and the detided pressure. The summation extends over all N points of the time series. The r.m.s. ΔP_i represents the r.m.s. ocean pressure signal. Time is in hours; t_0 is the time when the drift starts.

Power law: $P_{drift} = P_1 (t - t_0)^{P_2} + P_3$

Logarithmic law: $P_{drift} = P_1 \ln(t - t_0) + P_2$

Exponential law: $P_{drift} = P_1 [1 - \exp(P_2 t)] + P_3$

Exponential-linear law: $P_{drift} = P_1 [1 - \exp(P_2 t)] + P_3 + P_4 t$

		r.m.s. ΔP_i (dbar)			
Record	Sensor	Power Law	Logarithmic Law	Exponential Law	Exponential-Linear Law
PIES84B2	1	0.0372	0.0428	0.0372	0.0370
PIES85BCM2	1	0.0491	0.0474	0.0368	0.0368
PIES85CCM2	2	0.0361	0.0363	0.0421	0.0349
PIES84CCM2	4	0.0543	0.0542	0.0448	0.0449
PIES85CCM3	7	0.0412	0.0416	0.0370	0.0370

TABLE 5.2 Drift parameters for log-law least-squares fit:

$$P_{drift} = P_1 \ln [(t - t_0)] + P_2$$

or, in the case of no drift, P_{drift} is zero.

Parameters as in Table 5.1.

Record	Sensor	P_1 (dbar)	P_2 (dbar)	r.m.s. ΔP_i (dbar)
PIES84B2	1	-0.037278	0.231444	0.043
PIES85BCM2	1	-0.048840	0.394873	0.047
PIES85CCM2	2	0.088609	-0.709164	0.036
PIES84C1	3	--	--	0.041
PIES84CCM2	4	-0.112501	0.852820	0.054
PIES85C1	4	--	--	0.030
PIES84CCM3	5	--	--	0.053
PIES85C0	5	--	--	0.042
PIES85CCM3	7	-0.035110	0.281740	0.042

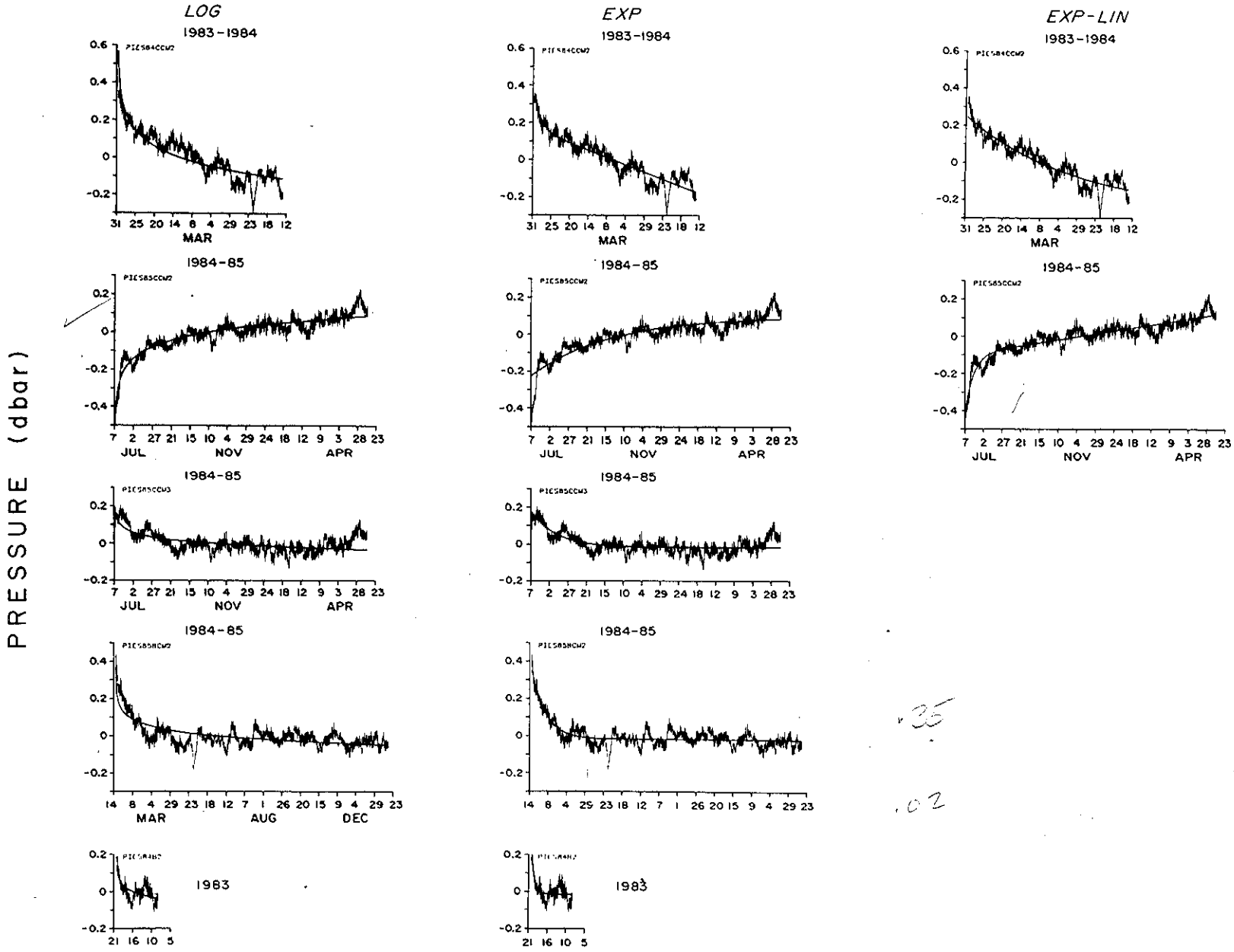

Figure 5.1 Plots of pressure drift vs. time with log-law, exponential, and exponential-linear curves superimposed.

5.3 Exponential and exponential-linear vs. log-law least-squares fit

We next made least-squares fits of exponential and exponential-linear curves to our data. The mathematical formulas we used were:

$$P_{drift} = P_1 [1 - \exp(P_2 t)] + P_3$$

for the exponential curve and

$$P_{drift} = P_1 [1 - \exp(P_2 t)] + P_3 + P_4 t$$

for the exponential-linear curve. Here P_1, P_2, P_3, and P_4 are again free parameters determined by the non-linear regression subroutine and t is time in hours, relative to 13 hours before the first data point used (as explained in Section 8.3 of Part II). (N.B.: Both models could use any other chosen start time, t_0, since any time shift, $t - t_0$, could be adjusted by corresponding changes in P_1 and P_3.)

The above models converge rapidly and the parameters are independent of initial values in the iteration process. Values of P_1, P_2, P_3 and P_4 for the exponential and exponential-linear drift curve models are listed in Table 5.3, with r.m.s. deviations repeated for each record. The predicted exponential and exponential-linear drift curves have in general smaller r.m.s. deviations from the original data than the logarithmic curves (Table 5.1). This was expected since they have more free parameters (four). However, curves for all the laws have similar shapes, and the r.m.s. residual is mainly from the oscillatory "ocean pressure signal". Plots of exponential and exponential-linear curves superimposed on the drift data are shown in the center and right-hand columns of Figure 5.1, respectively.

The regression subroutine detects no linear trends in records PIES85BCM2, PIES84B2 and PIES85CCM3. It gives $P_4 = 0$ and converges to the same values for P_1, P_2, and P_3 with the purely exponential type of drift. For these three records the exponential curves seem very satisfactory in

TABLE 5.3 Drift parameters for exponential $\{P_{drift} = P_1 [1 - \exp(P_2 t)] + P_3\}$ and exponential-linear $\{P_{drift} = P_1 [1 - \exp(P_2 t)] + P_3 + P_4 t\}$ least-squares fits. Parameters as in Table 5.1.

Record	Sensor	Drift law	P_1 (dbar)	P_2 (h^{-1})	P_3 (dbar)	P_4 (dbar/h)	r.m.s. ΔP_i (dbar)
PIES84B2	1	exp.	-0.226419	-0.0110545	0.210320	--	0.037
PIES85BCM2	1	exp.	-0.369187	-0.0022225	0.350771	--	0.037
PIES85CCM2	2	exp.-lin.	0.296492	-0.0036410	-0.395883	0.000027	0.034
PIES84C1	3	-	--	--	--	--	0.040
PIES84CCM2	4	exp.	-0.511474	-0.0002825	0.244648	--	0.045
PIES85C1	4	-	--	--	--	--	0.030
PIES84CCM3	5	-	--	--	--	--	0.052
PIES85C0	5	-	--	--	--	--	0.041
PIES85CCM3	7	exp.	-0.193927	-0.0012165	0.174750	--	0.037

tracking the drift and were preferred over the logarithmic ones. In records PIES84CCM2 and PIES85CCM2 we observe a probable tendency for the exponential law to underestimate the drift rates at the beginning of the records and for the exponential-linear law to overestimate the drift rates at the end of the records. In the case of PIES84CCM2 we preferred the exponential curve: with its fewer parameters, the r.m.s. deviation was the best; we chose to accept the risk of retaining a small additional drift error in the first ~10 days of the record. In the case of PIES85CCM2 we preferred the exponential-linear curve; the r.m.s. deviation was significantly smaller with this law and we chose to accept the risk of introducing a linear drift trend of unknown origin (perhaps due to the JAN crystals).

5.4 The final ("residual") pressure records

The "residual" pressure records (detided and dedrifted), which are our best estimate of the true deep-ocean pressure signal, were calculated by subtracting the fitted P_{drift} curve, represented by the fit described above (Table 5.3), from its respective detided set of measurements at each half-hourly data point.

A low-pass filtered version of the pressure records is given in Figures 12.4 to 12.6 of Part II. All coincident records are plotted on the same time axes and with consistent pressure scales. (January-May 1984 is plotted twice to show the coincidence with earlier and later deployment periods.) Visually, the coherence between pressure records at neighboring sites is quite high. We have identified some of the major pressure-events with the passage of Gulf Stream rings offshore and their coalescence into the Gulf Stream (Bane and Watts, 1985).

6. ESTIMATED ACCURACY OF FINAL PRESSURE RECORDS

6.1 General remarks

The final record described in the previous section is a pressure record from which a drift curve has been subtracted; the best estimated drift curve is the exponential or exponential-linear least-squares fit whose parameters are listed in Table 5.3. We now attempt to estimate the uncertainty in the drift-removal procedure or, equivalently, to estimate the long-term accuracy of the dedrifted records. (N.B.: This is a separate question from that of the absolute accuracy of the mean pressure, which is about ±1.5 dbar. The absolute accuracy has not been important thus far, because the absolute depth of the instrument site relative to the geoid is not known either.)

It is difficult to estimate the accuracy of the drift curves for these records. Each has a mixture of two unknown signals that differ for each site: the ocean pressure signal plus the drift. Some records are from different time periods, and others coincide in time but are from different sites (~15 to 50 km apart) with coherent, but different ocean pressure signals. We have no independent way to determine either the ocean pressure signal or the drift signal exactly, but the methods we have used to separate them essentially assume that they have different spectral characteristics.

Since the rate of drift decreases greatly with increasing time, another distinction is that the longer duration records (especially their later months) have a smaller proportion of their total variance associated with drift errors. Hence, they become more dominated by the ocean pressure signal.

6.2 Two methods to estimate uncertainties

We take advantage of these differences to estimate the errors in two ways. In the first method, we use records from two sites at which an instrument that had been deployed for several months was recovered and replaced almost immediately with another instrument at the same site. Figure 12.5 in Part II shows these cases (records PIES84CCM2 and PIES85CCM2 at site C2; records PIES84CCM3 and PIES85CCM3 at site C3), with the recovery and redeployment time in June 1984. The drift-removal error at the end of one record is probably small compared to that at the beginning of the subsequent record, since it seems reasonable to expect that the magnitude of error is roughly proportional to the amount of drift being removed. Hence, any pressure "jump" occurring between the records gives an estimate of the size of drift-removal error that characterizes the beginning of a record. The "jump" magnitudes are about 0.02 dbar at site C2 and 0.06 dbar at site C3 (also listed in Table 6.1A).

The second method to estimate the error was to regress the law selected for dedrifting on segments of the records. These segments have the same (true) drift curve, but our estimate of it will differ for different segments due to the contribution of the ocean pressure signal. An inferrence of how much the ocean pressure signal "contaminates" or causes the regressed drift curve to differ from the true drift can be taken from the difference between the regressed drift curves obtained from different segments of the record.

We used the second method only on the four longest records (7 to 12 months), because it was felt that dividing the records into segments shorter than 3 months was inadvisable, given the obviously energetic ocean pressure signals at shorter periodicities. Each of the four records was divided into two segments at a point which had a pressure near the overall

TABLE 6.1 Pressure offsets between drift curves estimated on different, sequential records (6.1A) and on segments of the same record (6.1B); estimated accuracy of final, "dedrifted" pressure records. The detection threshold (due to "noise" of the ocean pressure signal) of the exponential and exponential-linear least-squares fit is < 0.01 dbar in 1 year. $\Delta P = \Delta P_b - \Delta P_a$.

t_a: Length of first segment or record
t_b: Length of second segment or record
ΔP: Pressure offset between drift curves of two segments at join-point or of two full records
ΔP_a: Pressure offset between drift curve of first segment and drift curve of the full record at the end of first segment
ΔP_b: Pressure offset between drift curve of second segment and drift curve of the full record at the beginning of second segment

6.1A Pressure offsets between different, sequential records

Records	t_a (months)	t_b (months)	ΔP (dbar)
PIES84CCM2 and PIES85CCM2	8	11	0.02
PIES84CCM3 and PIES85CCM3	6	11	0.06

6.1B Pressure offsets between segments of the same record

Record	t_a (months)	t_b (months)	ΔP (dbar)	ΔP_a (dbar)	ΔP_b (dbar)
PIES85BCM2	4.4	8	-0.015	0.013	-0.002
PIES85BCM2	7.4	5	0.000	0.001	0.001
PIES84CCM2	3	4.3	-0.016	-0.052	-0.036
PIES84CCM2	4.6	2.6	0.042	-0.020	0.022
PIES85CCM2	2.6	8.6	-0.007	-0.004	-0.011
PIES85CCM2	5.6	5.6	0.037	-0.028	0.009
PIES85CCM2	8.3	2.9	0.053	-0.004	0.049
PIES85CCM3	2.6	8.6	0.003	0.014	0.017
PIES85CCM3	5.6	5.6	-0.006	0.006	0.000
r.m.s. ΔP for segments:			0.027	0.021	0.022
r.m.s. ΔP for full 12-month record*:			0.019	0.015	0.016

* Obtained by dividing by $(2)^{1/2}$, because the degrees of freedom are doubled.

drift curve, to avoid introducing new "end effects". A curve was fitted to model the drift for each segment. Then we computed the offsets between these fitted curves at the point where one joins or overlaps another. At the same point, we also computed the differences between the curves fitted on the segments and the curve originally fitted on the whole record. The results of these calculations are summarized in Table 6.1B. The magnitudes of the offsets range from 0.000 to 0.053 dbar, with a r.m.s. offset of 0.023 dbar.

6.3 Discussion of drift uncertainty estimates

We now argue that the offsets between the above exponential-law regressions on segments of each given record are probably overestimates of the uncertainty of the drift regression on the full record. Two reasons support this contention: (1) The offsets occur at the beginning of each segment, where the regressed curve has its maximum amplitude and probably maximum error. However, in the regression curve for the full record, the corresponding time is not at the beginning, but farther out in the tail of the true drift curve, where the drift rate is slower and the error should be smaller. (2) The full-record regression curve is 2 or 4 times as long as the independent segments, with consequently greater degrees of freedom and more confidence in "averaging out" the ocean pressure signal; invoking a "central-limit theorem" that the ocean signal ought to be normally distributed given sufficient degrees of freedom, would suggest that doubling (or quadrupling) a record length would improve the removal of ocean pressure signal from the drift by a factor of $2^{1/2}$ (or 2, respectively). These arguments are applied in the footnote to Table 6.1B.

7. SUMMARY OF PART I

Ten records from seven Digiquartz deep-ocean bottom pressure sensors (Paroscientific, Inc.) have been obtained in eleven deployments of 3 to 12 months between September 1983 and May 1985. The deployments were under the Gulf Stream northeast of Cape Hatteras in depths of 3300 to 3900 m, as part of the Gulf Stream Dynamics Experiment. Two of the pressure sensors had bellows; five had Bourdon tubes. The records were examined with particular attention to estimating and removing any observed drift in calibration. (For this set of deployments, much of the drift may unfortunately be due to drift of the control crystals for the time base. Using better clock crystals in future deployments should result in less drift.)

All three records from the two bellows-type sensors exhibited significant drift. (Surprisingly, one sensor drifted in the opposite sense of the other sensor.)

Seven records were obtained with the five Bourdon-tube sensors. Two of these sensors were deployed twice; of these four records, three records had no detectable drift and one record (a first deployment) had a large drift. Three sensors were deployed once; of these three records, one had no detectable drift, one had significant drift, and one was jumpy and unreliable.

The drift was removed from five pressure records as follows: Least-squares fits of the power-law, logarithmic, exponential, and exponential-linear dependencies on time were made to each detided pressure record. The best-fit drift curve was subtracted from the record at each data point, yielding the "residual" pressure record. For four records,

the exponential drift curve had the best fit; for one record, the exponential-linear drift curve had the best fit.

We estimate that the errors in our drift-removal procedure are as much as 0.06 dbar (range ±0.02 to ±0.06 dbar; Table 6.1A) if the entire record is considered. However, the pressure error is estimated to be about 0.02 dbar r.m.s. (range ±0.01 to ±0.05 dbar; Table 6.1B) if the first week of a record is not included.

The residual uncertainties in the final "dedrifted" pressure records are small compared to the r.m.s. ocean pressure signal observed, and will tend to contaminate only the relatively long periodicities ($\geq$60 to 90 d) in these records. This opens many possibilities for studies requiring knowledge of the deep-ocean dynamic pressures. Moreover, bottom pressure gauges in combination with inverted echo sounders can provide highly accurate definition of variations in the sea-surface height.

PART II. DATA

8. DATA PROCESSING

8.1 Program Flow Chart and Description

The data processing for all the IES, pressure, and temperature records was done on a PRIME 750 computer, using FORTRAN 77 with some extensions for bit manipulation. The basic procedural steps on the pressure data are illustrated by the flow chart in Figure 8.1 and are accomplished by a series of routines developed specifically for the IES (Tracey and Watts, 1987). The raw data are recorded within the IES on Sea Data model 610 recorders. The cassette tape contains the counts associated with sequential record number, acoustic travel time, pressure, and temperature measurements as a series of integer words of varying lengths. The subsequent processing steps are outlined below.

CARP: Transfers the data from cassettes to 9-track magnetic tape for subsequent processing.

BUNS: Converts the series of integer words of varying lengths into standard length 32-bit integer words.

MEMOD: Establishes the time base from the sequence number. Converts all travel time, pressure and temperature counts into scientific units of seconds, decibars, and degrees Celsius, respectively.

FILL: Checks for proper increment of the time base. Missing data points are filled by inserting interpolated values.

DESPIKE: Identifies and replaces travel time, pressure and temperature spikes with interpolated values.

RESPO: Determines the mean and the tidal constituents by using tidal response analysis (Munk and Cartwright, 1977). The mean and

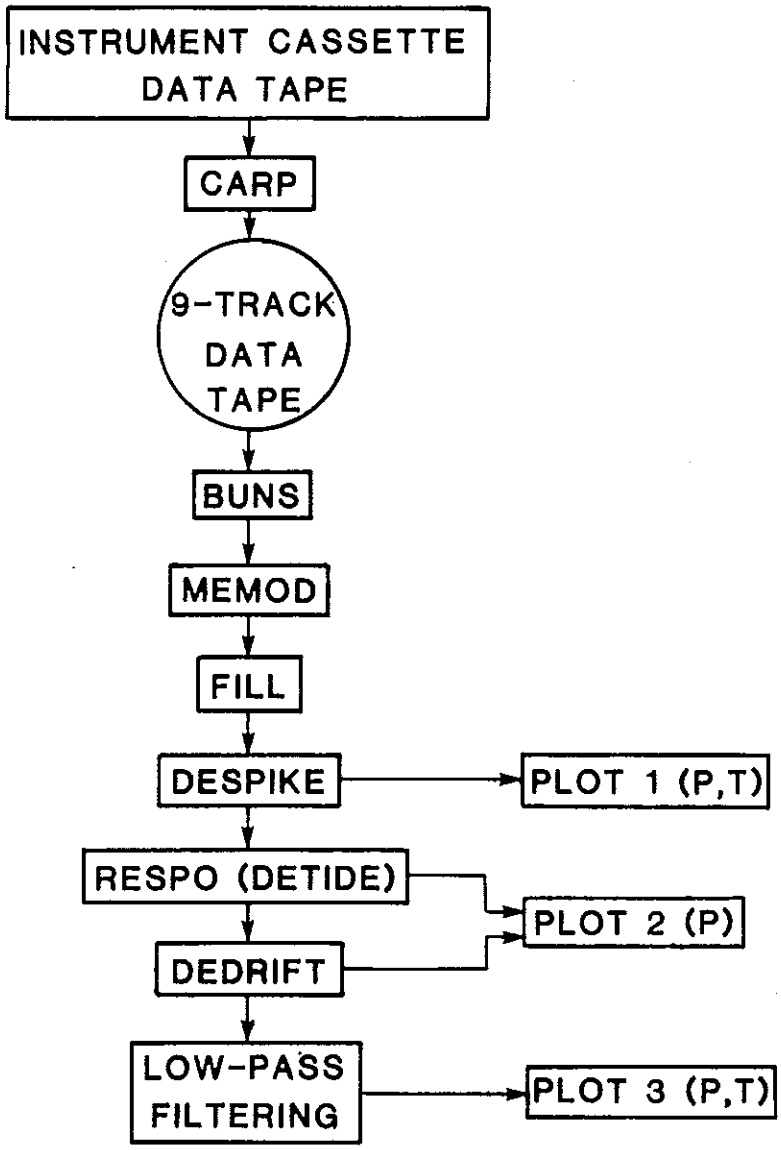

Figure 8.1 Pressure data processing flowchart

the calculated tides are then removed from the pressure values.

DEDRIFT: Identifies and removes the long-term drift of the detided pressures. The drift is tracked through the non-linear regression subroutine P3R of BMDP-79, a package of computer programs developed at UCLA (Dixon and Brown, 1979).

LOW-PASS FILTERING: Convolves the residual (detided and dedrifted) pressures with a 40-hour low-pass Lanczos filter. The FESTSA time series analysis package (Brooks, 1976), modified for the PRIME 750, was used to remove the higher frequency (tidal and inertial) motions from those with periods of several days or longer. The symmetric filter, with a Lanczos taper, was designed with the half power (-6 db) at 0.025 cph and -60 db attenuation at tidal frequencies (0.0833 cph). The smoothed output time series ("40HRLP") for pressure and temperature were subsampled at six-hour intervals.

8.2 Conversion to Scientific Units

Both the temperatures (T) and the pressures (P) are determined by counting frequencies that vary in accord with individually calibrated relationships for T and P. These are described below and the individual parameters for each instrument are given in the tables in Section 9.

8.2.1 Temperature

The T measurement is independent of P; that is, the thermistor does not vary with pressure. Thus, only the temperature-dependent resistance, R(T), of the thermistor controls a variable-frequency oscillator on the DC37 electronics card (Sea Data Corp.). This circuitry is designed such that it linearizes the output frequency, f_T, as a function of T within the range $0^{\circ}C$ to $25^{\circ}C$. (This linearization is

set for a standard R(T) curve for this model YSI thermistor and is supposed to be accurate to 0.1°C.) The frequency, f_T, is counted for a measurement interval, Z, and divided by a scale factor, S (= 1 in this case), to fit into a 16-bit integer word prior to recording on the cassette tape. Therefore, the recorded count is $N_T = Zf_T/S$. From N_T one can find T (°C), which is the true average temperature over the sampling interval, Z. For these deployments, the sampling interval was 30 min (1800 s).

The conversion from counts to temperature is

$$(N_T - N_a)/(N_b - N_a) = (T - T_a)/(T_b - T_a) ,$$

where the constants (N_a,N_b) and (T_a,T_b), listed in Table 8.1 for each sensor, are determined from laboratory calibrations. The accuracy of the temperature measurements is about 0.1°C and the resolution is 0.0002°C. The half-hourly temperature records are shown in Section 10 (Figures 10.1-10). The temperatures were low-pass filtered and are shown in Section 12 (Figures 12.1-3).

8.2.2 Pressure

The pressure sensor, suited for deep-ocean applications, has an output frequency, f_p, that not only depends strongly on P, but also depends significantly on T. The full-range change in frequency is typically from 36 to 40 kHz, depending on the applied pressure and type of construction. It is common practice to deal with the period, $\tau = 1/f_p$, rather than the frequency; the period ranges from 25 to 28 μsec. Accompanying each sensor, we purchased individual calibrations from Paroscientific, Inc. along with polynomial expressions to determine $P(\tau,T)$.

An XP35 electronics card (Sea Data Corp.) counts the pressure sensor oscillations for the measurement interval, Z, and divides the

TABLE 8.1 Constants T_a, N_a, T_b, and N_b used for conversion of temperature counts, N_T, to temperature in ^{o}C.

Record	Sensor	T_a (^{o}C)	N_a	T_b (^{o}C)	N_b
PIES84B2	1	1	4554	10	46260
PIES85BCM2	1	1	4554	10	46260
PIES85CCM2	2	1	4518	10	46080
PIES84C1	3	1	4518	10	45900
PIES85CCM1	3	1	4518	10	45900
PIES84CCM2	4	1	4428	10	45720
PIES85C1	4	0	0	12.5	57600
PIES84CCM3	5	0	0	12.5	57600
PIES85C0*	5	0	0	12.5	57600
PIES85BCM3	6	0	0	12.5	57600
PIES85CCM3	7	1	4428	10	46080

* Note added in proofreading: For record PIES85C0, the constants listed in this table were used in processing the data; however, a more accurate set of constants (T_a = 1, N_a = 4428, T_b = 10, and N_b = 45720) would give temperatures 0.045^{o}C warmer with the same range of temperatures observed (near 2.4^{o}C). This offset is smaller than the uncertainty in the thermistor calibration and has been ignored in subsequent processing. The effect of this warmer temperature would shift the absolute pressure calculations 0.008 dbar lower, which is also insignificant.

counts by the scale factor, S, to fit into a 24-bit integer word for recording on the cassette tape. The sampling interval was 30 min (1800 s) and the scale factor was 4 for these deployments. Therefore, the recorded count is $N_P = Zf_P/S = 450/\tau$.

The polynomial relationships $P(\tau,T)$ from Paroscientific, Inc. are listed in Table 8.2 for each sensor. τ_0 is the vibrational period at zero applied pressure, with polynomial temperature dependence. The older sensors come with "A,B,τ_0" coefficients, each of which has its own polynomial equation in temperature, T (^oF). The newer sensors preferably have "C,D,τ_0" coefficients, again each with a polynomial T dependence (again in ^oF, except sensor 7, which is in ^oC).

The half-hourly measured pressure records are shown in Figures 10.11 to 10.20. The absolute accuracy of the long-term average pressure measurements is within 1.5 dbar, but the resolution is much better. The pressure change corresponding to a change in N_P of one count, under typical conditions of applied pressures (~3500 dbar) and deep temperatures (~2^oC), ranges from 0.0010 to 0.0025 dbar for these deployments with a measurement interval of Z = 1800 s. The stability of these pressures is discussed in Section 8.3.

8.2.3 Time Base

The date and time were assigned to each sampling period. The tables in Section 9 report the hour, minutes, and seconds associated with the first and last sampling period as a six-digit number. All times are given as Greenwich Mean Time (GMT). For processing convenience, the times were converted into yearhours. Table 8.3 lists the yearhour that corresponds to 0000 GMT of each day for non-leap years. (For leap years, the yearhours can be determined by adding 24 to each day after February 28.) There are a total of 8760 hours in a

TABLE 8.2 Pressure sensor calibration equations, $P(\tau,T)$, to convert sensor oscillation period, τ (s), into pressure, P (psi), with functional dependence on temperature, T (either °F or °C), and on the output period at zero pressure, τ_0 (s).

Set 1: (for sensors 1 and 2)

$$P = A(1- \tau_0/\tau) - B(1- \tau_0/\tau)^2$$

$$A = A_0 + A_1 T + A_2 T^2$$
$$B = B_0 + B_1 T + B_2 T^2$$
$$\tau_0 = \tau_{00} + \tau_1 T + \tau_2 T^2 ,$$

$$\tau = 450/N_P$$

T : (°F) (Fahrenheit)

Sensor: 1. Serial #: 8181

A_0: $5.18004 \cdot 10^{4}$
A_1: $-9.70308 \cdot 10^{-1}$
A_2: $1.71739 \cdot 10^{-3}$

B_0: $3.17505 \cdot 10^{4}$
B_1: $-7.80773 \cdot 10^{-1}$
B_2: $1.04970 \cdot 10^{-2}$

τ_{00}: $25.97996 \cdot 10^{-6}$
τ_1: $-1.99543 \cdot 10^{-11}$
τ_2: $1.70393 \cdot 10^{-13}$

Sensor: 2. Serial #: 8180

A_0: $4.87536 \cdot 10^{4}$
A_1: $-9.17509 \cdot 10^{-2}$
A_2: $-5.94345 \cdot 10^{-4}$

B_0: $2.81395 \cdot 10^{4}$
B_1: 8.01378
B_2: $-9.13550 \cdot 10^{-3}$

τ_{00}: $25.95124 \cdot 10^{-6}$
τ_1: $-6.38494 \cdot 10^{-11}$
τ_2: $2.28777 \cdot 10^{-13}$

Set 2: (for sensors 3, 4, 5, 6)

$$P = C[(1-(\tau_0/\tau)^2) - D(1-(\tau_0/\tau)^2)^2]$$

$$C = C_0 + C_1 T + C_2 T^2$$
$$D = D_0 + D_1 T + D_2 T^2$$
$$\tau_0 = \tau_{00} + \tau_1 T + \tau_2 T^2 ,$$

$$\tau = 450/N_P$$

T : (°F) (Fahrenheit)

Sensor: 3. Serial #: 17848

C_0: $-2.95074 \cdot 10^{4}$
C_1: $-1.40724 \cdot 10^{-1}$
C_2: $6.61457 \cdot 10^{-4}$

D_0: $5.00619 \cdot 10^{-2}$
D_1: $4.19904 \cdot 10^{-5}$
D_2: $-1.20873 \cdot 10^{-7}$

τ_{00}: $28.05943 \cdot 10^{-6}$
τ_1: $-1.72125 \cdot 10^{-10}$
τ_2: $6.73124 \cdot 10^{-13}$

Sensor: 4. Serial #: 17849

C_0: $-2.48035 \cdot 10^{4}$
C_1: $5.17487 \cdot 10^{-1}$
C_2: $-4.92268 \cdot 10^{-4}$

D_0: $4.55063 \cdot 10^{-2}$
D_1: $1.06118 \cdot 10^{-4}$
D_2: $-2.66707 \cdot 10^{-7}$

τ_{00}: $28.92787 \cdot 10^{-6}$
τ_1: $-1.45426 \cdot 10^{-10}$
τ_2: $7.89478 \cdot 10^{-13}$

Sensor: 5. Serial #: 17911

C_0: $-2.27081 \cdot 10^{4}$
C_1: $-5.35951 \cdot 10^{-1}$
C_2: $2.09832 \cdot 10^{-3}$

D_0: $5.62671 \cdot 10^{-2}$
D_1: $-3.31430 \cdot 10^{-5}$
D_2: $1.16763 \cdot 10^{-7}$

τ_{00}: $29.75394 \cdot 10^{-6}$
τ_1: $-1.95993 \cdot 10^{-10}$
τ_2: $7.66406 \cdot 10^{-13}$

Sensor: 6 Serial #: 18426

C_0: $-2.64209 \cdot 10^{4}$
C_1: $-2.91091 \cdot 10^{-1}$
C_2: $1.09997 \cdot 10^{-3}$

D_0: $6.22649 \cdot 10^{-2}$
D_1: $-2.16853 \cdot 10^{-5}$
D_2: $7.50013 \cdot 10^{-8}$

τ_{00}: $29.16313 \cdot 10^{-6}$
τ_1: $-1.94124 \cdot 10^{-10}$
τ_2: $5.35286 \cdot 10^{-13}$

Set 3: (for sensor 7)

$$P = C[(1-(\tau_0/\tau)^2) - D(1-(\tau_0/\tau)^2)^2]$$

$$C = C_0 + C_1 T + C_2 T^2$$
$$D = D_0$$
$$\tau_0 = \tau_{00} + \tau_1 T + \tau_2 T^2 + \tau_3 T^3,$$

$$\tau = 450/N_P$$

T : (°C) (Centigrade)

Sensor: 7. Serial #: 19327

C_0: $-2.505732 \cdot 10^{4}$
C_1: $-6.270068 \cdot 10^{-1}$
C_2: $5.399068 \cdot 10^{-3}$

D_0: $3.720884 \cdot 10^{-2}$

τ_{00}: $29.613417 \cdot 10^{-6}$
τ_1: $-5.454051 \cdot 10^{-10}$
τ_2: $3.093264 \cdot 10^{-12}$
τ_3: $8.444666 \cdot 10^{-16}$

TABLE 8.3 Yearhour calendar for non-leap years. Only the yearhour corresponding to 0000 GMT is listed for each day.

JAN			FEB			MAR			APR			MAY			JUNE		
DATE	YEAR DAY	HOUR (0000Z)	DATE	YEAR DAY	HOUR (0000Z)	DATE	YEAR DAY	HOUR (0000Z)	DATE	YEAR DAY	HOUR (0000Z)	DATE	YEAR DAY	HOUR (0000Z)	DATE	YEAR DAY	HOUR (0000Z)
1	1	0	1	32	744	1	60	1416	1	91	2160	1	121	2880	1	152	3624
2	2	24	2	33	768	2	61	1440	2	92	2184	2	122	2904	2	153	3648
3	3	48	3	34	792	3	62	1464	3	93	2208	3	123	2928	3	154	3672
4	4	72	4	35	816	4	63	1488	4	94	2232	4	124	2952	4	155	3696
5	5	96	5	36	840	5	64	1512	5	95	2256	5	125	2976	5	156	3720
6	6	120	6	37	864	6	65	1536	6	96	2280	6	126	3000	6	157	3744
7	7	144	7	38	888	7	66	1560	7	97	2304	7	127	3024	7	158	3768
8	8	168	8	39	912	8	67	1584	8	98	2328	8	128	3048	8	159	3792
9	9	192	9	40	936	9	68	1608	9	99	2352	9	129	3072	9	160	3816
10	10	216	10	41	960	10	69	1632	10	100	2376	10	130	3096	10	161	3840
11	11	240	11	42	984	11	70	1656	11	101	2400	11	131	3120	11	162	3864
12	12	264	12	43	1008	12	71	1680	12	102	2424	12	132	3144	12	163	3888
13	13	288	13	44	1032	13	72	1704	13	103	2448	13	133	3168	13	164	3912
14	14	312	14	45	1056	14	73	1728	14	104	2472	14	134	3192	14	165	3936
15	15	336	15	46	1080	15	74	1752	15	105	2496	15	135	3216	15	166	3960
16	16	360	16	47	1104	16	75	1776	16	106	2520	16	136	3240	16	167	3984
17	17	384	17	48	1128	17	76	1800	17	107	2544	17	137	3264	17	168	4008
18	18	408	18	49	1152	18	77	1824	18	108	2568	18	138	3288	18	169	4032
19	19	432	19	50	1176	19	78	1848	19	109	2592	19	139	3312	19	170	4056
20	20	456	20	51	1200	20	79	1872	20	110	2616	20	140	3336	20	171	4080
21	21	480	21	52	1224	21	80	1896	21	111	2640	21	141	3360	21	172	4104
22	22	504	22	53	1248	22	81	1920	22	112	2664	22	142	3384	22	173	4128
23	23	528	23	54	1272	23	82	1944	23	113	2688	23	143	3408	23	174	4152
24	24	552	24	55	1296	24	83	1968	24	114	2712	24	144	3432	24	175	4176
25	25	576	25	56	1320	25	84	1992	25	115	2736	25	145	3456	25	176	4200
26	26	600	26	57	1344	26	85	2016	26	116	2760	26	146	3480	26	177	4224
27	27	624	27	58	1368	27	86	2040	27	117	2784	27	147	3504	27	178	4248
28	28	648	28	59	1392	28	87	2064	28	118	2808	28	148	3528	28	179	4272
29	29	672				29	88	2088	29	119	2832	29	149	3552	29	180	4296
30	30	696				30	89	2112	30	120	2856	30	150	3576	30	181	4320
31	31	720				31	90	2136				31	151	3600			

JULY			AUG			SEPT			OCT			NOV			DEC		
DATE	YEAR DAY	HOUR (0000Z)	DATE	YEAR DAY	HOUR (0000Z)	DATE	YEAR DAY	HOUR (0000Z)	DATE	YEAR DAY	HOUR (0000Z)	DATE	YEAR DAY	HOUR (0000Z)	DATE	YEAR DAY	HOUR (0000Z)
1	182	4344	1	213	5088	1	244	5832	1	274	6552	1	305	7296	1	335	8016
2	183	4368	2	214	5112	2	245	5856	2	275	6576	2	306	7320	2	336	8040
3	184	4392	3	215	5136	3	246	5880	3	276	6600	3	307	7344	3	337	8064
4	185	4416	4	216	5160	4	247	5904	4	277	6624	4	308	7368	4	338	8088
5	186	4440	5	217	5184	5	248	5928	5	278	6648	5	309	7392	5	339	8112
6	187	4464	6	218	5208	6	249	5952	6	279	6672	6	310	7416	6	340	8136
7	188	4488	7	219	5232	7	250	5976	7	280	6696	7	311	7440	7	341	8160
8	189	4512	8	220	5256	8	251	6000	8	281	6720	8	312	7464	8	342	8184
9	190	4536	9	221	5280	9	252	6024	9	282	6744	9	313	7488	9	343	8209
10	191	4560	10	222	5304	10	253	6048	10	283	6768	10	314	7512	10	344	8232
11	192	4584	11	223	5328	11	254	6072	11	284	6792	11	315	7536	11	345	8256
12	193	4608	12	224	5352	12	255	6096	12	285	6816	12	316	7560	12	346	8280
13	194	4632	13	225	5376	13	256	6120	13	286	6840	13	317	7584	13	347	8304
14	195	4656	14	226	5400	14	257	6144	14	287	6864	14	318	7608	14	348	8328
15	196	4680	15	227	5424	15	258	6168	15	288	6888	15	319	7632	15	349	8352
16	197	4704	16	228	5448	16	259	6192	16	289	6912	16	320	7656	16	350	8376
17	198	4728	17	229	5472	17	260	6216	17	290	6936	17	321	7680	17	351	8400
18	199	4752	18	230	5496	18	261	6240	18	291	6960	18	322	7704	18	352	8424
19	200	4776	19	231	5520	19	262	6264	19	292	6984	19	323	7728	19	353	8448
20	201	4800	20	232	5544	20	263	6288	20	293	7008	20	324	7752	20	354	8472
21	202	4824	21	233	5568	21	264	6312	21	294	7032	21	325	7776	21	355	8496
22	203	4848	22	234	5592	22	265	6336	22	295	7056	22	326	7800	22	356	8520
23	204	4872	23	235	5616	23	266	6360	23	296	7080	23	327	7824	23	357	8544
24	205	4896	24	236	5640	24	267	6384	24	297	7104	24	328	7848	24	358	8568
25	206	4920	25	237	5664	25	268	6408	25	298	7128	25	329	7872	25	359	8592
26	207	4944	26	238	5688	26	269	6432	26	299	7152	26	330	7896	26	360	8616
27	208	4968	27	239	5712	27	270	6456	27	300	7176	27	331	7920	27	361	8640
28	209	4992	28	240	5736	28	271	6480	28	301	7200	28	332	7944	28	362	8664
29	210	5016	29	241	5760	29	272	6504	29	302	7224	29	333	7968	29	363	8688
30	211	5040	30	242	5784	30	273	6528	30	303	7248	30	334	7992	30	364	8712
31	212	5064	31	243	5808				31	304	7272				31	364	8736

standard year and 8784 hours in a leap year. The yearhours given in this report are referenced to 0000 GMT on either January 1, 1984 or January 1, 1985, depending on the year in which the instrument was recovered; the two-digit number of the instrument name indicates which date is the reference. Positive yearhours correspond to sampling periods which occur during the same calendar year as the reference date; negative yearhours correspond to those which occur in the calendar year prior to the reference date.

8.3 Pressure Sensor Drift Estimation and Removal

Prior to determining the long-term drift of our measurements, the mean and the tides were removed from the original pressure measurements. The time origin (when the drift started; t_o) was assumed to be the time when the instrument was about halfway to the sea floor, or 1 hour before the first sample on the bottom. We also removed the first 12 hours of data (24 points) after the instrument landed on the sea floor because during this time the sensors inside the glass instrument housing were still coming to thermal equilibrium, causing these initial measurements to change rapidly. Hence, the time origin was 13 hours before the first data point used. For computational ease and speed in estimating the drift curve, we temporarily subsampled the time series every two hours; however, the drift curve was later removed from the half-hourly time series.

The method of estimating and removing the long-term drift from the pressure records was described in Section 5, and the fitted drift parameters were listed in Table 5.3. The regressed drift curves are superimposed on the detided pressures in Figures 11.1 to 11.10.

The residual pressure records (detided and dedrifted), representing our best estimate of the true deep-ocean pressure signal, were calculated as the result of subtracting the fitted P_{drift} curve from the detided sets of measurements at each half-hourly data point. These dedrifted pressures were then low-pass filtered, and are shown in Figures 12.4 to 12.6.

9. PARAMETERS AND STATISTICS OF INDIVIDUAL SITES AND RECORDS

The location, dates, and basic statistics of the eleven instrument records are given in Tables 9.1 to 9.11. Each table documents a single instrument deployment. The useful data records are plotted in Sections 10, 11, and 12. General site information, such as position, bottom depth, and launch and recovery times, are given first, followed by details about the bottom pressure and temperature data sets. The times associated with the first and last data points are supplied. The time origin (t_0) is 13 hours before the first data point used. Yearhours are referenced to 0000 GMT on January 1 of the year indicated by the two-digit number in the instrument name. Positive yearhours occur during the same calendar year as the two-digit number; negative yearhours occur during the previous one.

The first order statistics (minimum, maximum, mean, and standard deviation) were calculated for the half-hourly and the 40HRLP records for each variable. These are also presented in the following tables. In Section 10 are plots of the measured (half-hourly) temperature and pressure data. The plots in Section 11 illustrate the detided pressure records, P_{detide}, <u>before</u> subtracting the drift, with the drift curve superimposed. The $P_{residual}$ records, plotted in Section 12, were obtained by subtracting the mean pressure, the drift curve (if nonzero), and the tide record from the half-hourly measured pressures. The statistics for $P_{residual}$ are included in the following tables.

TABLE 9.1
PIES84B2

IES Serial Number: 055
Pressure Sensor Serial Number: 8181

Position: 35°47.81 N
73°26.99 W
Depth: 3570 m

	DATE	GMT	CRUISE
LAUNCH:	Sep 24, 1983	1023	EN106
RECOVERY:	Jan 11, 1984	2004	OC144

MEASURED PRESSURE RECORDS
(Fig. 10.11)

	DATE	GMT	YEARHOUR
1st DATA POINT:	Sep 24, 1983	112952	-2364.5025
LAST DATA POINT:	Nov 18, 1983	052952	-1050.5025

Number of points: 2629
Sampling Interval: 0.50 hrs

Minimum = 3623.79 dbar
Maximum = 3625.17 dbar
Mean = 3624.43 dbar
Standard deviation = 0.325 dbar

RESIDUAL PRESSURE RECORDS

$$P_{residual} = P_{meas} - MEAN - DRIFT - TIDE$$

$$DRIFT = P_1 [1 - \exp(P_2\ t)] + P_3$$

where t = Time of sample in hours, starting with t = 13.0 for the first data point.

P_1 = -0.255695 dbar
P_2 = -0.0110545 h^{-1}
P_3 = 0.239596 dbar

TIDE calculated from the following constituents:

	M2	N2	S2	K2	K1	O1	P1	Q1
H (dbar):	.42427	.10616	.08304	.01971	.09128	.06666	.02991	.01460
G°:	353.50	335.77	20.90	21.65	183.08	186.63	182.51	194.59

	DATE	GMT	YEARHOUR
1st DATA POINT:	Sep 24, 1983	232952	-2352.5025
LAST DATA POINT:	Nov 18, 1983	052952	-1050.5025

Number of points: 2605
Sampling Interval: 0.50 hrs

Minimum = -0.1059 dbar
Maximum = 0.1140 dbar
Mean = 0.0000 dbar
Standard deviation = 0.0370 dbar

40HRLP PRESSURE RECORDS
(Fig. 12.4)

	DATE	GMT	YEARHOUR
1st DATA POINT:	Sep 26, 1983	060000	-2322.0000
LAST DATA POINT:	Nov 17, 1983	000000	-1080.0000

Number of points: 208
Sampling Interval: 6.00 hrs

Minimum = -0.0790 dbar
Maximum = 0.0814 dbar
Mean = 0.0000 dbar
Standard deviation = 0.0330 dbar

TEMPERATURE RECORDS
(Fig. 10.1)

	DATE	GMT	YEARHOUR
1st DATA POINT:	Sep 24, 1983	232952	-2352.5025
LAST DATA POINT:	Nov 18, 1983	052952	-1050.5025

Number of points: 2605
Sampling Interval: 0.50 hrs

Minimum = 2.173 °C
Maximum = 2.272 °C
Mean = 2.218 °C
Standard deviation = 0.035 °C

40HRLP TEMPERATURE RECORDS
(Fig. 12.1)

	DATE	GMT	YEARHOUR
1st DATA POINT:	Sep 26, 1983	060000	-2322.0000
LAST DATA POINT:	Nov 17, 1983	000000	-1080.0000

Number of points: 208
Sampling Interval: 6.00 hrs

Minimum = 2.173 °C
Maximum = 2.264 °C
Mean = 2.219 °C
Standard deviation = 0.026 °C

TABLE 9.2
PIES85BCM2

IES Serial Number: 055
Pressure Sensor Serial Number: 8181

Position: 35°48.09 N
73°25.88 W
Depth: 3560 m

	DATE	GMT	CRUISE
LAUNCH:	Jan 16, 1984	2344	OC144
RECOVERY:	Jan 17, 1985	0104	EN124

MEASURED PRESSURE RECORDS
(Fig. 10.12)

	DATE	GMT	YEARHOUR
1st DATA POINT:	Jan 17, 1984	005927	-8399.009
LAST DATA POINT:	Jan 16, 1985	235927	383.9915

Number of points: 17567
Sampling Interval: 0.50 hrs

Minimum = 3645.84 dbar
Maximum = 3647.71 dbar
Mean = 3646.57 dbar
Standard deviation = 0.338 dbar

RESIDUAL PRESSURE RECORDS

$$P_{residual} = P_{meas} - MEAN - DRIFT - TIDE$$

$$DRIFT = P_1 [1 - \exp(P_2 t)] + P_3$$

where t = Time of sample in hours, starting with t = 13.0 for the first data point

P_1 = -0.378324 dbar
P_2 = -0.0022225 h^{-1}
P_3 = 0.359908 dbar

TIDE calculated from the following constituents:

	M2	N2	S2	K2	K1	O1	P1	Q1
H (dbar):	.43233	.10587	.08715	.02063	.09064	.06984	.02990	.01485
G°:	352.84	333.99	19.68	20.286	181.05	186.12	181.76	184.73

	DATE	GMT	YEARHOUR
1st DATA POINT:	Jan 17, 1984	125927	-8387.009
LAST DATA POINT:	Jan 16, 1985	235927	383.991

Number of points: 17543
Sampling Interval: 0.50 hrs

Minimum = -0.1680 dbar
Maximum = 0.1190 dbar
Mean = 0.0000 dbar
Standard deviation = 0.0369 dbar

40HRLP PRESSURE RECORDS
(Fig. 12.5)

	DATE	GMT	YEARHOUR
1st DATA POINT:	Jan 19, 1984	000000	-8352.0000
LAST DATA POINT:	Jan 15, 1985	180000	354.0000

Number of points: 1452
Sampling Interval: 6.00 hrs

Minimum = -0.150 dbar
Maximum = 0.087 dbar
Mean = 0.0000 dbar
Standard deviation = 0.0334 dbar

TEMPERATURE RECORDS
(Figs. 10.2a and 10.2b)

	DATE	GMT	YEARHOUR
1st DATA POINT:	Jan 17 1984	125927	-8387.009
LAST DATA POINT:	Jan 16, 1985	235927	383.991

Number of points: 17543
Sampling Interval: 0.50 hrs

Minimum = 2.166 °C
Maximum = 2.435 °C
Mean = 2.232 °C
Standard deviation = 0.080 °C

40HRLP TEMPERATURE RECORDS
(Fig. 12.2)

	DATE	GMT	YEARHOUR
1st DATA POINT:	Jan 19, 1984	000000	-8352.0000
LAST DATA POINT:	Jan 15, 1985	180000	354.0000

Number of points: 1452
Sampling Interval: 6.00 hrs

Minimum = 2.168 °C
Maximum = 2.432 °C
Mean = 2.234 °C
Standard deviation = 0.054 °C

TABLE 9.3
PIES85BCM3

IES Serial Number: 034
Pressure Sensor Serial Number: 18426

Position: 35°31.00 N
73°08.02 W
Depth: 3930 m

	DATE	GMT	CRUISE
LAUNCH:	Jan. 15, 1984	0352	OC144
RECOVERY:	Washed up on beach in Bermuda		

MEASURED PRESSURE RECORDS
(Figs. 10.13a and 10.13b)

	DATE	GMT	YEARHOUR
1st DATA POINT:	Jan. 15, 1984	04 51 25	- 8443.143
LAST DATA POINT:	Jan. 3, 1985	02 51 25	52.356

Number of points: 16991
Sampling Interval: 0.50 hrs

(Pressure record is jumpy.)

TEMPERATURE RECORDS
(Figs. 10.3a and 10.3b)

	DATE	GMT	YEARHOUR
1st DATA POINT:	Jan. 15, 1984	045125	- 8443.143
LAST DATA POINT:	Jan. 3, 1985	035125	52.356

Number of points: 16991
Sampling Interval: 0.50 hrs

Minimum = 2.440 °C
Maximum = 10.719 °C
Mean = 2.467 °C
Standard deviation = 0.107 °C

TABLE 9.4
PIES85C0

IES Serial Number: 053
Pressure Sensor Serial Number: 17911

Position: 36°25.25 N
73°19.75 W
Depth: 3310 m

	DATE	GMT	CRUISE
LAUNCH:	Jan 18, 1985	2007	EN124
RECOVERY:	May 12, 1985	1459	EN130

MEASURED PRESSURE RECORDS
(Fig. 10.14)

	DATE	GMT	YEARHOUR
1st DATA POINT:	Jan 18, 1985	210004	429.0011
LAST DATA POINT:	May 12, 1985	143004	3158.5011

Number of points: 5460
Sampling Interval: 0.50 hrs

Minimum = 3342.76 dbar
Maximum = 3344.35 dbar
Mean = 3343.51 dbar
Standard deviation = 0.335 dbar

RESIDUAL PRESSURE RECORDS

$$P_{residual} = P_{meas} - MEAN - TIDE$$

TIDE calculated from the following constituents:

	M2	N2	S2	K2	K1	O1	P1	Q1
H (dbar):	.43132	.10572	.09210	.02238	.09088	.07117	.03012	.01475
G°:	351.03	334.45	18.33	19.56	182.00	185.80	182.65	183.86

	DATE	GMT	YEARHOUR
1st DATA POINT:	Jan 19, 1985	090004	441.0011
LAST DATA POINT:	May 12, 1985	143004	3158.0011

Number of points: 5436
Sampling Interval: 0.50 hrs

Minimum = -0.1731 dbar
Maximum = 0.1222 dbar
Mean = 0.0000 dbar
Standard deviation = 0.0417 dbar

40HRLP PRESSURE RECORDS
(Fig. 12.6)

	DATE	GMT	YEARHOUR
1st DATA POINT:	Jan 20, 1985	180000	474.0000
LAST DATA POINT:	May 11, 1985	060000	3126.0000

Number of points: 443
Sampling Interval: 6.00 hrs

Minimum = -0.0802 dbar
Maximum = 0.0831 dbar
Mean = 0.0000 dbar
Standard deviation = 0.0369 dbar

TEMPERATURE RECORDS
(Fig. 10.4)

	DATE	GMT	YEARHOUR
1st DATA POINT:	Jan 18, 1985	210004	429.0011
LAST DATA POINT:	May 12, 1985	143004	3158.5011

Number of points: 5460
Sampling Interval: 0.50 hrs

Minimum = 2.300 °C
Maximum = 10.436 °C
Mean = 2.373 °C
Standard deviation = 0.140 °C

40HRLP TEMPERATURE RECORDS
(Fig. 12.3)

	DATE	GMT	YEARHOUR
1st DATA POINT:	Jan 20, 1985	180000	474.0000
LAST DATA POINT:	May 11, 1985	060000	3126.0000

Number of points: 443
Sampling Interval: 6.00 hrs

Minimum = 2.312 °C
Maximum = 2.461 °C
Mean = 2.369 °C
Standard deviation = 0.032 °C

TABLE 9.5
PIES84C1

IES Serial Number: 056
Pressure Sensor Serial Number: 17848

Position: 36°17.20 N
73°11.40 W

Depth: 3450 m

	DATE	GMT	CRUISE
LAUNCH:	Nov 01, 1983	1903	EN107
RECOVERY:	Jan 11, 1984	1459	OC144

MEASURED PRESSURE RECORDS
(Fig. 10.15)

	DATE	GMT	YEARHOUR
1st DATA POINT:	Nov 01, 1983	200406	-1443.9316
LAST DATA POINT:	Jan 11, 1984	143406	254.5683

Number of points: 3398
Sampling Interval: 0.50 hrs

Minimum = 3513.51 dbar
Maximum = 3515.04 dbar

Mean = 3514.20 dbar
Standard deviation = 0.331 dbar

RESIDUAL PRESSURE RECORDS

$$P_{residual} = P_{measured} - MEAN - TIDE$$

TIDE calculated from the following constituents:

	M2	N2	S2	K2	K1	O1	P1	Q1
H (dbar):	.42659	.09910	.08669	.02037	.09116	.06876	.03045	.01264
G°:	353.61	335.45	21.82	23.81	181.16	188.76	182.42	185.16

	DATE	GMT	YEARHOUR
1st DATA POINT:	Nov 02, 1983	080406	-1431.9316
LAST DATA POINT:	Jan 11, 1984	143406	254.5683

Number of points: 3374
Sampling Interval: 0.50 hrs

Minimum = -0.1433 dbar
Maximum = 0.1374 dbar

Mean = 0.0000 dbar
Standard deviation = 0.0405 dbar

40HRLP PRESSURE RECORDS
(Fig. 12.4)

	DATE	GMT	YEARHOUR
1st DATA POINT:	Nov 3, 1983	180000	-1398.0000
LAST DATA POINT:	Jan 10, 1984	060000	222.0000

Number of points: 271
Sampling Interval: 6.00 hrs

Minimum = -0.0828 dbar
Maximum = 0.0818 dbar

Mean = 0.0000 dbar
Standard deviation = 0.0341 dbar

TEMPERATURE RECORDS
(Fig. 10.5)

	DATE	GMT	YEARHOUR
1st DATA POINT:	Nov 2, 1983	080406	-1431.9316
LAST DATA POINT:	Jan 11, 1984	143406	254.5683

Number of points: 3374
Sampling Interval: 0.50 hrs

Minimum = 2.219 °C
Maximum = 2.349 °C

Mean = 2.257 °C
Standard deviation = 0.038 °C

40HRLP TEMPERATURE RECORDS
(Fig. 12.1)

	DATE	GMT	YEARHOUR
1st DATA POINT:	Nov 3, 1983	180000	-1398.0000
LAST DATA POINT:	Jan 19, 1984	060000	222.0000

Number of points: 271
Sampling Interval: 6.00 hrs

Minimum = 2.221 °C
Maximum = 2.347 °C

Mean = 2.257 °C
Standard deviation = 0.029 °C

TABLE 9.6
PIES85CCM1

IES Serial Number: 056
Pressure Sensor Serial Number: 17848

Position: 36°15.23 N
73°09.89 W

Depth: 3475 m

	DATE	GMT	CRUISE
LAUNCH:	Jan. 17, 1984	0505	OC144
RECOVERY:	Jan. 14, 1985	0120	EN124

(Pressure sensor did not work.)

TABLE 9.7
PIES85C1

IES Serial Number: 035
Pressure Sensor Serial Number: 17849

Position: 36°15.26 N
73°09.70 W

Depth: 3475 m

	DATE	GMT	CRUISE
LAUNCH:	Jan 14, 1985	0217	EN124
RECOVERY:	May 12, 1985	1243	EN130

MEASURED PRESSURE RECORDS
(Fig. 10.16)

	DATE	GMT	YEARHOUR
1st DATA POINT:	Jan 14, 1985	032453	315.4147
LAST DATA POINT:	May 12, 1985	122453	3156.4147

Number of points: 5683
Sampling Interval: 0.50 hrs

Minimum = 3529.66 dbar
Maximum = 3531.21 dbar

Mean = 3530.39 dbar
Standard deviation = 0.333 dbar

RESIDUAL PRESSURE RECORDS

$$P_{residual} = P_{meas} - MEAN - TIDE$$

TIDE calculated from the following constituents:

	M2	N2	S2	K2	K1	O1	P1	Q1
H (dbar):	.43174	.10568	.09249	.02246	.09047	.06960	.03003	.01404
G°:	351.20	334.39	18.03	19.09	182.40	185.18	182.91	183.49

	DATE	GMT	YEARHOUR
1st DATA POINT:	Jan 14, 1985	152453	327.4147
LAST DATA POINT:	May 12, 1985	122453	3156.4147

Number of points: 5659
Sampling Interval: 0.50 hrs

Minimum = -0.0891 dbar
Maximum = 0.1065 dbar

Mean = 0.0000 dbar
Standard deviation = 0.0310 dbar

40HRLP PRESSURE RECORDS
(Fig. 12.6)

	DATE	GMT	YEARHOUR
1st DATA POINT:	Jan 16, 1985	000000	360.0000
LAST DATA POINT:	May 11, 1985	060000	3126.0000

Number of points: 462
Sampling Interval: 6.00 hrs

Minimum = -0.0632 dbar
Maximum = 0.0763 dbar
Mean = 0.0000 dbar
Standard deviation = 0.0271 dbar

TEMPERATURE RECORDS
(Fig. 10.6)

	DATE	GMT	YEARHOUR
1st DATA POINT:	Jan 14, 1985	032453	315.4147
LAST DATA POINT:	May 12, 1985	122453	3156.4147

Number of points: 5683
Sampling Interval: 0.50 hrs

Minimum = 2.188 °C
Maximum = 8.291 °C
Mean = 2.280 °C
Standard deviation = 0.111 °C

40HRLP TEMPERATURE RECORDS
(Fig. 12.3)

	DATE	GMT	YEARHOUR
1st DATA POINT:	Jan 16, 1985	000000	360.0000
LAST DATA POINT:	May 11, 1985	060000	3126.0000

Number of points: 462
Sampling Interval: 6.00 hrs

Minimum = 2.190 °C
Maximum = 2.387 °C
Mean = 2.277 °C
Standard deviation = 0.042 °C

TABLE 9.8
PIES84CCM2

IES Serial Number: 057
Pressure Sensor Serial Number: 17849

Position: 36°05.02 N
72°59.94 W

Depth: 3660 m

	DATE	GMT	CRUISE
LAUNCH:	Nov 1, 1983	2158	EN107
RECOVERY:	June 7, 1984	1514	EN118

MEASURED PRESSURE RECORDS
(Fig. 10.17)

	DATE	GMT	YEARHOUR
1st DATA POINT:	Nov 1, 1983	230740	-1440.8723
LAST DATA POINT:	Jun 7, 1984	150740	3807.1277

Number of points: 10497
Sampling Interval: 0.50 hrs

Minimum = 3732.73 dbar
Maximum = 3734.59 dbar

Mean = 3733.56 dbar
Standard deviation = 0.354 dbar

RESIDUAL PRESSURE RECORDS

$$P_{residual} = P_{meas} - MEAN - DRIFT - TIDE$$

$$DRIFT = P_1 [1 - \exp(P_2\ t)] + P_3$$

where t = Time of sample in hours, starting with t = 13.0 for the first data point

P_1 = -0.513066 dbar
P_2 = -0.0002825 h^{-1}
P_3 = 0.246240 dbar

TIDE calculated from the following constituents:

	M2	N2	S2	K2	K1	O1	P1	Q1
H (dbar):	.43285	.10601	.08994	.02138	.09200	.06898	.03032	.01438
G°:	352.23	332.50	19.29	19.71	180.70	185.78	181.45	183.89

	DATE	GMT	YEARHOUR
1st DATA POINT:	Nov 2, 1983	110740	-1428.8723
LAST DATA POINT:	Jun 7, 1984	150740	3807.1277

Number of points: 10473
Sampling Interval: 0.50 hrs

Minimum = -0.190 dbar
Maximum = 0.118 dbar

Mean = 0.0000 dbar
Standard deviation = 0.0449 dbar

40HRLP PRESSURE RECORDS
(Fig. 12.4 and 12.5)

	DATE	GMT	YEARHOUR
1st DATA POINT:	Nov 3, 1983	180000	-1398.0000
LAST DATA POINT:	Jun 6, 1984	060000	3774.0000

Number of points: 863
Sampling Interval: 6.00 hrs

Minimum = -0.1658 dbar
Maximum = 0.0916 dbar
Mean = 0.0000 dbar
Standard deviation = 0.0416 dbar

TEMPERATURE RECORDS
(Fig. 10.7)

	DATE	GMT	YEARHOUR
1st DATA POINT:	Nov 2, 1983	110740	-1428.8723
LAST DATA POINT:	June 7, 1984	150740	3807.1277

Number of points: 10473
Sampling Interval: 0.50 hrs

Minimum = 2.244 °C
Maximum = 2.482 °C
Mean = 2.317 °C
Standard deviation = 0.076 °C

40HRLP TEMPERATURE RECORDS
(Fig. 12.1 and 12.2)

	DATE	GMT	YEARHOUR
1st DATA POINT:	Nov 3, 1983	180000	-1398.0000
LAST DATA POINT:	Jun 6, 1984	060000	3774.0000

Number of points: 863
Sampling Interval: 6.00 hrs

Minimum = 2.246 °C
Maximum = 2.475 °C
Mean = 2.319 °C
Standard deviation = 0.058 °C

TABLE 9.9
PIES85CCM2

IES Serial Number: 054
Pressure Sensor Serial Number: 8180

Position: 36°05.07 N
72°59.86 W

Depth: 3660 m

	DATE	GMT	CRUISE
LAUNCH:	June 7, 1984	1705	EN118
RECOVERY:	May 12, 1985	1004	EN130

MEASURED PRESSURE RECORDS
(Fig. 10.18)

	DATE	GMT	YEARHOUR
1st DATA POINT:	June 7, 1984	181007	-4973.8314
LAST DATA POINT:	May 12, 1985	094007	3153.6686

Number of points: 16256
Sampling Interval: 0.50 hrs

Minimum = 3732.42 dbar
Maximum = 3734.33 dbar

Mean = 3733.34 dbar
Standard deviation = 0.344 dbar

RESIDUAL PRESSURE RECORDS

$$P_{residual} = P_{meas} - MEAN - DRIFT - TIDE$$

$$DRIFT = P_1 [1 - \exp(P_2\ t)] + P_3 + P_4\ t$$

where t = Time of sample in hours, starting with t = 13.0 for the first data point

P_1 = 0.308608 dbar
P_2 = -0.0036410 h^{-1}
P_3 = -0.407702 dbar
P_4 = 0.000027 dbar/h

TIDE calculated from the following constituents:

	M2	N2	S2	K2	K1	O1	P1	Q1
H (dbar):	.43341	.10592	.08873	.02120	.08852	.06976	.02935	.01447
G°:	352.60	335.00	19.74	20.77	181.13	186.05	181.82	184.82

	DATE	GMT	YEARHOUR
1st DATA POINT:	June 8, 1984	061007	-4961.8314
LAST DATA POINT:	May 12, 1985	094007	3153.6686

Number of points: 16232
Sampling Interval: 0.50 hrs

Minimum = -0.1120 dbar
Maximum = 0.1215 dbar

Mean = 0.0000 dbar
Standard deviation = 0.0350 dbar

40HRLP PRESSURE RECORDS
(Fig. 12.5 and 12.6)

	DATE	GMT	YEARHOUR
1st DATA POINT:	June 9, 1984	120000	-4932.0000
LAST DATA POINT:	May 11, 1985	000000	3120.0000

Number of points: 1343
Sampling Interval: 6.00 hrs

Minimum = -0.082 dbar
Maximum = 0.099 dbar
Mean = 0.0000 dbar
Standard deviation = 0.0315 dbar

TEMPERATURE RECORDS
(Fig. 10.8)

	DATE	GMT	YEARHOUR
1st DATA POINT:	June 7, 1984	181007	-4973.8314
LAST DATA POINT:	May 12, 1985	094007	3153.6686

Number of points: 16256
Sampling Interval: 0.50 hrs

Minimum = 2.204 °C
Maximum = 4.619 °C
Mean = 2.256 °C
Standard deviation = 0.071 °C

40HRLP TEMPERATURE RECORDS
(Fig. 12.2 and 12.3)

	DATE	GMT	YEARHOUR
1st DATA POINT:	June 9, 1984	120000	-4932.0000
LAST DATA POINT:	May 11, 1985	000000	3120.0000

Number of points: 1343
Sampling Interval: 6.00 hrs

Minimum = 2.205 °C
Maximum = 2.334 °C
Mean = 2.257 °C
Standard deviation = 0.036 °C

TABLE 9.10
PIES84CCM3

IES Serial Number: 036
Pressure Sensor Serial Number: 17911

Position: 35°48.42 N
72°42.55 W
Depth: 3900 m

	DATE	GMT	CRUISE
LAUNCH:	Jan 15, 1984	0822	OC144
RECOVERY:	June 7, 1984	2109	EN118

MEASURED PRESSURE RECORDS
(Fig. 10.19)

	DATE	GMT	YEARHOUR
1st DATA POINT:	Jan 15, 1984	092953	345.4981
LAST DATA POINT:	Jun 7, 1984	205953	3812.9981

Number of points: 6396
Sampling Interval: 0.50 hrs

Minimum = 3990.15 dbar
Maximum = 3991.77 dbar
Mean = 3990.94 dbar
Standard deviation = 0.337 dbar

RESIDUAL PRESSURE RECORDS

$$P_{residual} = P_{measured} - MEAN - TIDE$$

TIDE calculated from the following constituents:

	M2	N2	S2	K2	K1	O1	P1	Q1
H (dbar):	.43048	.10519	.09131	.02181	.09100	.06813	.02987	.01475
G°:	352.05	332.17	19.27	19.72	181.50	185.05	181.98	184.06

	DATE	GMT	YEARHOUR
1st DATA POINT:	Jan 15, 1984	212953	357.4981
LAST DATA POINT:	Jun 7, 1984	205953	3812.9981

Number of points: 6912
Sampling Interval: 0.50 hrs

Minimum = -0.1641 dbar
Maximum = 0.1060 dbar
Mean = 0.0000 dbar
Standard deviation = 0.0529 dbar

40HRLP PRESSURE RECORDS
(Fig. 12.4 and 12.5)

	DATE	GMT	YEARHOUR
1st DATA POINT:	Jan 17, 1984	060000	390.0000
LAST DATA POINT:	Jun 6, 1984	120000	3780.0000

Number of points: 566
Sampling Interval: 6.00 hrs

Minimum = -0.1363 dbar
Maximum = 0.0881 dbar
Mean = 0.0000 dbar
Standard deviation = 0.0511 dbar

TEMPERATURE RECORDS
(Fig. 10.9)

	DATE	GMT	YEARHOUR
1st DATA POINT:	Jan 15, 1984	212953	357.4981
LAST DATA POINT:	Jun 7, 1984	205953	3812.9981

Number of points: 6912
Sampling Interval: 0.50 hrs

Minimum = 2.365 °C
Maximum = 2.494 °C
Mean = 2.396 °C
Standard deviation = 0.039 °C

40HRLP TEMPERATURE RECORDS
(Fig. 12.1 and 12.2)

	DATE	GMT	YEARHOUR
1st DATA POINT:	Jan 17, 1984	060000	390.0000
LAST DATA POINT:	Jun 6, 1984	120000	3780.0000

Number of points: 566
Sampling Interval: 6.00 hrs

Minimum = 2.367 °C
Maximum = 2.486 °C
Mean = 2.397 °C
Standard deviation = 0.019 °C

TABLE 9.11
PIES85CCM3

IES Serial Number: 058
Pressure Sensor Serial Number: 19327

Position: 35°48.23 N
72°42.57 W

Depth: 3890 m

	DATE	GMT	CRUISE
LAUNCH:	June 7, 1984	2239	EN118
RECOVERY:	May 12, 1985	0635	EN130

MEASURED PRESSURE RECORDS
(Fig. 10.20)

	DATE	GMT	YEARHOUR
1st DATA POINT:	June 7, 1984	235920	-4968.0111
LAST DATA POINT:	May 12, 1985	062920	3150.4889

Number of points: 16238
Sampling Interval: 0.50 hrs

Minimum = 3988.67 dbar
Maximum = 3990.26 dbar

Mean = 3989.38 dbar
Standard deviation = 0.334 dbar

RESIDUAL PRESSURE RECORDS

$$P_{residual} = P_{meas} - MEAN - DRIFT - TIDE$$

$$DRIFT = P_1 [1 - \exp(P_2 t)] + P_3$$

where t = Time of sample in hours, starting with
t = 13.0 for the first data point

P_1 =-0.196539 dbar
P_2 =-0.0012165 h^{-1}
P_3 = 0.177363 dbar

TIDE calculated from the following constituents:

	M2	N2	S2	K2	K1	O1	P1	Q1
H (dbar):	.43211	.10560	.08885	.02127	.08816	.06896	.02922	.01424
G°:	352.83	335.33	20.12	21.21	181.19	186.55	181.94	185.23

	DATE	GMT	YEARHOUR
1st DATA POINT:	June 8, 1984	115920	-4956.0111
LAST DATA POINT:	May 12, 1985	062920	3150.4889

Number of points: 16214
Sampling Interval: 0.50 hrs

Minimum = -0.121 dbar
Maximum = 0.148 dbar

Mean = 0.0000 dbar
Standard deviation = 0.0369 dbar

40HRLP PRESSURE RECORDS
(Fig. 12.5 and 12.6)

	DATE	GMT	YEARHOUR
1st DATA POINT:	June 9, 1984	180000	-4926.0000
LAST DATA POINT:	May 11, 1985	000000	3120.0000

Number of points: 1342
Sampling Interval: 6.00 hrs

Minimum = -0.100 dbar
Maximum = 0.120 dbar
Mean = 0.0000 dbar
Standard deviation = 0.0334 dbar

TEMPERATURE RECORDS
(Fig. 10.10)

	DATE	GMT	YEARHOUR
1st DATA POINT:	June 7, 1984	235920	-4968.0111
LAST DATA POINT:	May 12, 1985	062920	3150.4889

Number of points: 16238
Sampling Interval: 0.50 hrs

Minimum = 2.375 °C
Maximum = 5.983 °C
Mean = 2.414 °C
Standard deviation = 0.077 °C

40HRLP TEMPERATURE RECORDS
(Fig. 12.2 and 12.3)

	DATE	GMT	YEARHOUR
1st DATA POINT:	June 9, 1984	180000	-4926.0000
LAST DATA POINT:	May 11, 1985	000000	3120.0000

Number of points: 1342
Sampling Interval: 6.00 hrs

Minimum = 2.377 °C
Maximum = 2.512 °C
Mean = 2.415 °C
Standard deviation = 0.024 °C

10. HALF-HOURLY DATA FOR EACH INSTRUMENT

Plots of the measured bottom pressure and temperature are presented. The time scale is the same for all plots, with each increment corresponding to 5 days. The axis begins on 0000 GMT of the first date labelled.

The vertical scale for each variable is consistent between instruments. Each increment corresponds to 0.5 dbar for the bottom pressure data and to 0.02°C for the temperatures.

The sampling interval is 0.5 hours for all instruments. The length and start and end times of the data records are tabulated in the previous section.

10.1 Temperature Data

The raw temperature records are shown in Figures 10.1 to 10.10. All the temperatures are in the range 2.2 to 2.5°C, with a tendency for the offshore (deeper) records to be warmer. We have observed this pattern in previous investigations in this region, where the colder core of the Western Boundary Undercurrent (WBUC) is somewhat onshore of (shallower than) the array. The temperature records are characterized by "square-pulse-like" warming events; i.e., they have many plateaus of relatively constant temperature (±0.02°C) separated by very rapid changes (~0.05 to 0.15°C within a few hours) to a different plateau that may last typically for 1 to 10 days. We tentatively associate this behavior with lateral shifts of the offshore temperature front of the WBUC, although it may also be caused by advective pulses of warmer or colder water.

10.2 Pressure Data

The raw pressure records are shown in Figures 10.11 to 10.20. The semidiurnal tidal oscillations of roughly 1 dbar range are prominent in these records, and the 29-day repeat-cycle of spring and neap tides is readily observed. Other features of these pressure records, which are only slightly noticeable on this coarse plotting scale, are discussed in Section 12, after the tides and the drift have been removed from them.

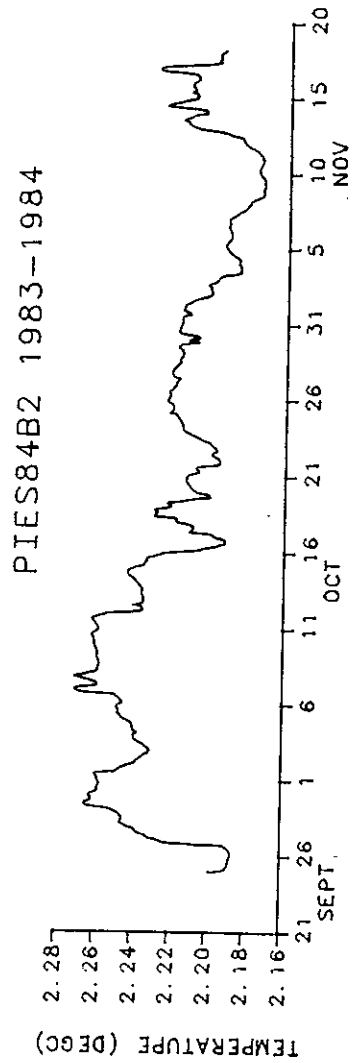

Figure 10:1 Raw temperature record of PIES84B2

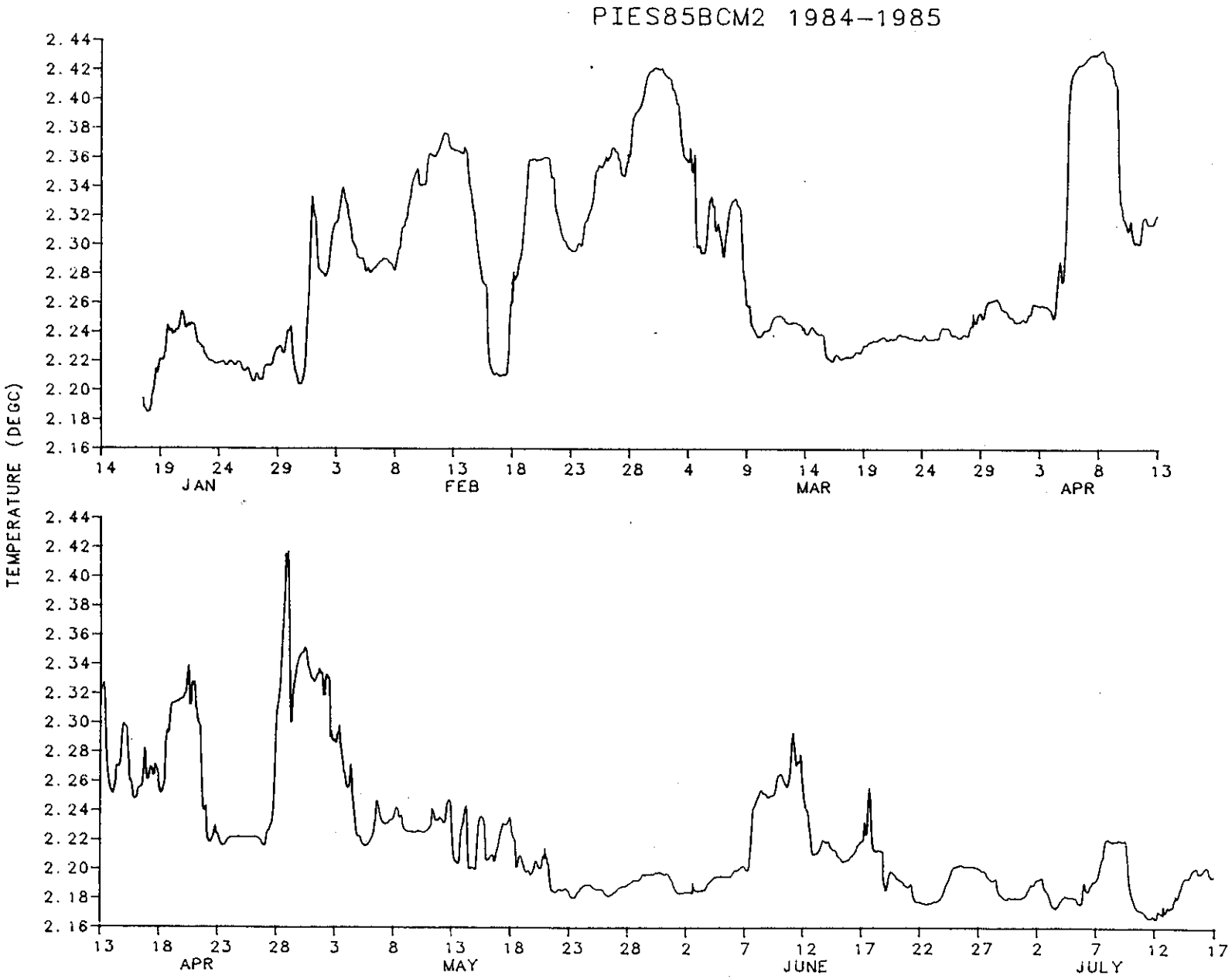

Figure 10.2a Raw temperature record of PIES85BCM2

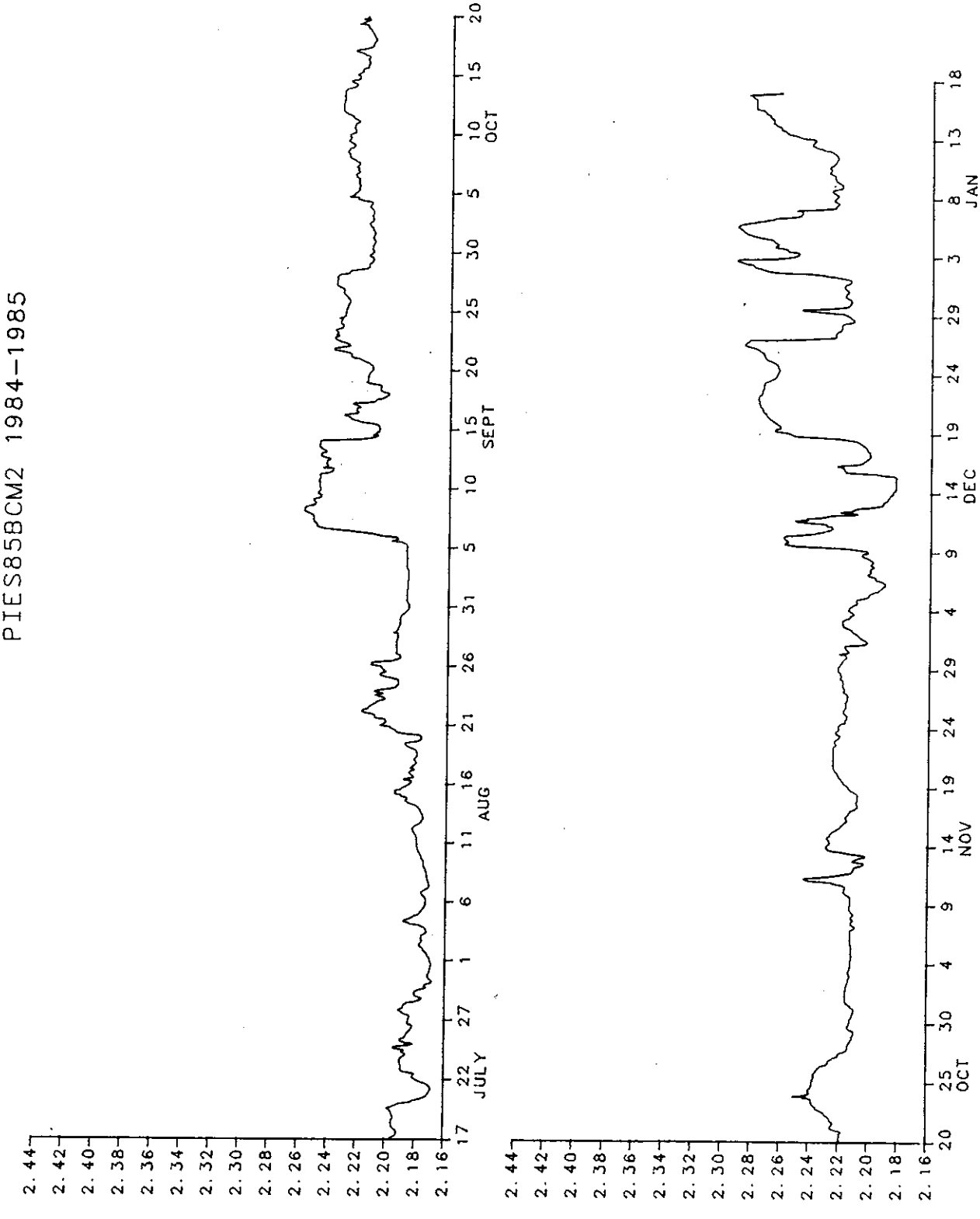

Figure 10.2b Raw temperature record of PIES85BCM2, continued

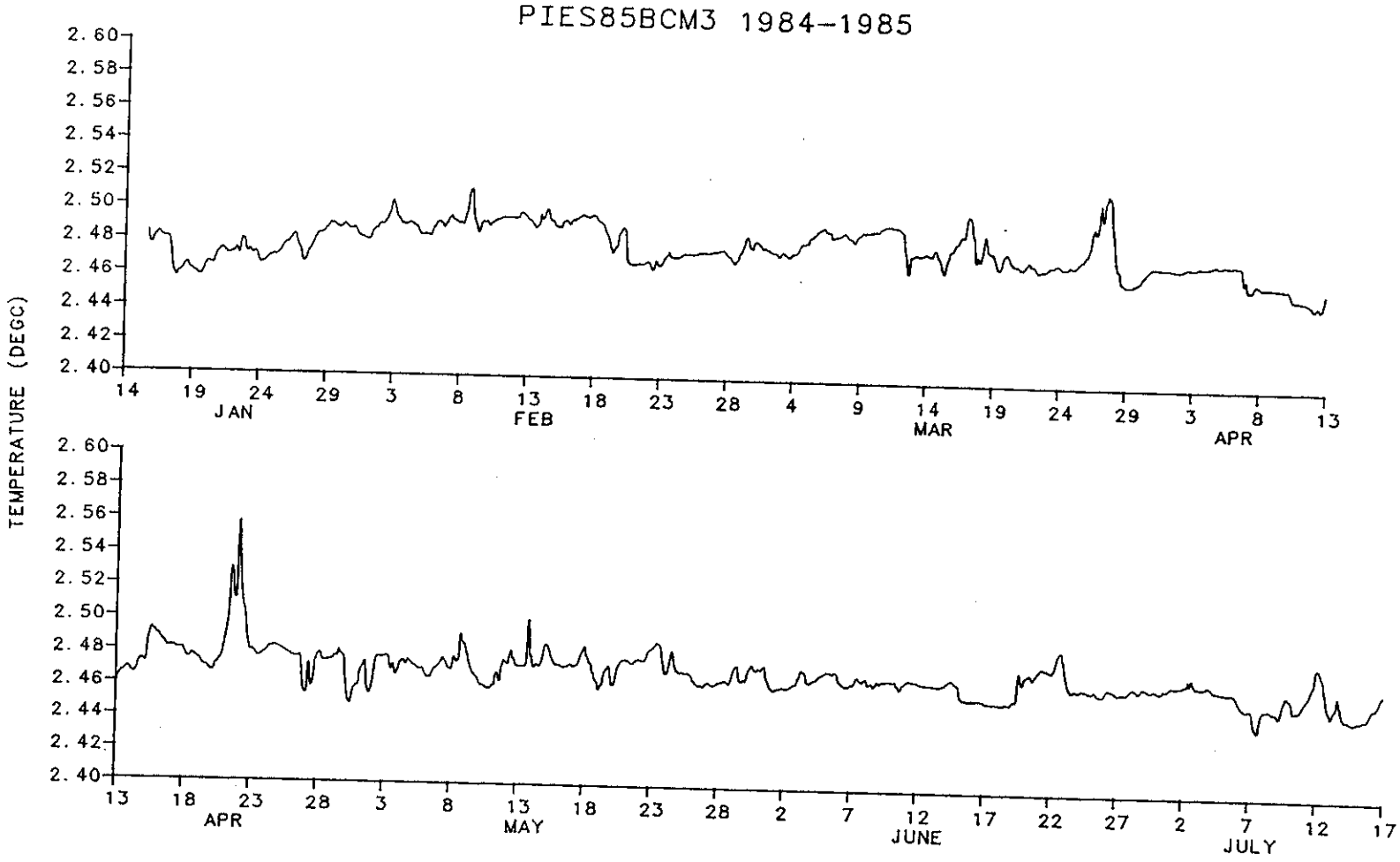

Figure 10.3a Raw temperature record of PIES85BCM3

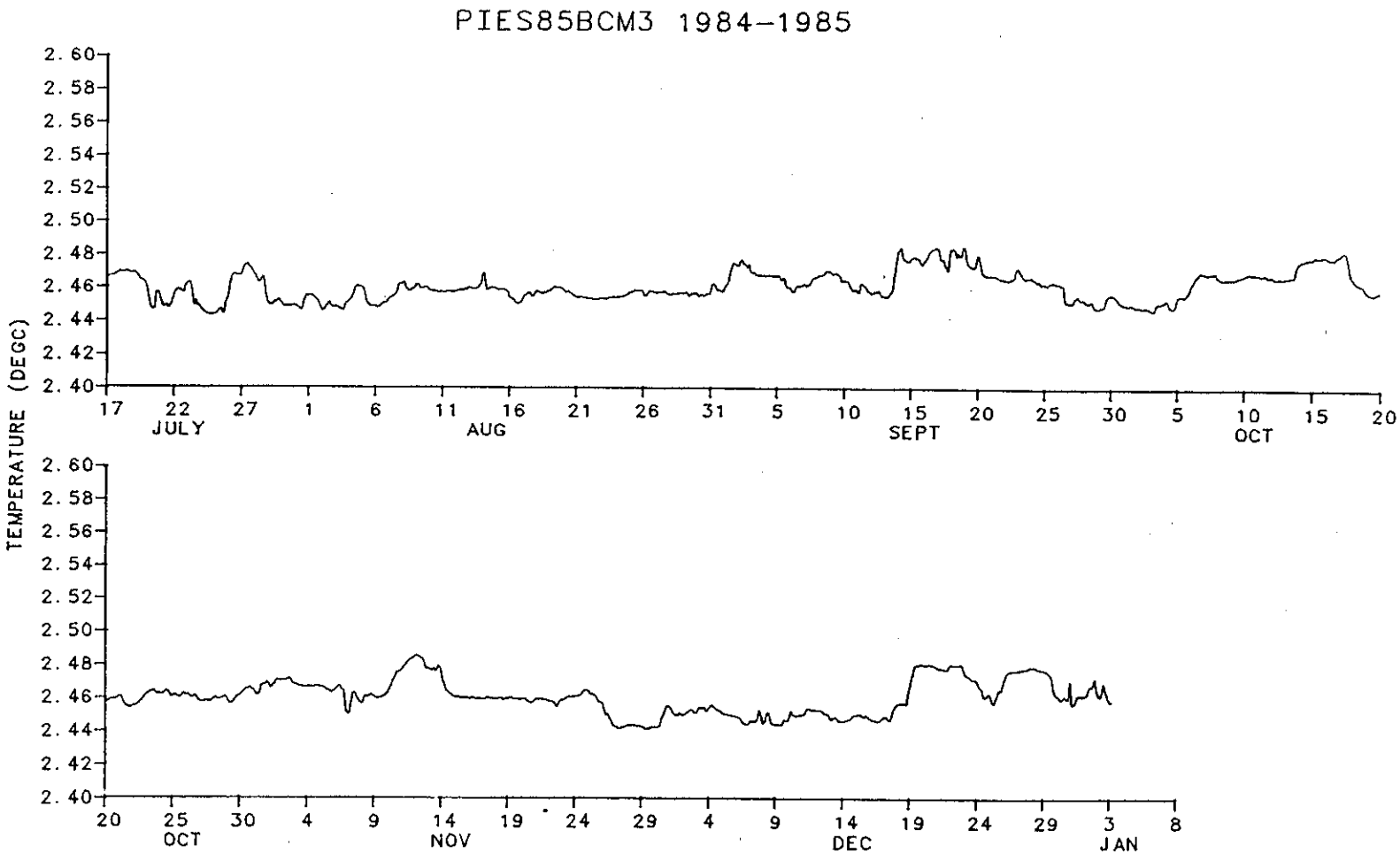

Figure 10.3b Raw temperature record of PIES85BCM3, continued

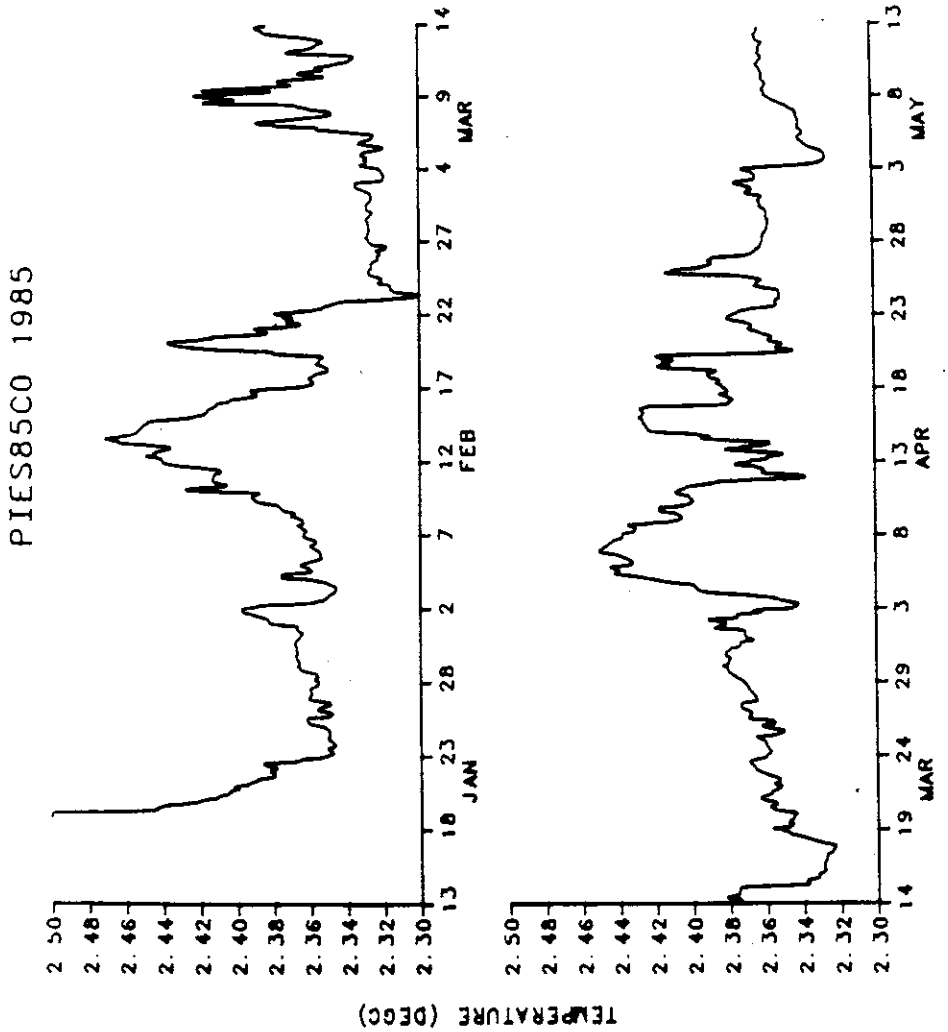

Figure 10.4 Raw temperature record of PIES85C0

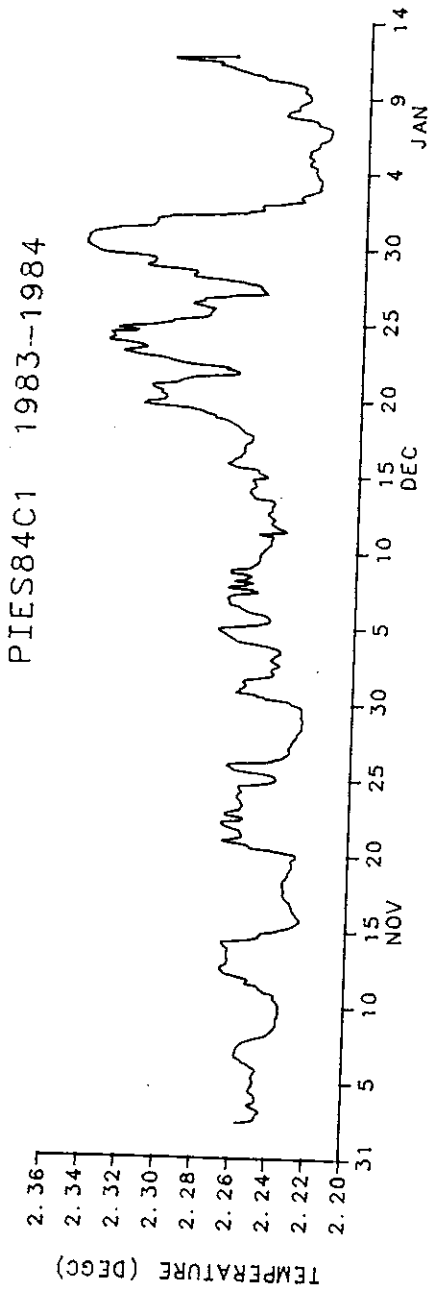

Figure 10.5 Raw temperature record of PIES84C1

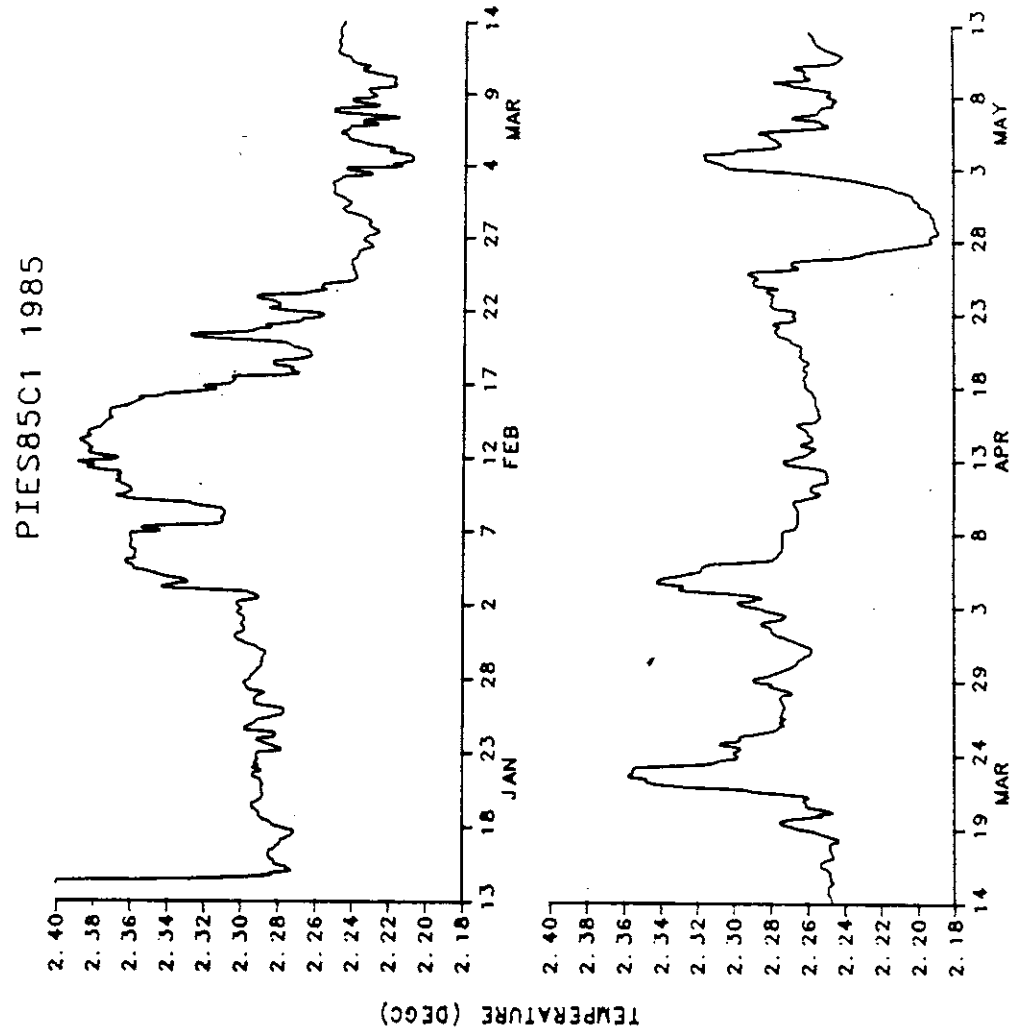

Figure 10.6 Raw temperature record of PIES85C1

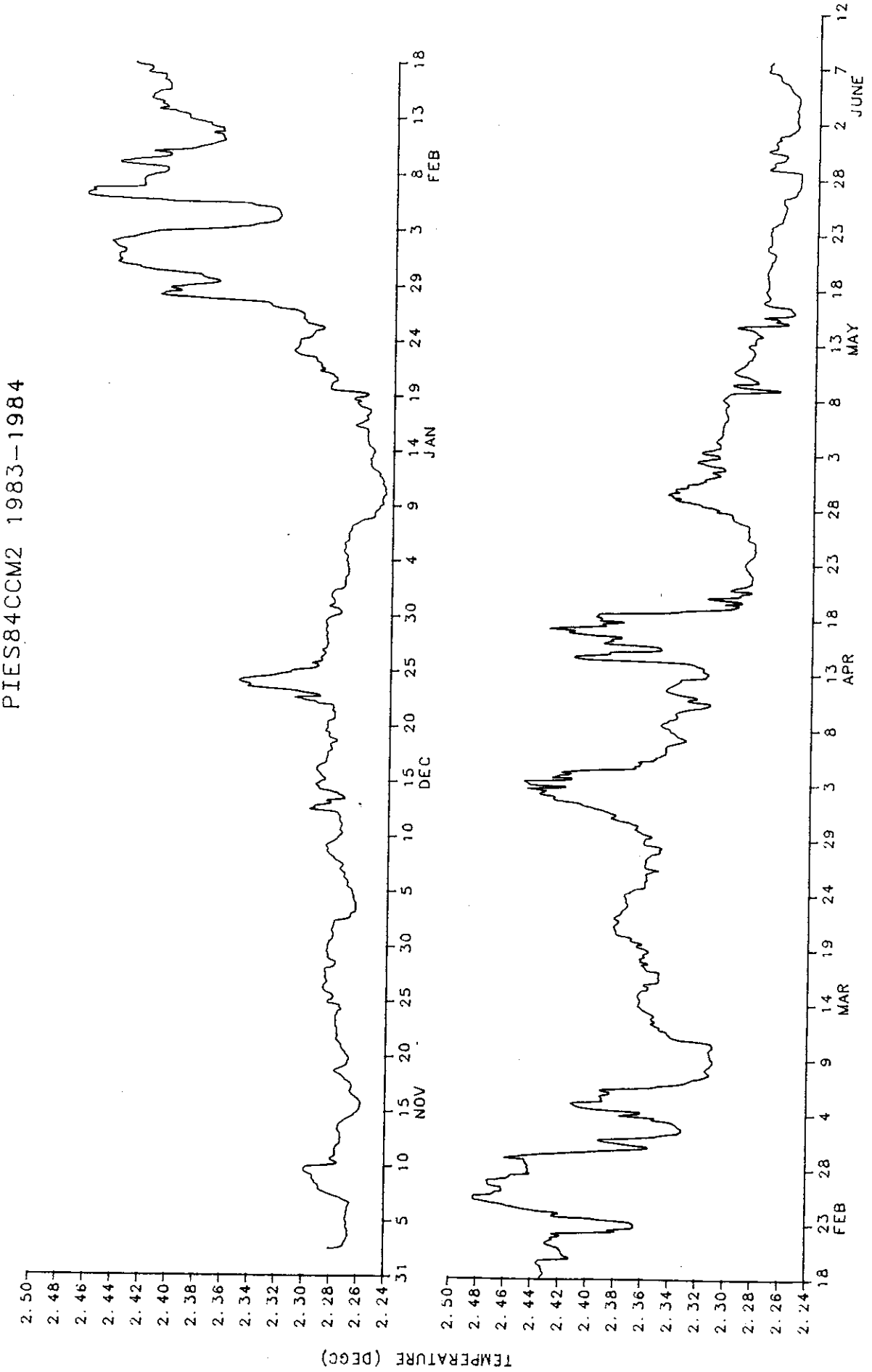

Figure 10.7 Raw temperature record of PIES84CCM2

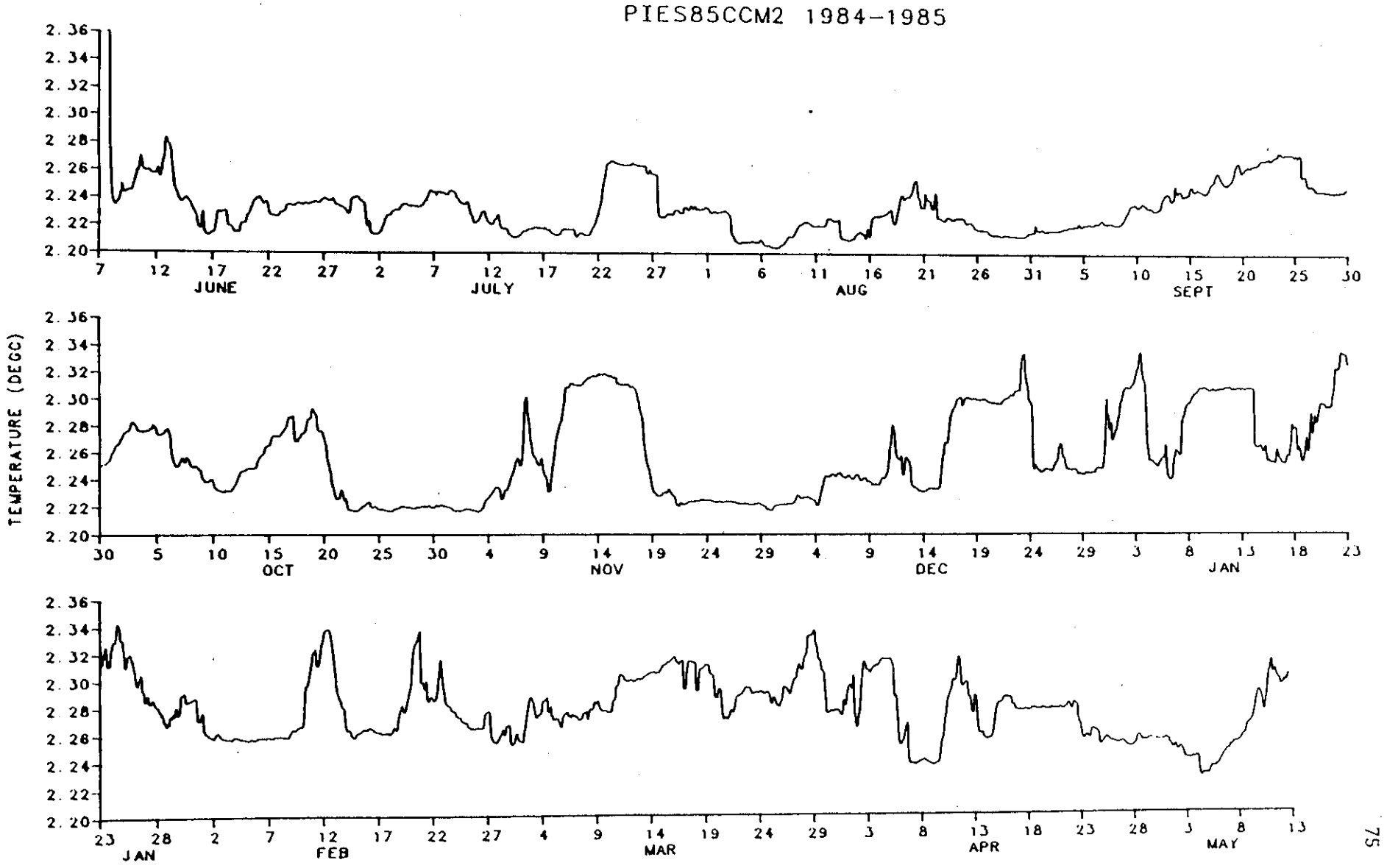

Figure 10.8 Raw temperature record of PIES85CCM2

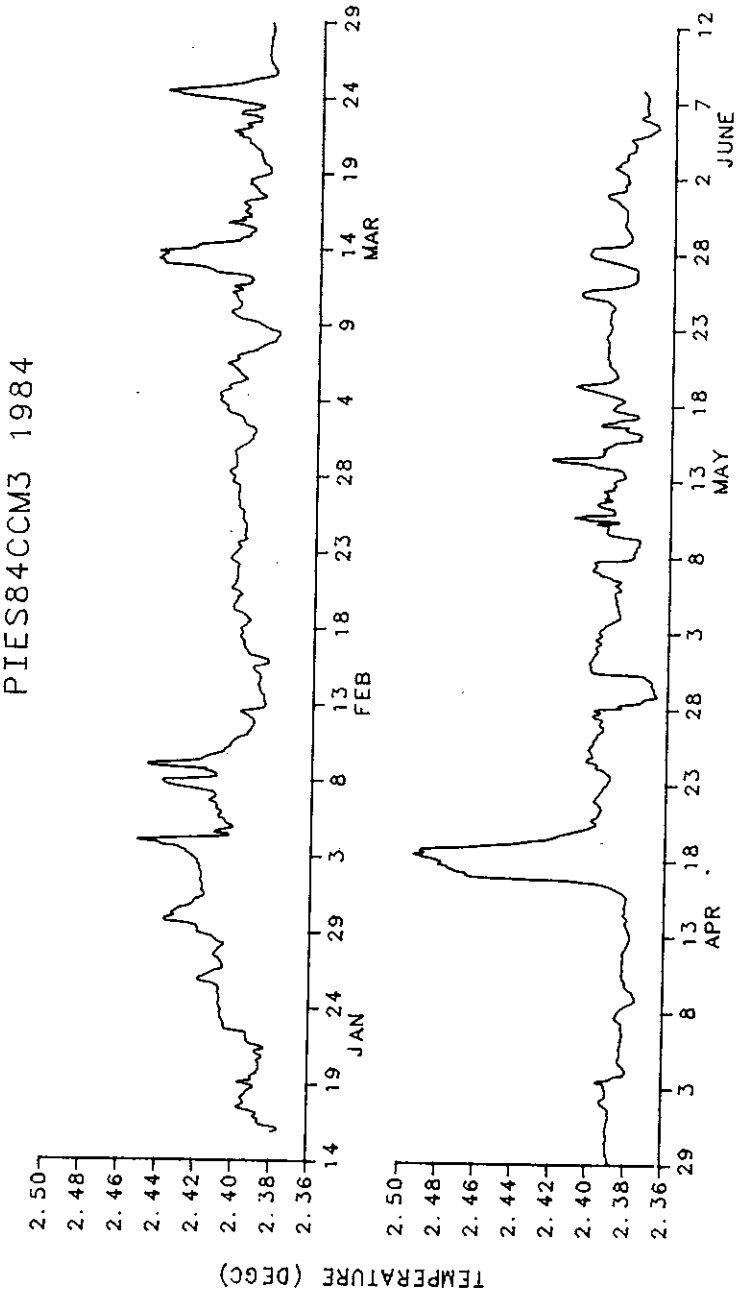

Figure 10.9 Raw temperature record of PIES84CCM3

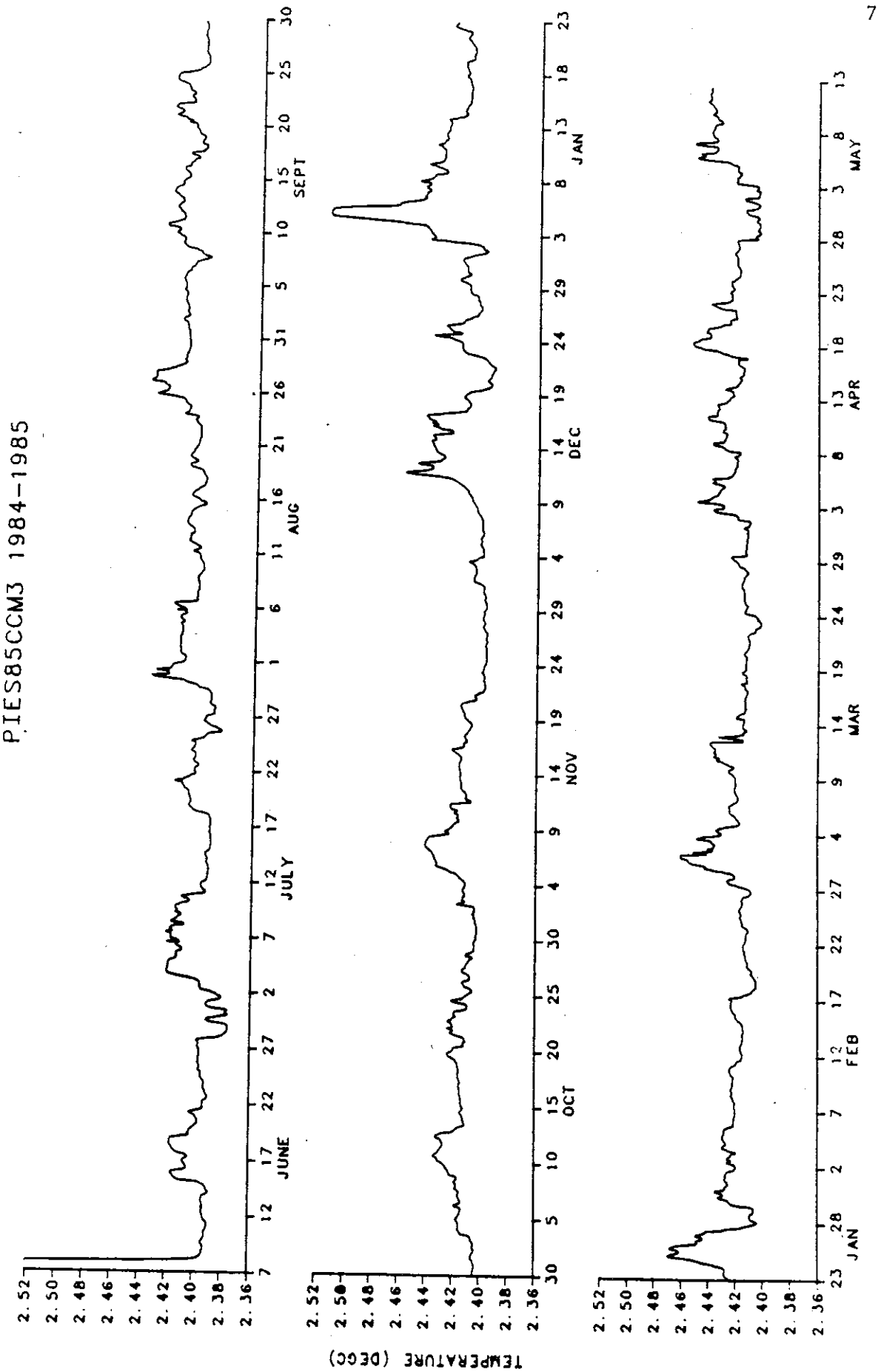

Figure 10.10 Raw temperature record of PIES85CCM3

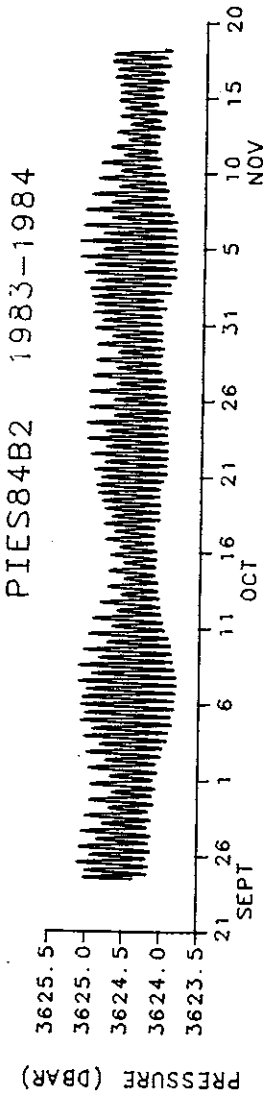

Figure 10.11 Raw pressure record of PIES84B2

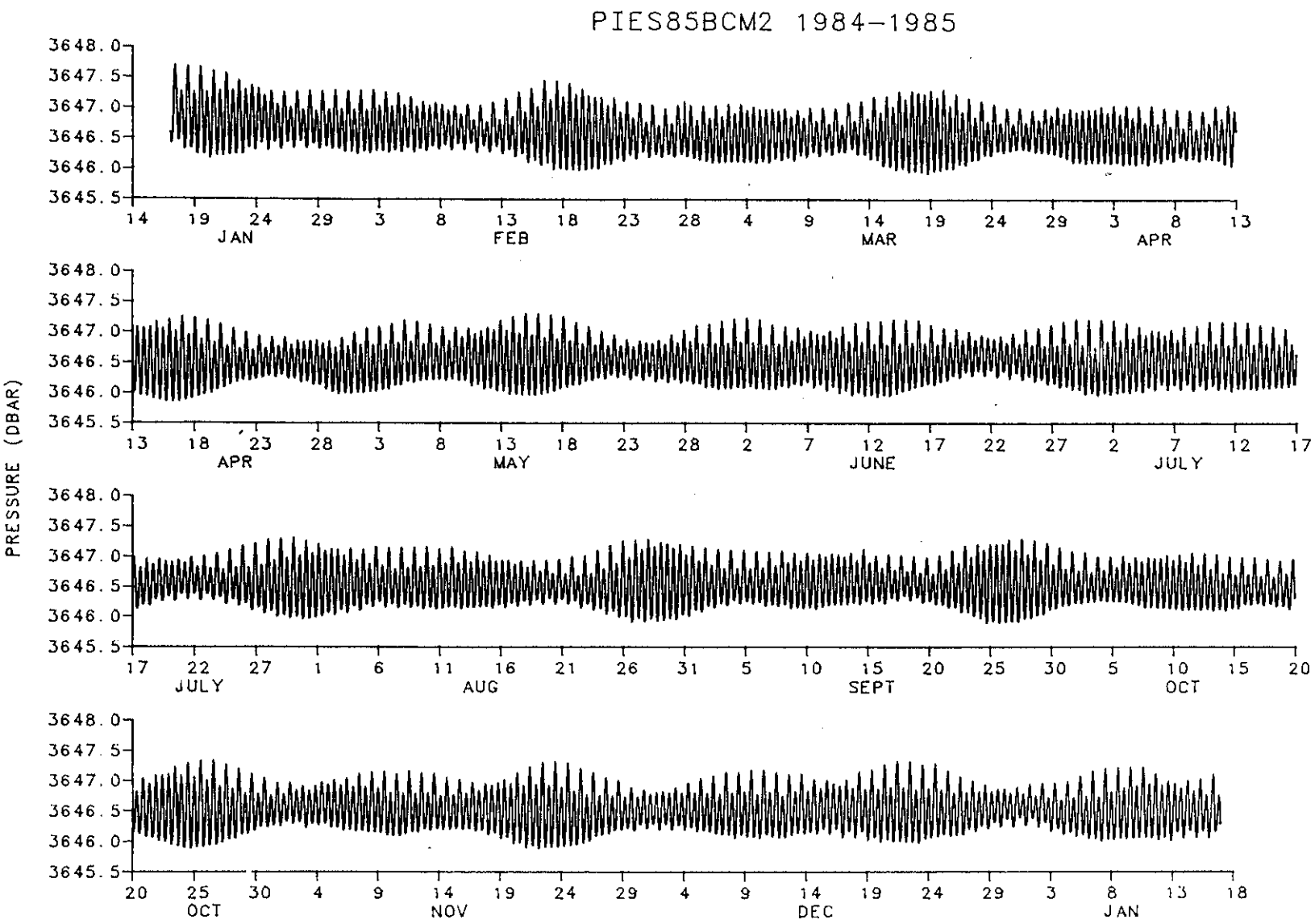

Figure 10.12 Raw pressure record of PIES85BCM2

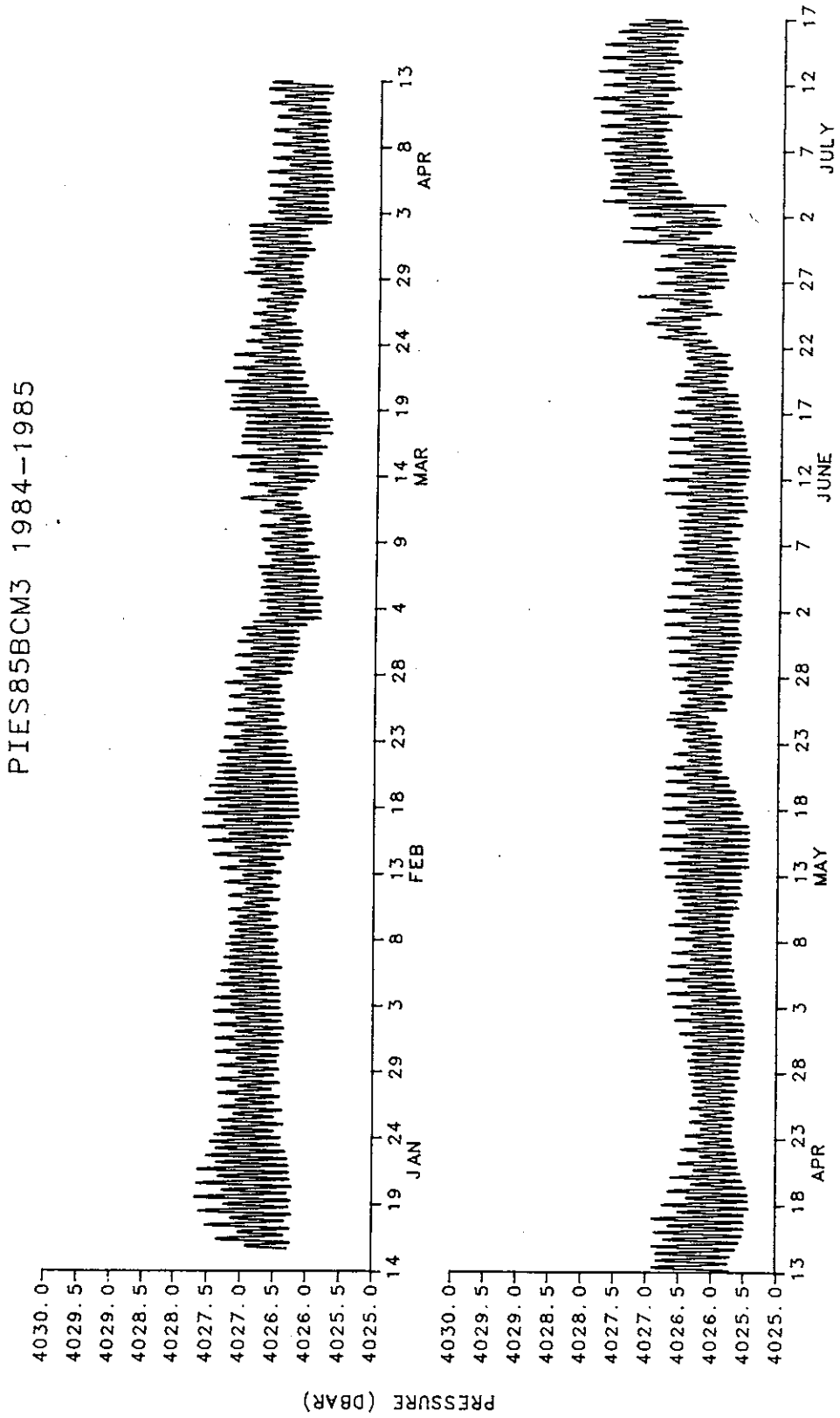

Figure 10.13a Raw pressure record of PIES85BCM3, an unreliable, "jumpy" record.

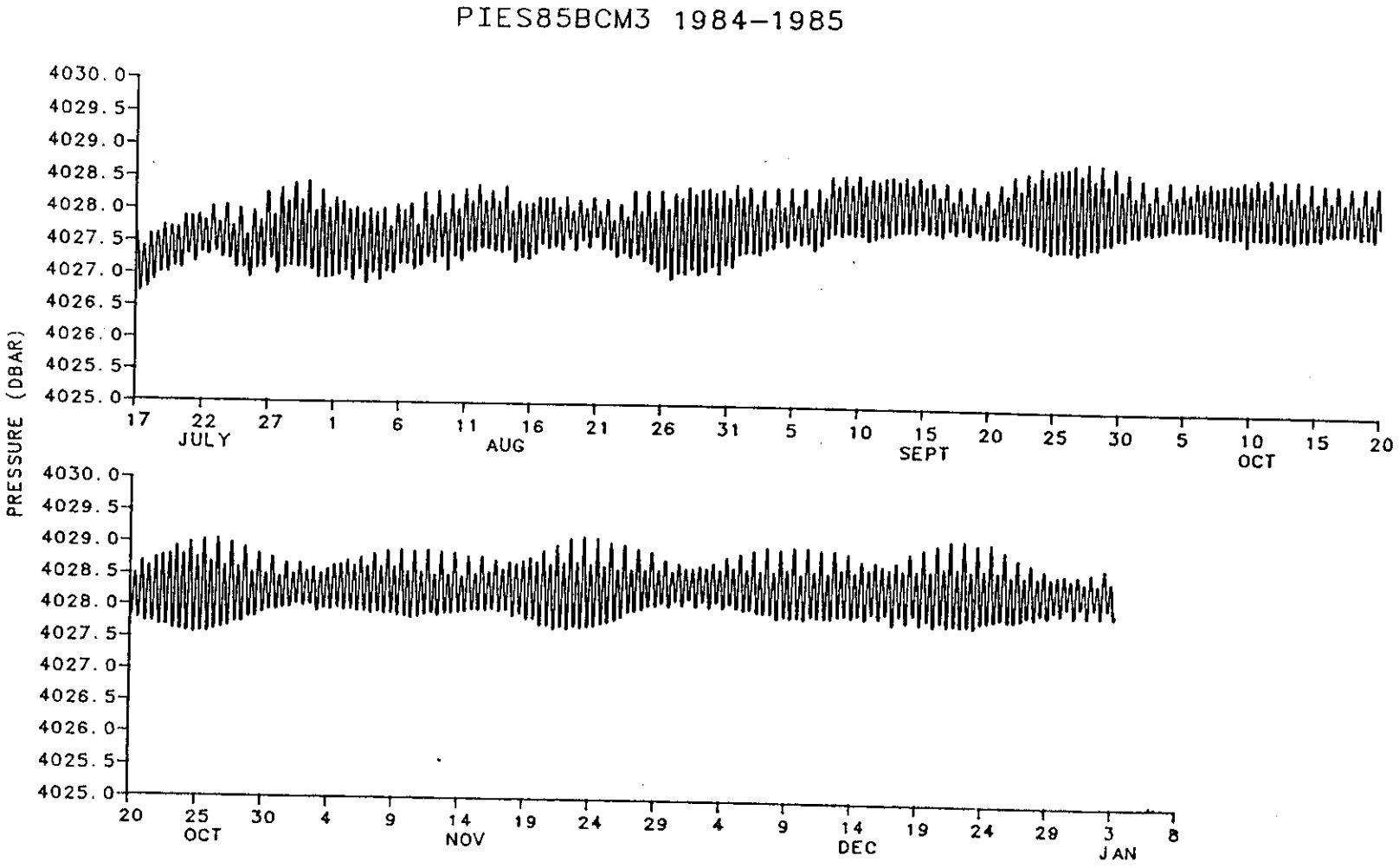

Figure 10.13b Raw pressure record of PIES85BCM3, an unreliable, "jumpy" record, continued.

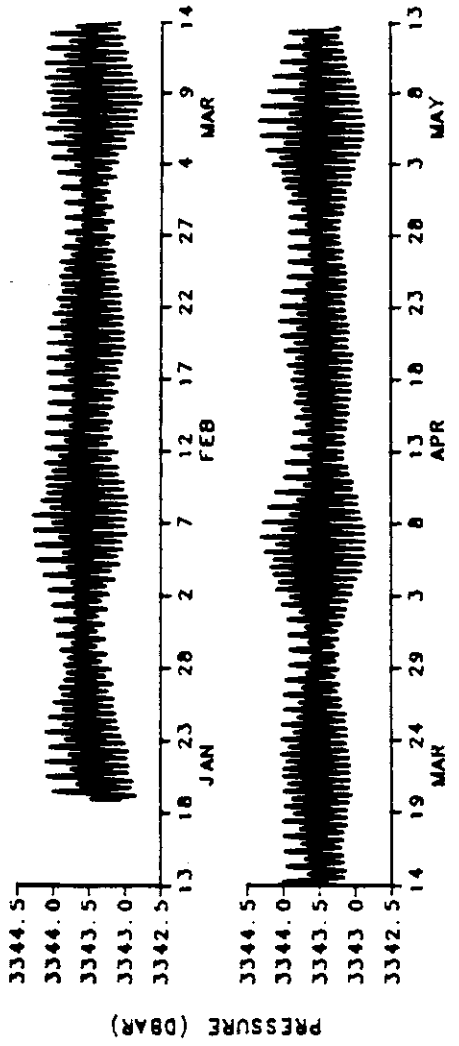

Figure 10.14 Raw pressure record of PIES85C0

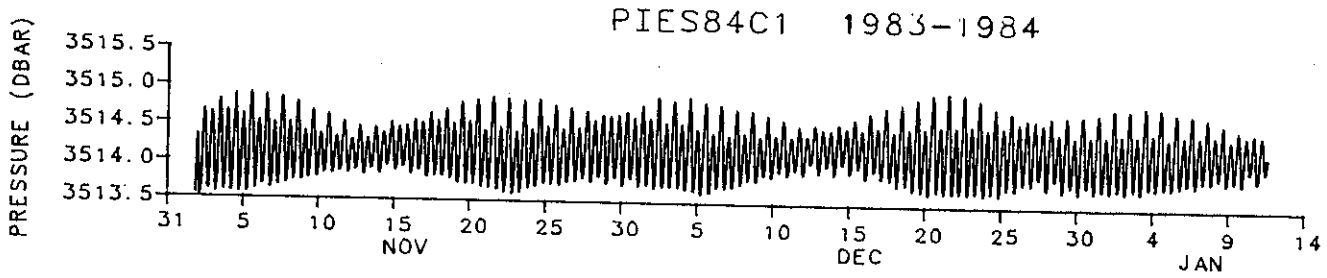

Figure 10.15 Raw pressure record of PIES84C1

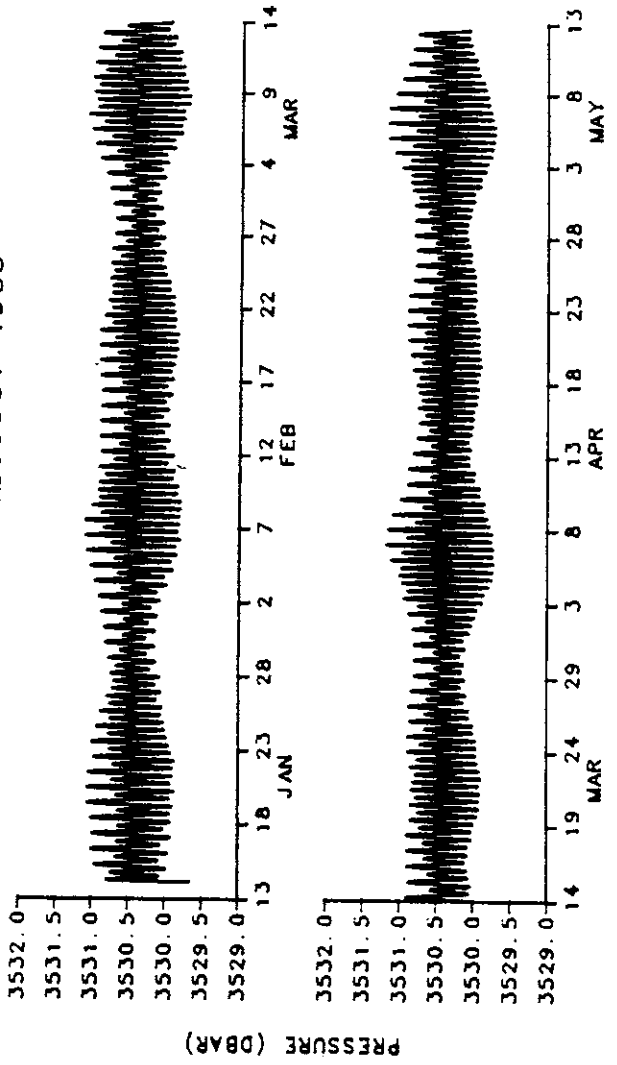

Figure 10.16 Raw pressure record of PIES85C1

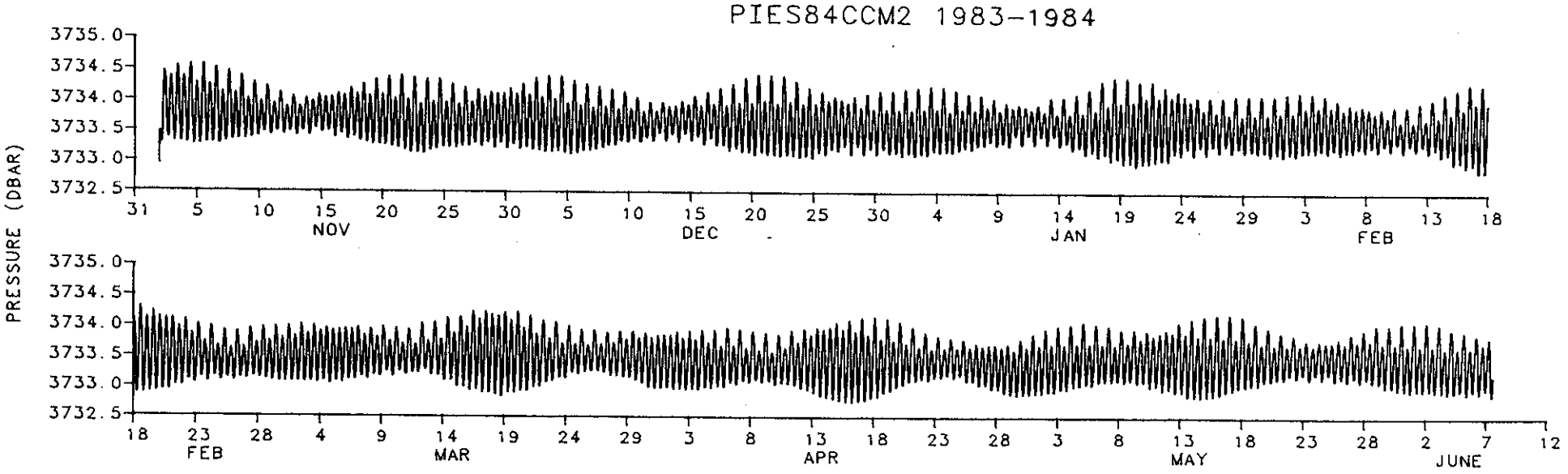

Figure 10.17 Raw pressure record of PIES84CCM2

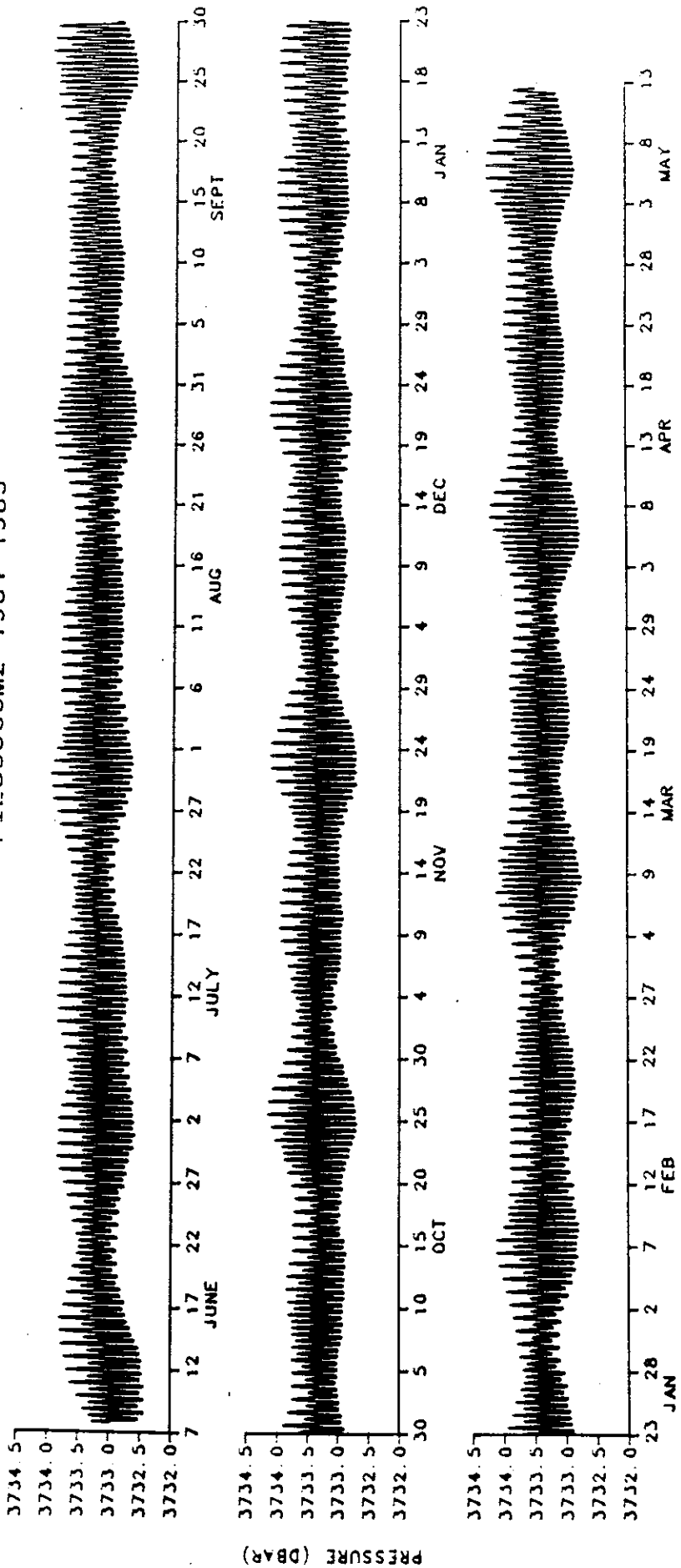

Figure 10.18 Raw pressure record of PIES85CCM2

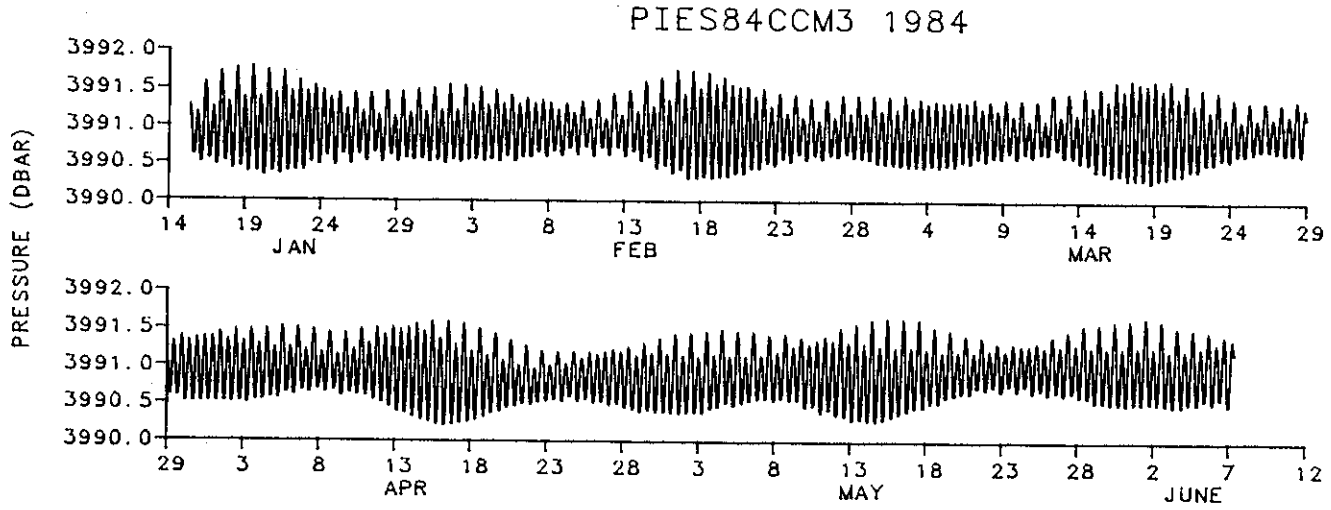

Figure 10.19 Raw pressure record of PIES84CCM3

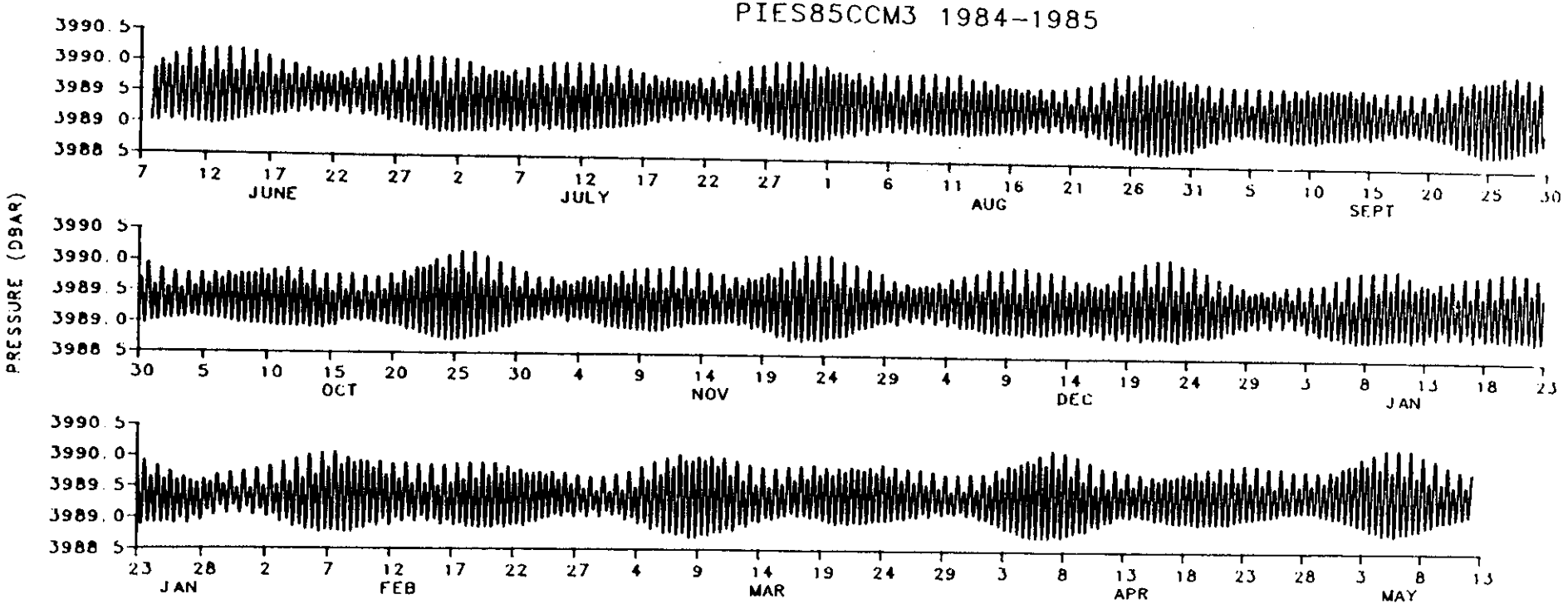

Figure 10.20 Raw pressure record of PIES85CCM3

11. DETIDED PRESSURE RECORDS AND DRIFT CURVES

The detided pressure (P_{detide}) records, which have had the mean and the tides removed, are presented in Figures 11.1 to 11.10. For the records which had a measurable long-term drift, the regressed drift curves are superimposed on the pressure curves.

The vertical scale of 0.1 dbar per increment is consistent between all records, except for PIES85BCM3 (Figure 11.3), which had large unexplained jumps. For that instrument, the vertical scale has been doubled to 0.2 dbar per increment.

The time scale is the same for all plots with each increment corresponding to 25 days. The axis begins on 0000 GMT of the first date labelled.

The sampling interval is 0.5 hours for all instruments. The length and start and end times of the data are tabulated in Section 9.

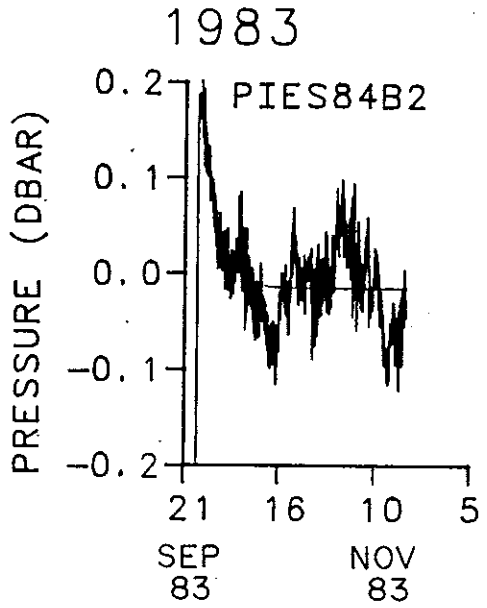

Figure 11.1 Detided pressure record of PIES84B2

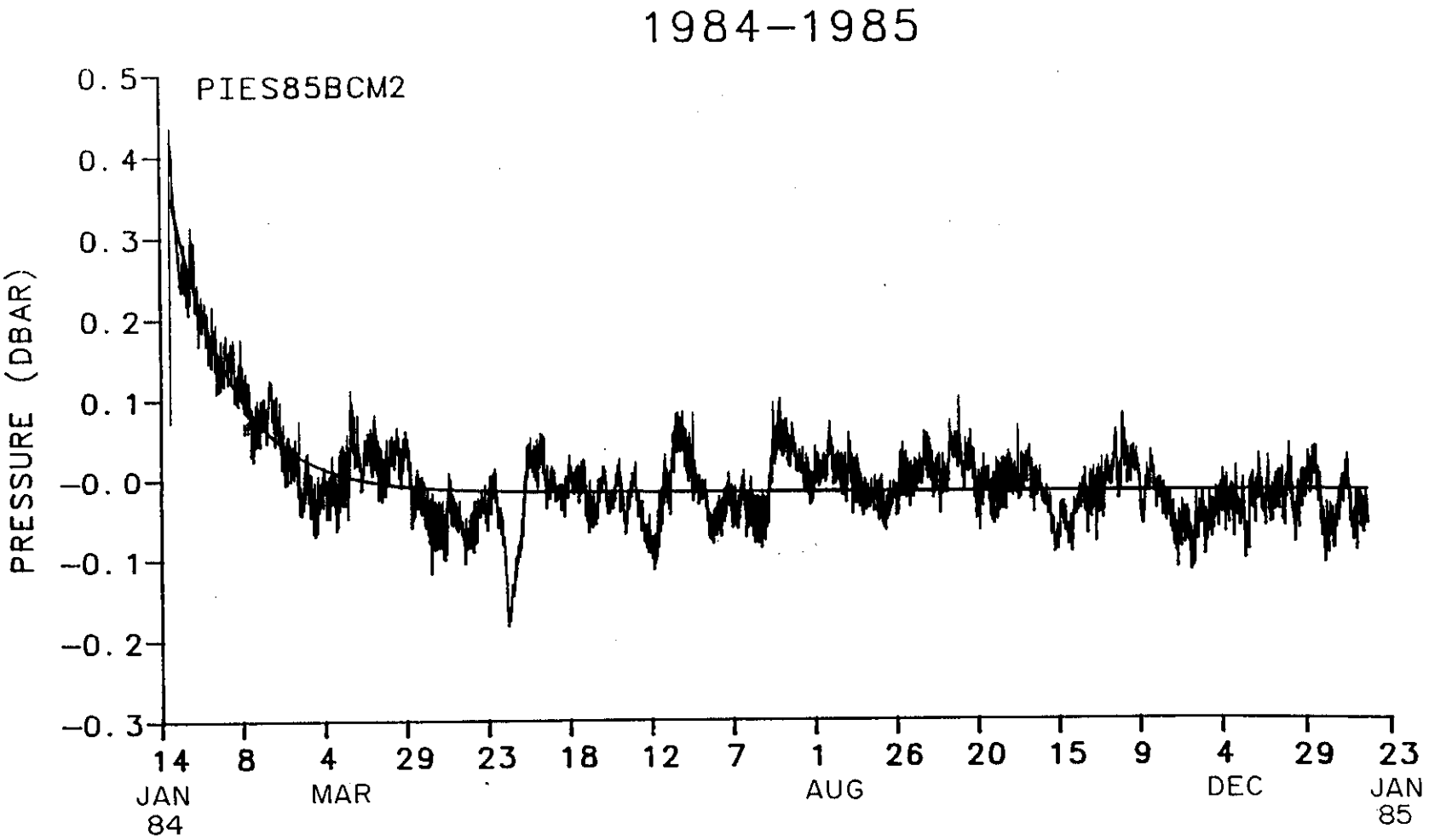

Figure 11.2 Detided pressure record of PIES85BCM2

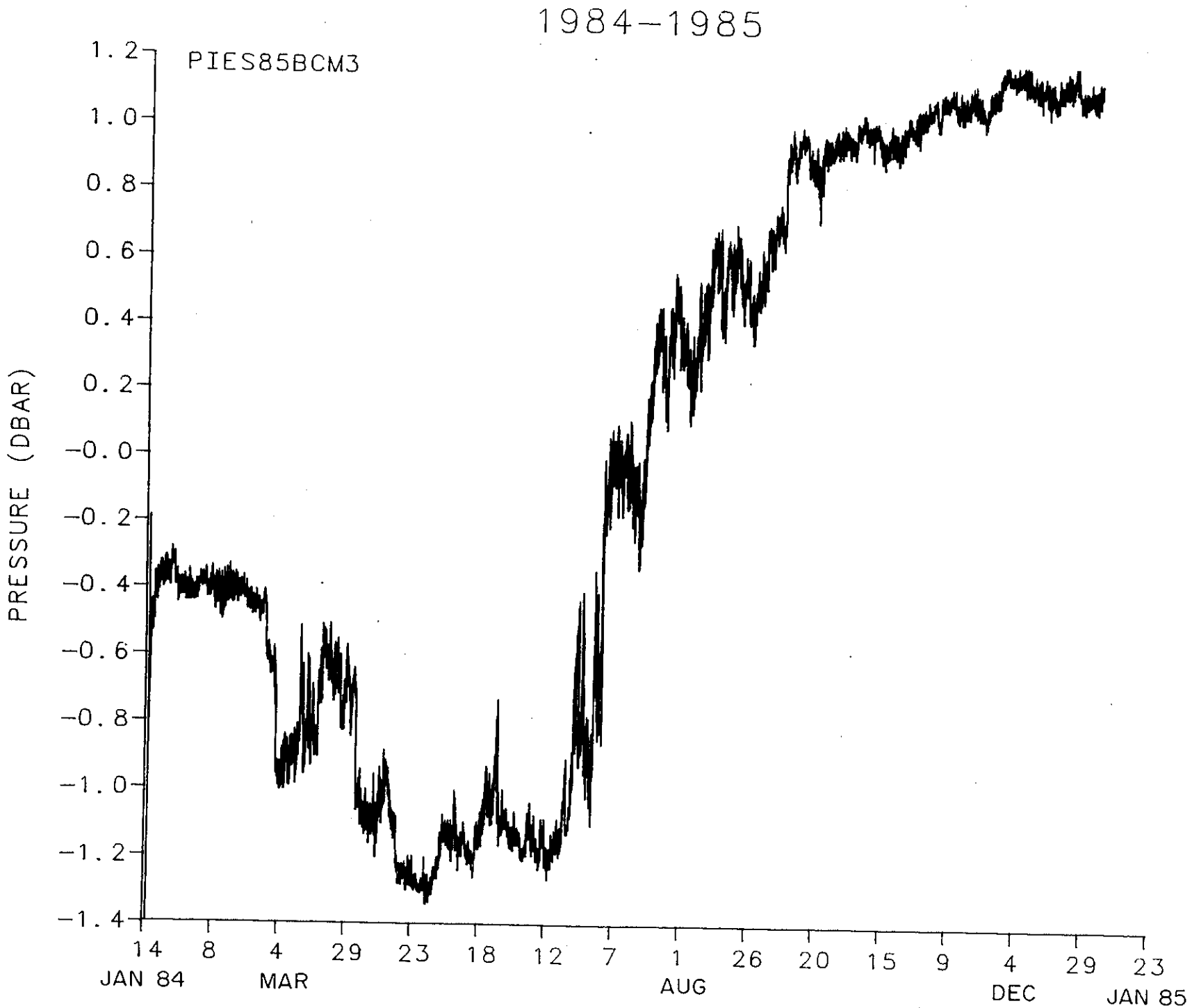

Figure 11.3 Detided pressure record of PIES85BCM3. This record has unexplained jumps and is unreliable.

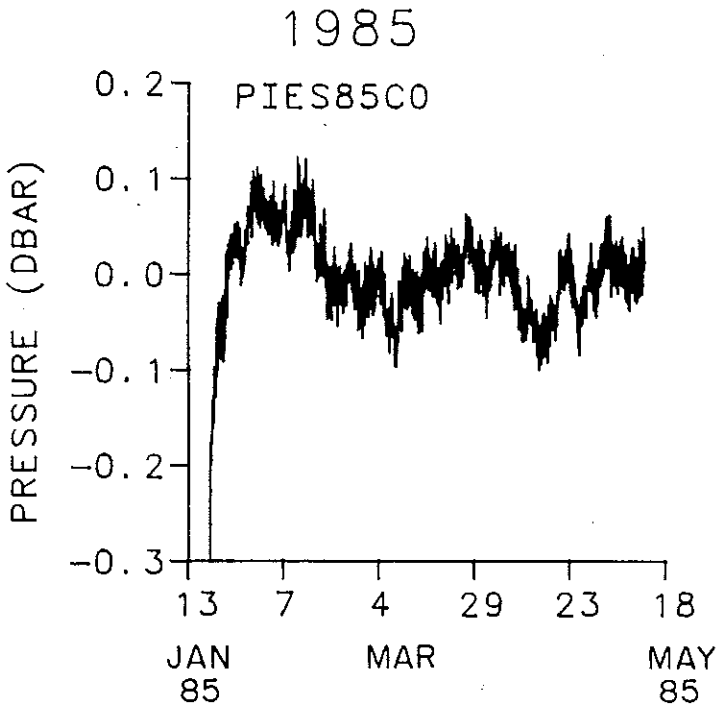

Figure 11.4 Detided pressure record of PIES85C0

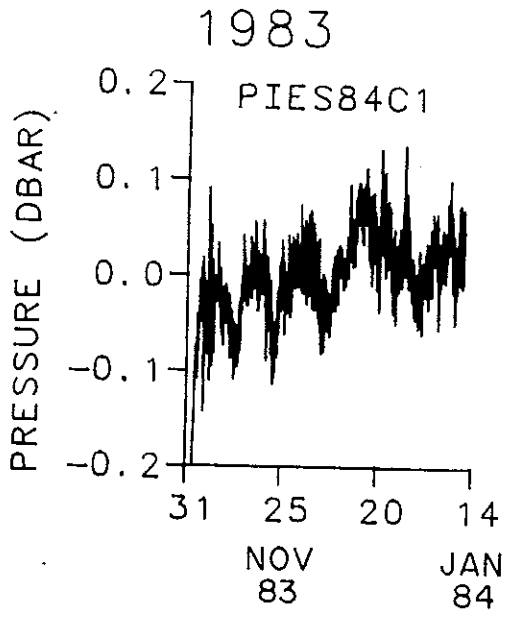

Figure 11.5 Detided pressure record of PIES84C1

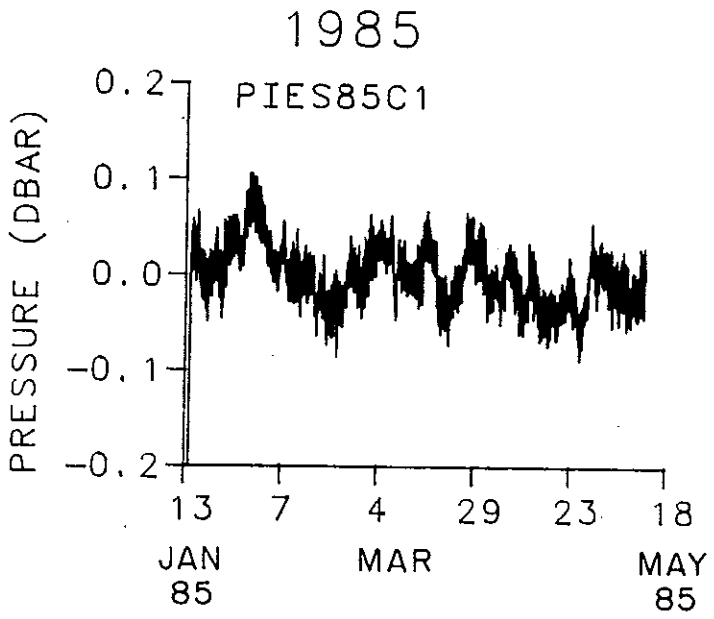

Figure 11.6 Detided pressure record of PIES85C1

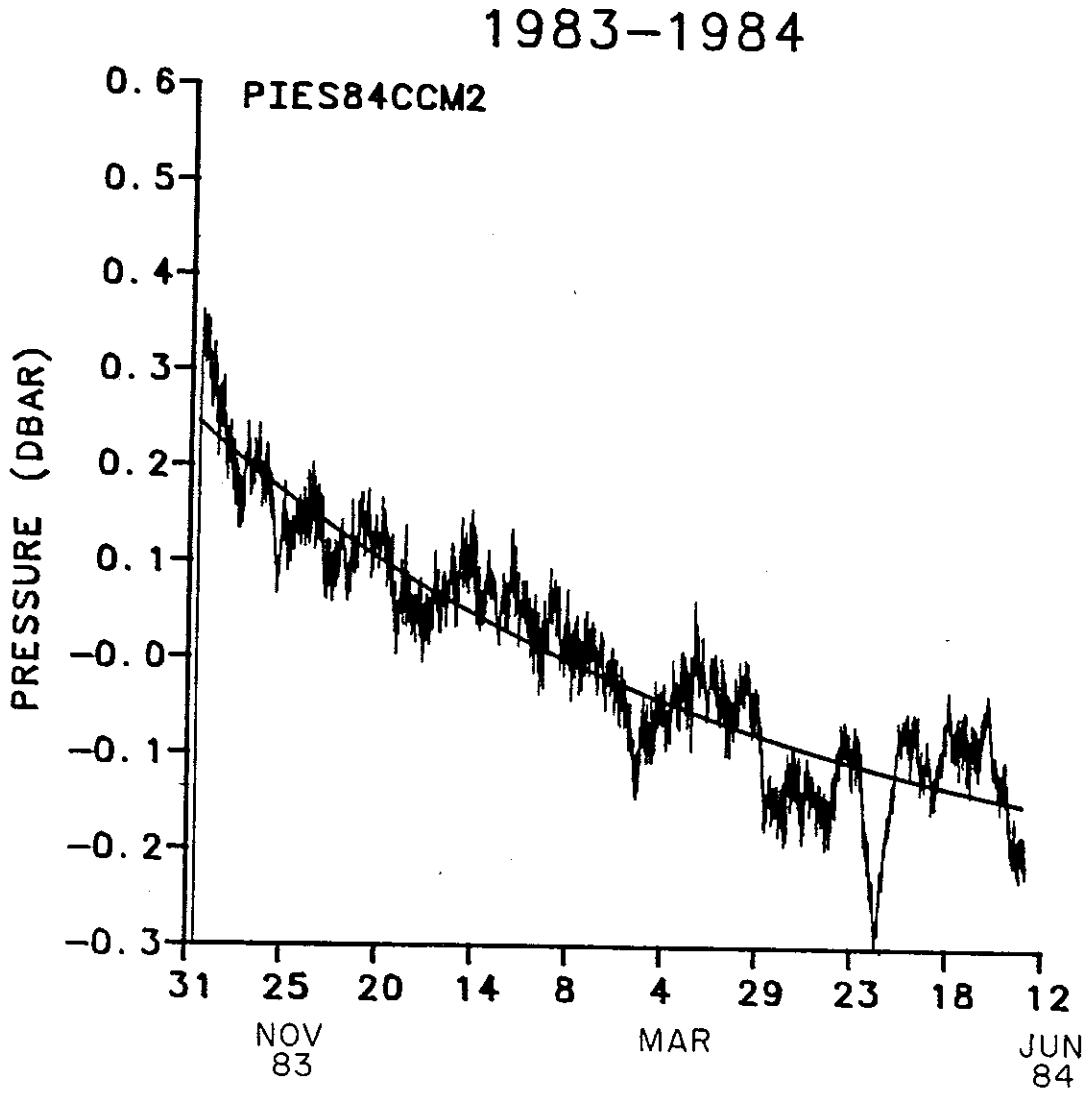

Figure 11.7 Detided pressure record of PIES84CCM2

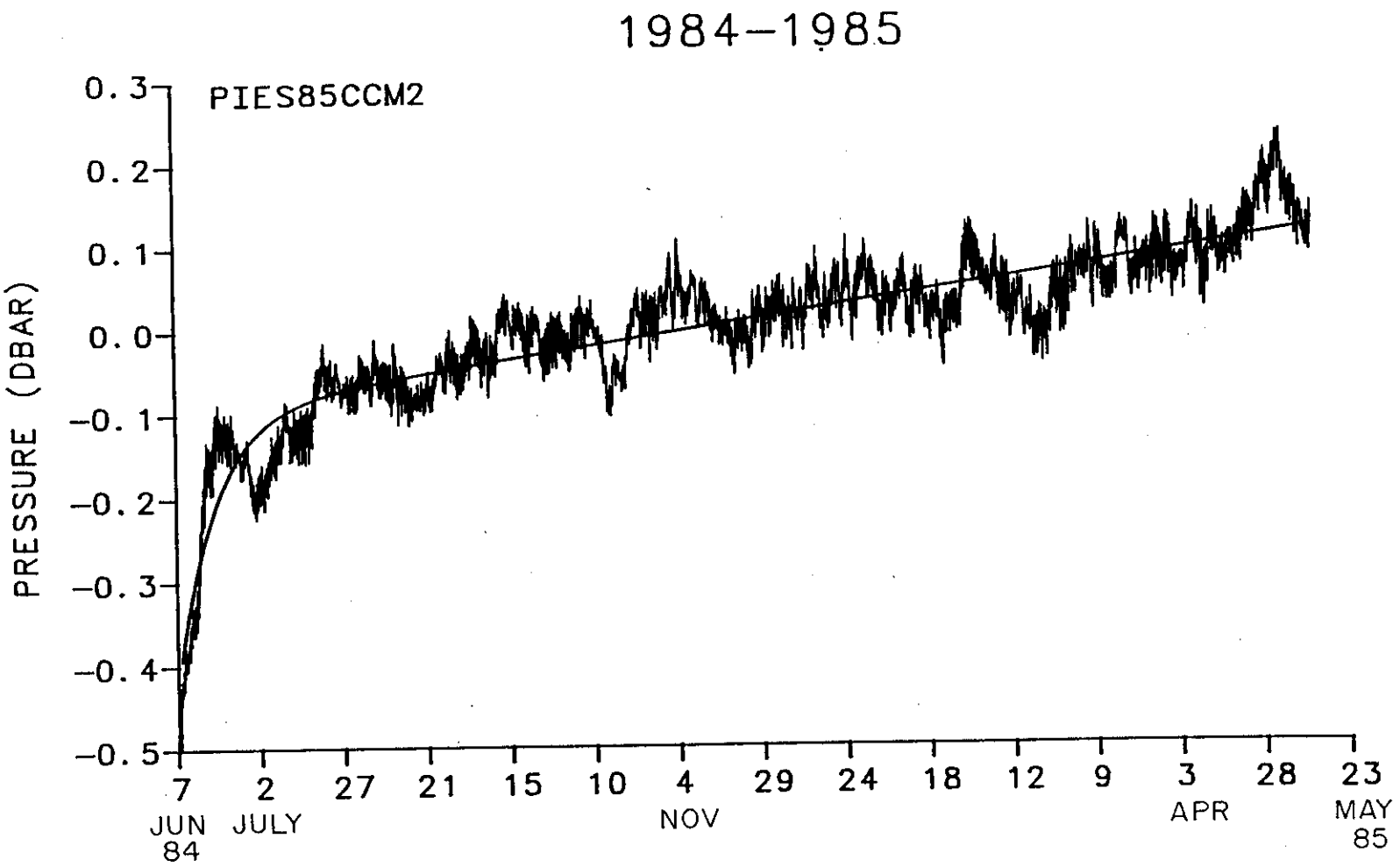

Figure 11.8 Detided pressure record of PIES85CCM2

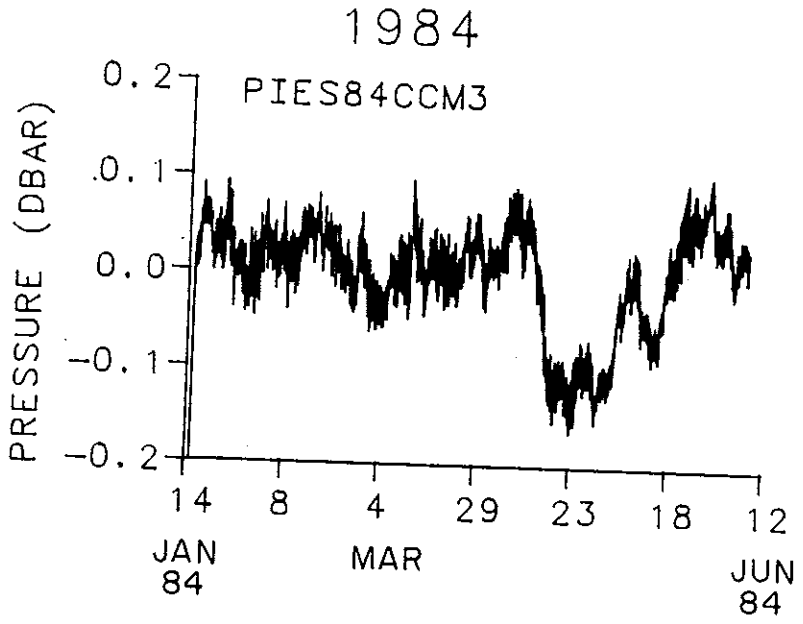

Figure 11.9 Detided pressure record of PIES84CCM3

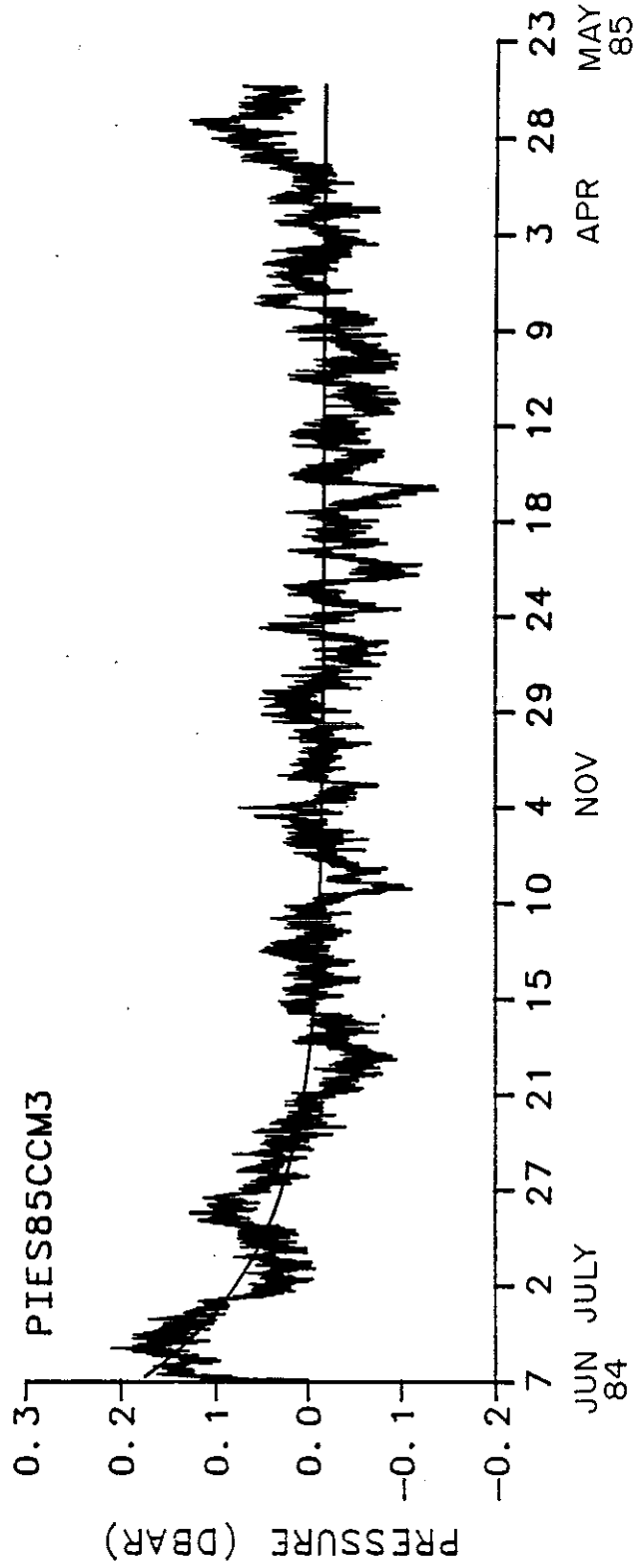

Figure 11.10 Detided pressure record of PIES85CCM3

12. FULLY PROCESSED RECORDS

The low-pass filtered temperature and bottom pressure records are presented for each instrument. The 40HRLP temperature records are shown first. These are followed by the 40HRLP, detided, dedrifted pressure records.

The time scale is the same for all plots, with each increment corresponding to 10 days. The axis begins on 0000 GMT of the first date labelled. Since the measurements at several of the sites were obtained by two or more instruments, the data for January to May 1984 is repeated in the figures to show coinciding measurements. Each record is labelled with the instrument names above the appropriate portions.

The vertical scale for each variable is consistent between instruments. Each increment corresponds to 0.05 dbar for the bottom pressure measurements and 0.04^{o}C for the temperatures.

The sampling interval is 6 hours for all the records. The length and start and end times of the data records are tabulated in Section 9.

12.1 Temperature: 40HRLP data

The 40HRLP temperature records are shown in Figures 12.1 to 12.3. the square-pulse nature of the temperature records has been rounded somewhat by the low-pass filtering. Visually, the temperature records from different sites have overall only a small amount of coherence; many pulses are quite different from one site to another.

12.2 Pressure: detided, dedrifted, 40HRLP data

The 40HRLP bottom pressure records are shown in Figures 12.4 to 12.6. Visually, the coherence between pressure records at neighboring sites is quite high. We have identified some of the major pressure events with the passage of Gulf Stream rings offshore and their

coalescence into the Gulf Stream (Bane and Watts, 1985). Pressure and temperature records at the same site do not appear to be very coherent, although some events occur simultaneously in both.

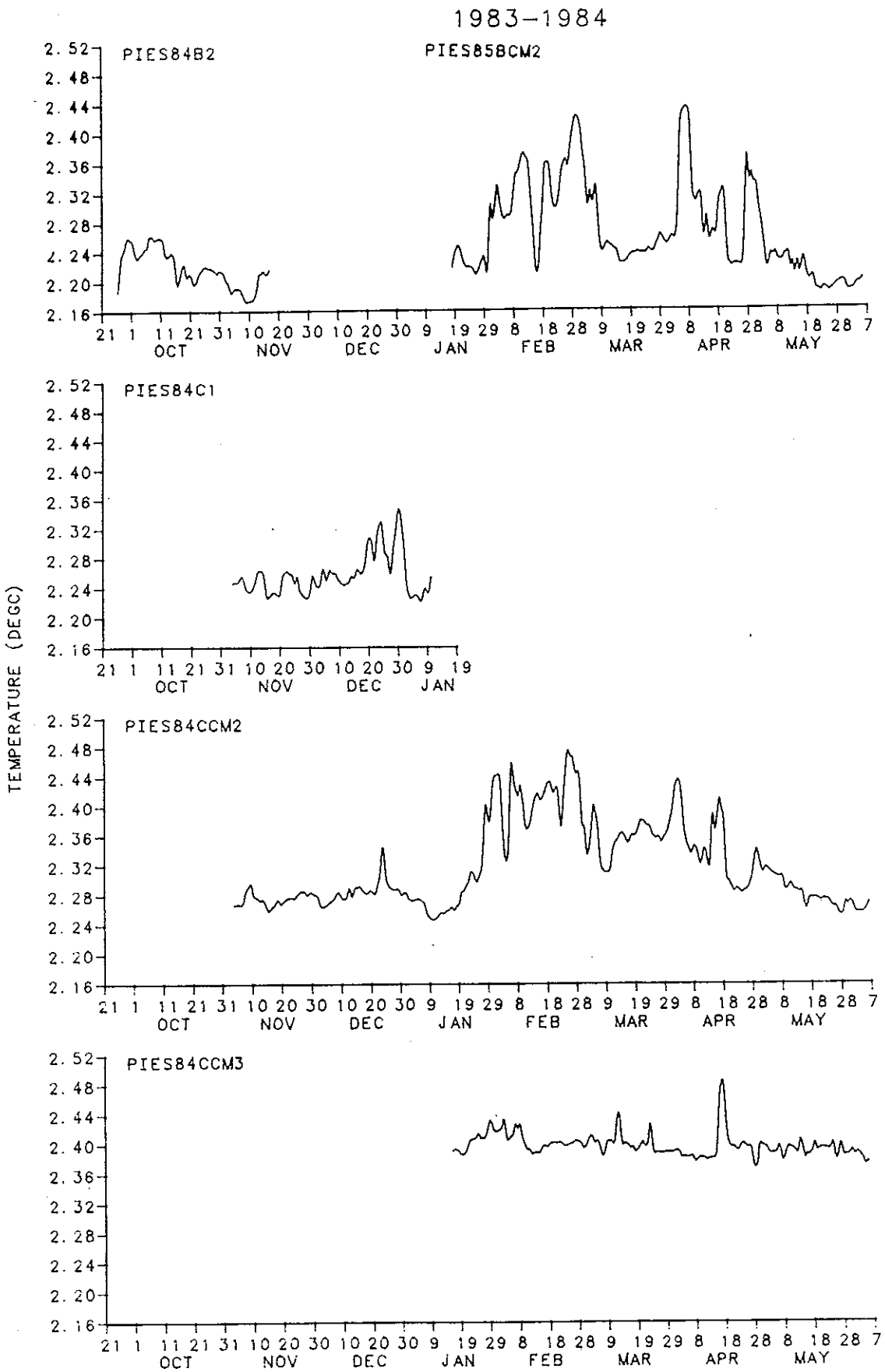

Figure 12.1 40HRLP temperature records for 1983-1984

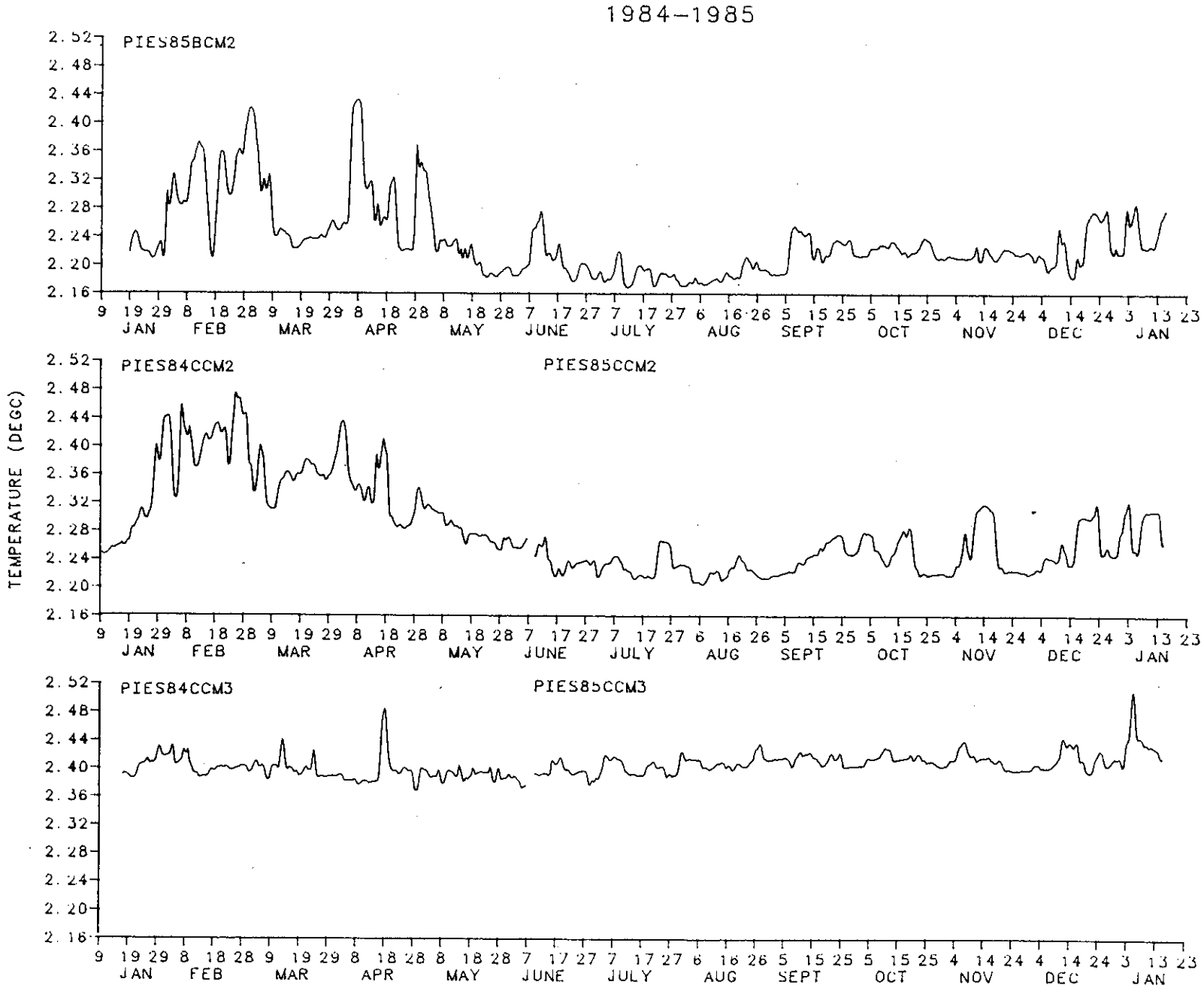

Figure 12.2 40HRLP temperature records for 1984-1985

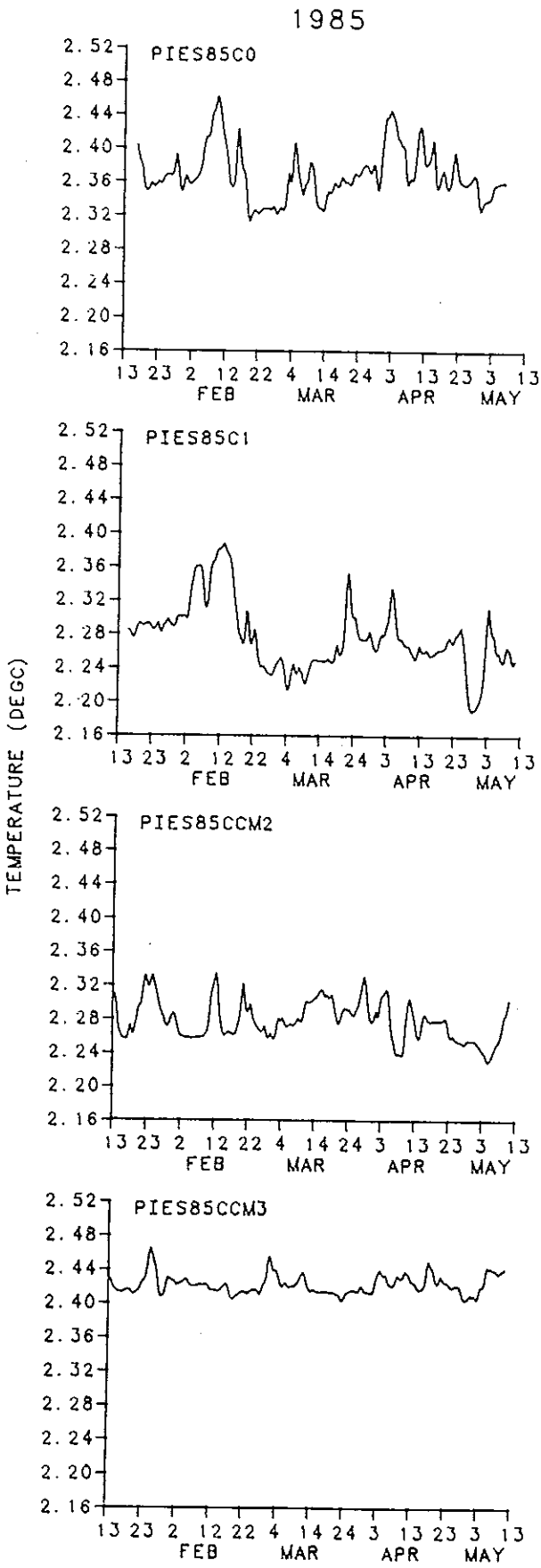

Figure 12.3 40HRLP temperature records for 1985

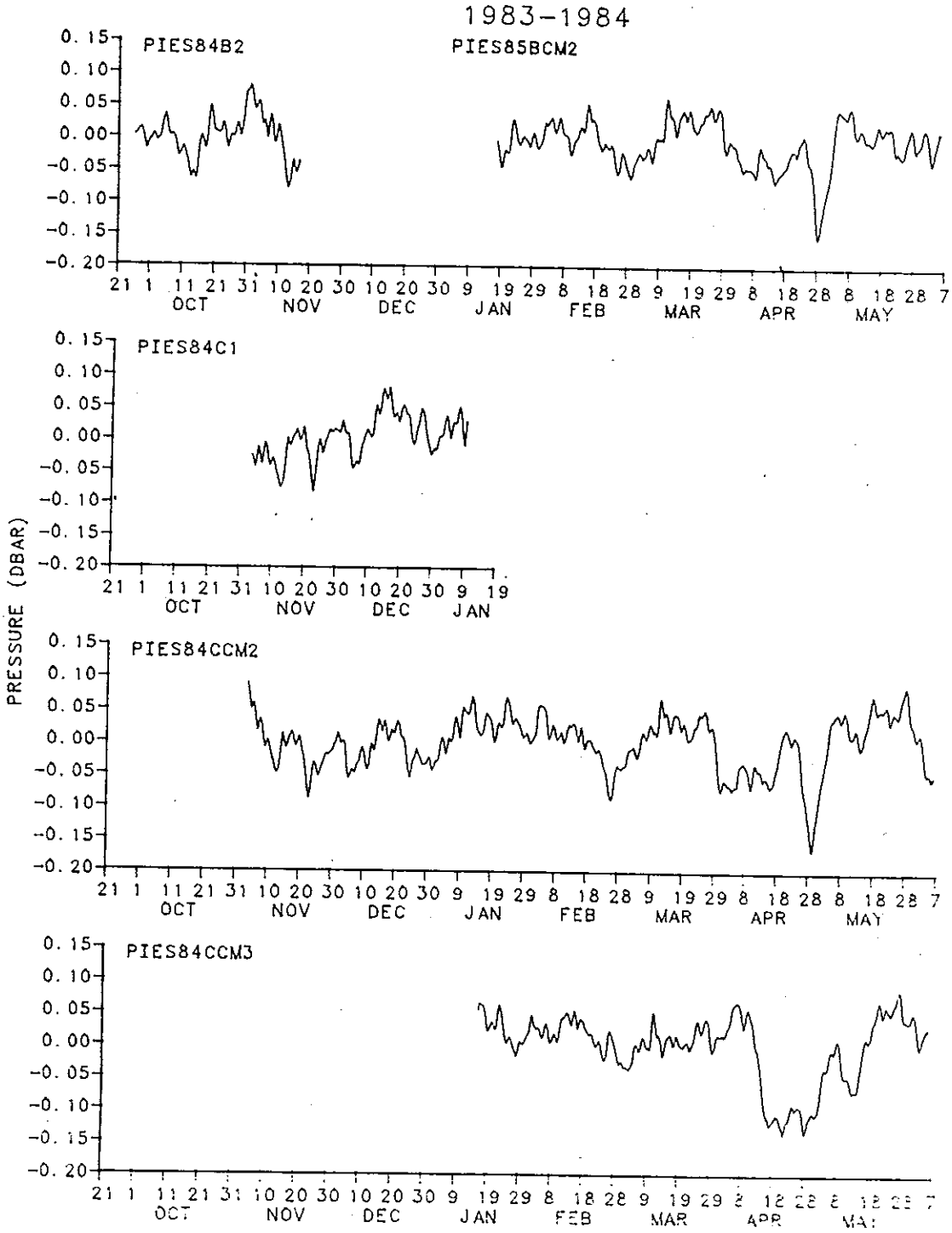

Figure 12.4 40HRLP bottom pressure records for 1983-1984

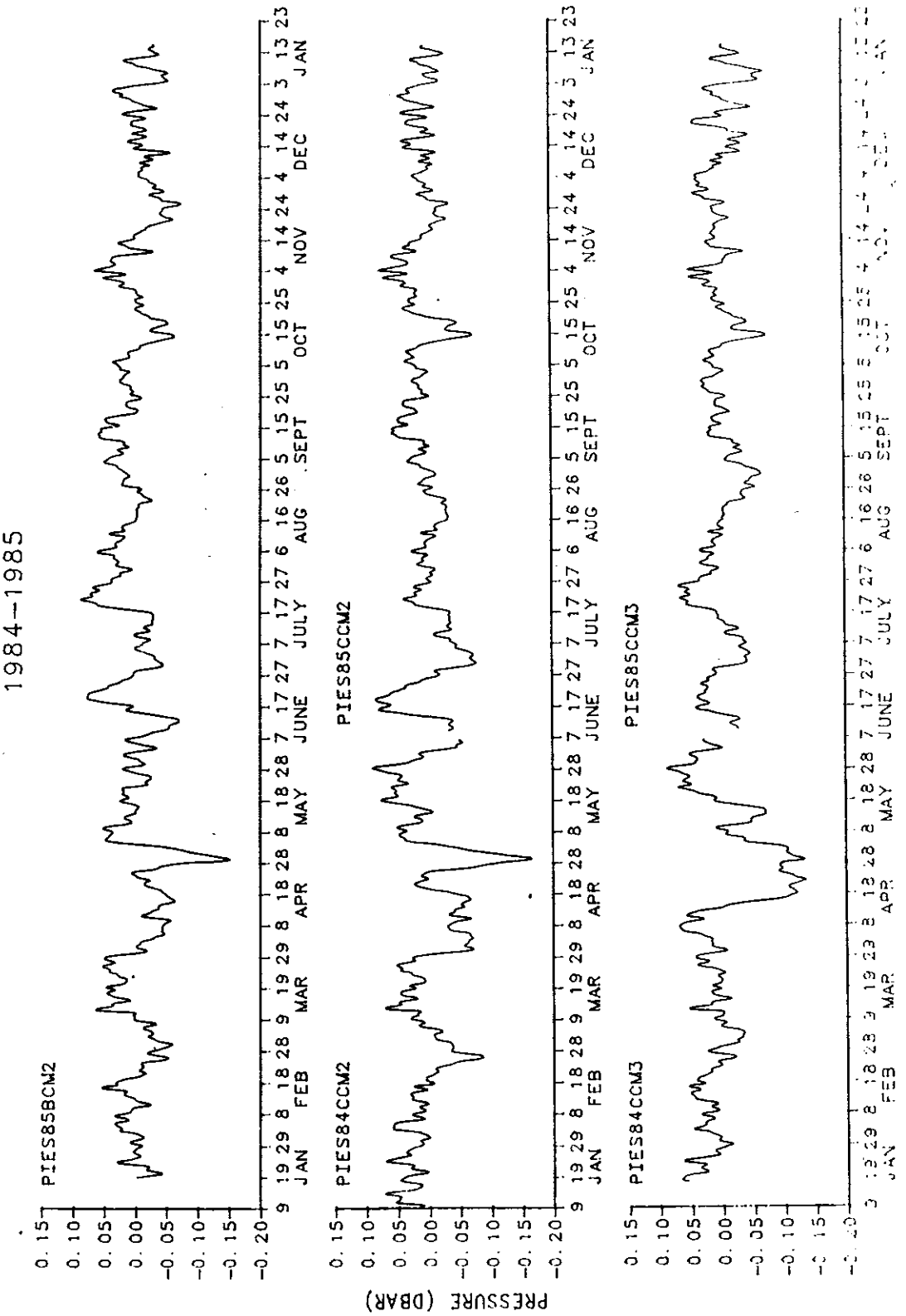

Figure 12.5 40HRLP bottom pressure records for 1984-1985

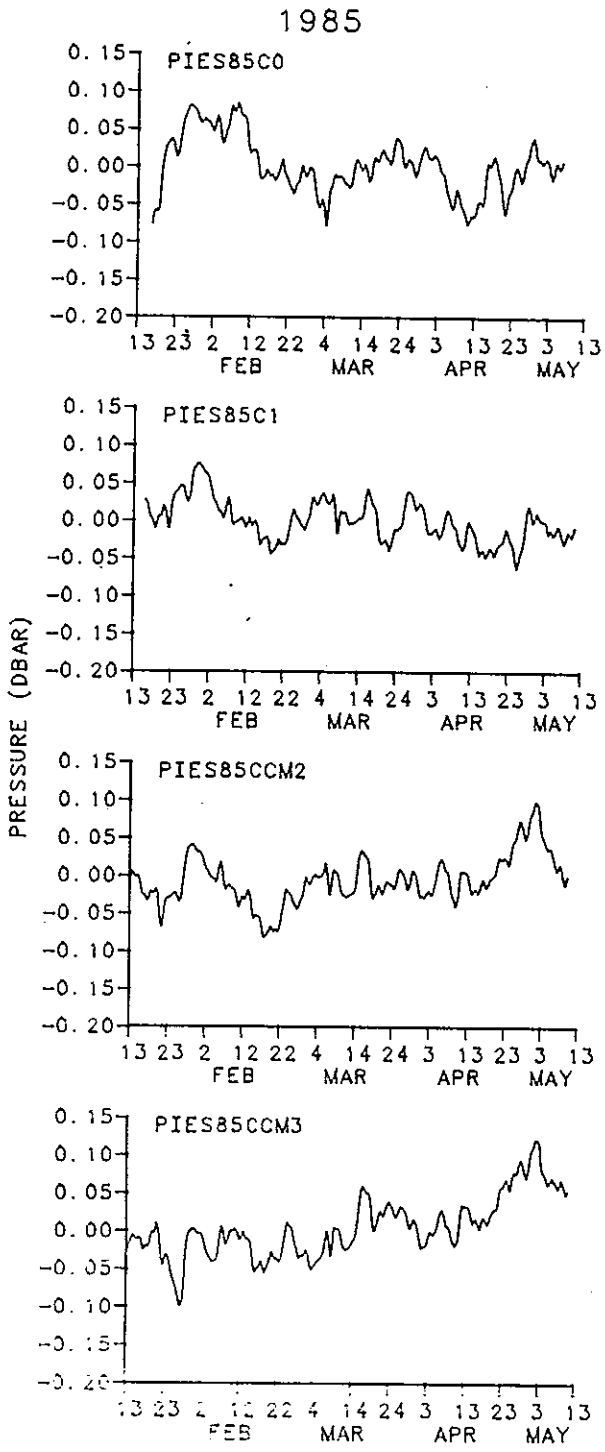

Figure 12.6 40HRLP bottom pressure records for 1985

ACKNOWLEDGEMENTS

This research program was funded by the National Science Foundation under grant number OCE82-01222 and by the Office of Naval Research under contract N00014-81-C-0062. We thank Karen Tracey, Mark Wimbush, and Steve Chiswell for their advice, Dr. Frank Gonzalez of NOAA/PMEL for suggestions on an early draft of this paper, and Julie Rahn for editorial assistance.

REFERENCES

Baker, D. J., Jr. 1981. Ocean instruments and experimental design. In: Evolution of Physical Oceanography. B. A. Warren and C. Wunsch, Eds. (Cambridge, MA: MIT Press), pp. 396-433.

Bane, J. M., Jr. and Watts, D. R. 1985. The Gulf Stream east of Cape Hatteras: the current and its events in 1984. EOS (Trans. Amer. Geoph. Union). 66. 1276.

Beardsley, R. C., H. Mofjeld, M. Wimbush, J. A. Vermersch, Jr. and C. N. Flagg. 1977. Ocean tides and weather-induced bottom pressure fluctuations in the middle-Atlantic bight. J. Geophys. Res. 82. 3175-3182.

Brooks, D. A. 1976. (Editor). Fast and Easy Time Series Analysis at NCSU. Technical Report. Center for Marine and Coastal Studies. North Carolina State University. Raleigh, NC.

Brown, W., W. Munk, F. Snodgrass, H. Mofjeld and B. Zetler. 1975. MODE bottom experiment. J. Phys. Oceanogr. 5. 75-85

Chaplin, G. and D. R. Watts. 1984. Inverted echo sounder development. Oceans '84 Conference Record. 1. 249-253.

Dixon, W. J. and M. B. Brown. 1979. (Editors). BMDP-79 Biomedical Computer Programs P-series. University of California Press. Berkeley, CA. 880 pp.

Filloux, J. H. 1971. Deep-sea tide observations from the northeastern Pacific. Deep-Sea Research. 18. 275-284.

Friedlander, A. I., K. L. Tracey, and D. R. Watts. 1986. The Gulf Stream Dynamics Experiment: Inverted Echo Sounder Data Report for the July 1982 to April 1983 Deployment Period. University of Rhode Island. GSO Technical Report 86-5.

Mofjeld, H. O. and M. Wimbush. 1977. Bottom pressure observations in the Gulf of Mexico and Caribbean Sea. Deep-Sea Research. 24. 987-1004.

Munk, W. H. and D. E. Cartwright. 1977. Tidal spectroscopy and prediction. Philos. Trans. R. Soc. London. 259. 533-581.

Paros, J. M. 1976. Digital pressure transducers. Measurements and Data. 10. 74-79.

Snodgrass, F., W. Brown, and W. Munk. 1975. MODE: IGPP measurements of bottom pressure and temperature. J. Phys. Oceanogr. 5. 63-74.

Tracey, K. L., M. Cronin, and D. R. Watts. 1985. The Gulf Stream Dynamics Experiment: Inverted Echo Sounder Data Report for the June 1984 to May 1985 Deployment Period. University of Rhode Island. GSO Technical Report 85-3.

Tracey, K. L., and D. R. Watts. 1986. The Gulf Stream Dynamics Experiment: Inverted echo sounder data report for the April 1983 to June 1984 deployment period. University of Rhode Island. GSO Technical Report 86-4.

Tracey, K. L., and D. R. Watts. 1987. Inverted echo sounder processing procedures. University of Rhode Island. GSO Technical Report (in preparation).

Wearn, R. B., Jr. and N. G. Larson. 1980. The Paroscientific pressure transducer, measurement of its sensitivities and drift. Applied Physics Laboratory, University of Washington. Technical Report APL-UW 8011.

Wearn, R. B., Jr. and N. G. Larson. 1982. Measurements of the sensitivities and drift of Digiquartz pressure sensors. Deep-Sea Research. 29. 111-134.

Wimbush, M.. 1977. An inexpensive sea-floor precision pressure recorder. Deep-Sea Research. 24. 493-497.

Wunsh, C. and M. Wimbush. 1977. Simultaneous pressure velocity and temperature measurements in the Florida Straits. J. of Marine Res. 35. 75-104.

Zetler, B., W. Munk, H. Mofjeld, W. Brown and F. Dormer. 1975. MODE Tides. J. Phys. Oceanogr. 5. 430-441.

Unclassified
SECURITY CLASSIFICATION OF THIS PAGE

REPORT DOCUMENTATION PAGE

1a. REPORT SECURITY CLASSIFICATION Unclassified	1b. RESTRICTIVE MARKINGS --
2a. SECURITY CLASSIFICATION AUTHORITY --	3. DISTRIBUTION/AVAILABILITY OF REPORT Distribution for public release; distribution is unlimited.
2b. DECLASSIFICATION/DOWNGRADING SCHEDULE --	
4. PERFORMING ORGANIZATION REPORT NUMBER(S) Graduate School of Oceanography Technical Report 86-8	5. MONITORING ORGANIZATION REPORT NUMBER(S)
6a. NAME OF PERFORMING ORGANIZATION University of Rhode Island Graduate School of Oceanography 6b. OFFICE SYMBOL (If applicable)	7a. NAME OF MONITORING ORGANIZATION
6c. ADDRESS (City, State, and ZIP Code) South Ferry Road Narragansett, R.I. 02882	7b. ADDRESS (City, State, and ZIP Code)
8a. NAME OF FUNDING/SPONSORING ORGANIZATION (1) National Science Foundation (2) Office of Naval Research 8b. OFFICE SYMBOL (If applicable) Physical Oceanography Program Code 422 P.O.	9. PROCUREMENT INSTRUMENT IDENTIFICATION NUMBER OCE82-01222 N00014-81-C-0062
8c. ADDRESS (City, State, and ZIP Code) (1) 1800 G St. NW, Washington D.C. 20550 (2) Code 422 P.O., 800 North Quincy, Arlington, VA 22217	10. SOURCE OF FUNDING NUMBERS PROGRAM ELEMENT NO. / PROJECT NO. / TASK NO. / WORK UNIT ACCESSION NO.

11. TITLE (Include Security Classification)
Deep-Ocean Bottom Pressure and Temperature Sensors Report: Methods and Data (Unclassified)

12. PERSONAL AUTHOR(S)
D.R. Watts and H. Kontoyiannis

13a. TYPE OF REPORT	13b. TIME COVERED	14. DATE OF REPORT (Year, Month, Day)	15. PAGE COUNT
Summary	FROM 9/1983 TO 5/1985	December, 1986	121

16. SUPPLEMENTARY NOTATION

17. COSATI CODES			18. SUBJECT TERMS (Continue on reverse if necessary and identify by block number)
FIELD	GROUP	SUB-GROUP	Gulf Stream meanders; Inverted Echo Sounders; Bottom Pressure; Pressure Sensor Drift

19. ABSTRACT (Continue on reverse if necessary and identify by block number)

This report documents ocean bottom pressure data collected from Sept. 1983 to May 1985 in eleven deployments of pressure sensors under the Gulf Stream northeast of Cape Hatteras in depths of 3300 to 3900 m, as part of the Gulf Stream Dynamics Experiment. In past experiments pressure sensors suitable for ocean depths have typically exhibited systematic drifts in calibration that seriously contaminate any observed periodicities longer than a few days. We used Digiquartz sensors (manufactured by Paroscientific, Inc.), because these sensors offered potentially much lower drift than other comercially available sensors. In these sensors, either a bellows or a Bourdon tube applies stress to an oscillating quartz-crystal beam, causing its oscillation frequency to vary. Several factors influence the amount of drift: bellows vs. Bourdon-tube construction, the applied pressure, the duration of deployment, and, for some sensors, high-pressure preconditioning in the lab. For the sensors deployed in the Gulf Stream, the total drift during deployments lasting from 3 to 12 months ranged from undetectable ($\leq$0.01 dbar) to 0.20 to 0.50 dbar. About half of the total drift typically occurred within

20. DISTRIBUTION/AVAILABILITY OF ABSTRACT ☒ UNCLASSIFIED/UNLIMITED ☒ SAME AS RPT. ☐ DTIC USERS	21. ABSTRACT SECURITY CLASSIFICATION unclassified
22a. NAME OF RESPONSIBLE INDIVIDUAL	22b. TELEPHONE (Include Area Code) / 22c. OFFICE SYMBOL

DD FORM 1473, 84 MAR 83 APR edition may be used until exhausted. All other editions are obsolete.

SECURITY CLASSIFICATION OF THIS PAGE

19.

the first six days of deployment.

We estimate the residual error in the final pressure records, after the "dedrifting" calculations, to be typically 0.02 dbar r.m.s. (or 0.06 dbar r.m.s.) if the first 6 days of the record are excluded (or included, respectively). This low drift-error opens many possibilities for studies that require knowledge of the low-frequency dynamic pressure signal in the deep ocean.

Part I on Methods contains a short review of bottom pressure measurement in the deep ocean, a description of the sensors that we used, a discussion of their performance and drift relative to type of construction and prior pressurization history ("preconditioning"), and estimates of the accuracy of the dedrifted pressure records.

In Part II of this report, the full data processing is described, including calibration parameters, corrections for the influence of temperature variations on the pressure sensor, and parameterization to remove sensor drift errors by least-squares regression onto an exponentially decaying time-dependence. Time series are plotted which illustrate several steps in the processing: the edited half-hourly pressure records, the detided pressures with drift-model curves superimposed, and the low-pass filtered, "dedrifted" pressure records (i.e., after subtracting the estimated drift curve).